Imperial College London
Department of Electrical and Electronic Engineering

Interconnection-based Model Order Reduction for Quadratic-bilinear Systems

Ph.D Candidate: Han Bai
Supervisor: Giordano Scarciotti

A thesis submitted to Imperial College London
for the degree of Doctor of Philosophy, March 2024

Declaration of Originality

I hereby declare that the material contained within this thesis is my own work, except where other work is appropriately referenced. Any use of the first-person plural is for reasons of clarity.

Han Bai

Department of Electrical and Electronic Engineering

Imperial College London, London, UK

March 2024

Copyright Declaration

Han Bai

Department of Electrical and Electronic Engineering

Imperial College London, London, UK

March 2024

Abstract

This thesis addresses the problem of model order reduction for quadratic-bilinear systems through an interconnection-based methodology. Initially, we compute the nonlinear moments for this type of systems by utilizing a formal power series representation. Two families of reduced-order model are proposed to achieve moment matching at specific interpolation points, while maintaining some key properties of the original system. Based on the model-based strategy, we then apply a data-driven algorithm to achieve reduced-order models by moment matching, using input and output data. This dual approach, both model-based and data-driven, is applied to the task of model order reduction for incompressible flows derived directly from the Navier-Stokes equations. Subsequently, we extend this approach to quadratic-bilinear time-delay systems by matching an approximated moment, achieved by truncating the power series. We present findings for both time-delay and non-time-delay systems represented in polynomial form. Finally, we introduce a two-sided interconnection for the model order reduction of quadratic-bilinear systems. This approach effectively doubles the number of matched moments in reduced-order models of the same size by considering both "direct" and "swapped" moments. We propose two families of reduced-order models: the first is designed based on the idea for general nonlinear systems, and the second leverages power series approximations.

Acknowledgements

I would like to express my deepest gratitude to all those who made the completion of this PhD thesis possible. First and foremost, I extend my sincere thanks to my supervisor, Giordano Scarciotti, for his invaluable guidance, patience, and unwavering support throughout this research journey. His expertise and insights have been crucial to my development as a scholar and to the successful completion of this work.

I am also immensely grateful to my co-supervisor, Thulasi Mylvaganam, whose expertise and advice have been instrumental in refining my research. Her contributions have significantly enhanced the quality of this thesis.

I also wish to express my thanks to my reviewers and examiners, Alessandro Astolfi and Mario Sassano, for their time and effort reviewing and evaluating this work.

I would like to thank many of my old friends for always being there. The time we share consistently aids in my relaxation and recharges me to continue with the research.

A special word of appreciation goes to my colleagues and friends at Imperial College London. This includes people in EEE 1111 and many other members in CAP group. I am particularly thankful for Junyu, Zilong, Zirui, Hanqing and Wangkun whose camaraderie and shared wisdom have made my PhD journey both enjoyable and enriching. Their support and encouragement have been a constant source of strength.

To my family, who has been my anchor and source of unconditional love and encouragement, I cannot thank you enough. I am thankful especially to my girlfriend, Wei Liu, who followed me to the UK to support and accompany me. Your belief in my abilities and unwavering support

have been my guiding light, and this achievement is as much yours as it is mine.

Last but not least, I acknowledge the countless authors and researchers whose works have informed and inspired my study. Their contributions have been indispensable to the development of this thesis.

This journey has been a testament to the power of collaboration, support, and shared knowledge. I am profoundly thankful to everyone who has been a part of it.

Contents

List of Figures

Chapter 1

Introduction

In this chapter relevant literature is reviewed, the motivations and objectives of the thesis are stated, and the thesis organization is described. The chapter is structured as follows. In Section 1.1, the motivations for model order reduction for quadratic-bilinear systems are discussed and the objectives of the thesis are stated. In Section 1.2 a brief review of the literature for model order reduction is given. In Section 1.3 the organization and the contributions of the thesis are discussed. Publications relating from the work in this thesis are listed in Section 1.4.

1.1 Motivation and Objectives

Model order reduction is a hot topic in fluid dynamics field as both linear and nonlinear techniques have been developed in this area [4]. The majority of established model order reduction methods have been designed primarily for linear systems and are frequently applied to linearized models of fluid dynamic systems, which simplifies the complexity inherent in these high-dimensional simulations [5]. When we turn to nonlinear systems, model order reduction techniques are much less developed due to the complexity of the system dynamics. However, in many situations, the problem is not so dire. For instance, the incompressible Navier-Stokes equations are nonlinear, but the nonlinearities have a specific form, i.e., they are quadratic, see [6]. Motivated by this, we focus on the problem of model order reduction for quadratic-bilinear

systems by using the interconnection-based method. Another motivation for studying this problem is that a large class of nonlinear systems can be written in quadratic-bilinear form by using exact transformations [7]. These transformations can be applied to many different fields, e.g. fluid mechanic systems, electrical circuit models, and biochemical rate equations [8]. Also, compared with more general nonlinear systems, quadratic-bilinear systems have a structure that is similar to that of linear systems (i.e., they are described by matrices) and can be exploited to simplify the model order reduction problem.

The objective of this thesis is to develop the interconnection-based moment matching method for quadratic-bilinear system. By exploiting the interconnection-based interpretation, we propose both one-sided and two-sided reduced-order models by moment matching for quadratic-bilinear systems. The one-sided moment matching method is then applied to Navier–Stokes type quadratic-bilinear descriptor systems together with the data-driven algorithm. The extension to quadratic-bilinear time-delay systems is also provided.

1.2 Model Order Reduction

The objective of model order reduction is to reduce the complexity issue that arises in the prediction, analysis, and control of modern complex systems. The complexity of a model is primarily described by its order, i.e., the number of state variables, which describe the dynamics of real-world systems. This problem, for both linear and nonlinear systems, has been extensively studied in the systems and control community due to its importance across various fields. For example, in fluid dynamics, the evolution of quantities of interest is typically described by the Navier-Stokes partial differential equation (PDE), which is difficult to find solutions. Since this equation lacks a closed-form solution, simulations and analysis rely on discretization techniques that convert the PDEs into ordinary differential equations (ODEs) with millions of states, as mentioned in [6]. Similarly, in the power systems sector, the interconnection of thousands of generators, buses, and interfacing devices increases the number of state variables to several thousands, as noted in [9–11]. Consequently, there is demand for simplified models of

smaller dimension that can provide essential insights for the simulation, analysis, and control of such systems at a lower computational cost, according to [12]. The model order reduction problem can be informally described as follows: given a higher order system, the goal is to find a reduced-order model that preserves some important behaviors (e.g., frequency response) or properties (e.g., stability).

Over the years, numerous strategies have been developed for effective model order reduction. Broadly speaking, these methods can be divided into those based on singular value decomposition (SVD) and those that rely on Krylov projectors and moment matching [13]. SVD-based techniques for model order reduction typically provide error bounds and enable the preservation of stability and structural properties. Balanced truncation, as an example, involves transforming a system into a balanced representation where two positive definite matrices are made diagonal and equal, as observed in [14], [15], [16], [17], [18] and [19]. Traditionally, controllability and observability Gramians are utilized in the Lyapunov balancing approach [13], [20]. In the balanced representation, states that require a substantial amount of input energy for control contribute minimal energy to the output, and vice versa. Consequently, these states are suitable candidates for truncation when reducing the system order. Other positive definite matrices have been explored for use in balanced truncation, such as stochastic balancing [21], [22], [23], and others [24], [25], [26], [27] and [28]. Balancing techniques have been extended to nonlinear systems [29], [30], [31], [32]; time-varying systems [33], [34], [35], [36]; and linear differential-algebraic equations (DAEs) [37], [38], [39], [40], [41], [42]. The Hankel-norm approximation approach aims to determine an approximant such that the associated error system is optimal in the Hankel-norm [43], [44], [45], [46]. This method has been developed for nonlinear systems [47], [48], [49], [50], time-varying systems [51], and linear DAEs [52].

Another widely-used family of model order reduction approaches is the interpolation or Krylov methods, which construct a reduced order model as a rational interpolant, as seen in [53], [54], [55], [56], [57], [58], [59]. (These methods are also known as *moment matching methods*, but in this paper we try to reserve this expression for the interpretation given in [60]). For a recent comprehensive overview of these methods, the readers are directed to [61]. The interpolation

framework described above has been reinterpreted using interconnection of systems and by relating moments with steady-state signals by [60]. This reinterpretation of the interconnection-based moment matching methods has allowed to create a theory of model order reduction by moment matching for general nonlinear systems. Compared with the classical interpolation approach, the interconnection-based method proposed in [60] has the advantage of allowing easy enforcement of some of the properties of the reduced order models for both linear and nonlinear systems. For instance, the technique allows imposing a set of eigenvalues or the relative degree of the reduced order model. The preservation of global stability for a class of nonlienar models has been published in [62]. This technique has been further generalized to wide classes of systems, e.g. linear and nonlinear time-delay systems [63], while a data-driven enhancement of this method has been given in [64], [65]. The moment matching approach has also been developed for DAEs, see [66], [67], [68], [69]; for stochastic systems, see [70], [71], [72]; for MIMO linear system, see [73]; and for 2-D discrete system, see [74]. The "moments" that we have mentioned above are related to the output via "direct" interconnection and are called "direct" moments. [75] introduces the "swapped" moments for a class of single-input, single-output, nonlinear systems, in terms of the evolution of the output of the "swapped" interconnection, which is an extension of the linear arguments developed in [76], [77]. By considering together the "direct" moment and the "swapped" moment, a so-called two-sided moment matching method for linear systems is proposed in [78]. Some data-driven results through "swapped" interconnection are available in [79] and then the extension to two-sided data-driven model reduction has been provided in [80], [81]. Moreover, [82] looks at the effect of noise in data-driven model reduction by moment matching. For further details, the readers are referred to [1].

Two other well-established approaches for model order reduction in fluids are Proper Orthogonal Decomposition (POD) and balanced truncation, as discussed in [83]. These methods have been integrated into a unified approach, known as balanced POD in [84], which also evaluates the performance of these three methods using the linearized flow in a plane channel as an example. [85] provides an insight into the modal decomposition/analysis techniques that are extensively employed to investigate a variety of fluid flows, discussing their strengths and weaknesses through several examples. [6] offers a comprehensive overview of some of the well-

developed model order reduction techniques for linear systems and explores methods applicable to nonlinear systems that describe flows. Various results have been proposed for addressing the model order reduction problem in such systems, including proper orthogonal decomposition (POD) [86], the trajectory piecewise-linear approach [87], and the discrete empirical interpolation method [88].

In the frequency domain, quadratic-bilinear systems can be represented by a nonlinear input-output mapping, which involves an infinite set of multivariate functions [89]. These functions, also called generalized transfer functions of the subsystems, represent the interconnected components within the system. Each subsystem contributes to the overall input-output behavior, and their collective dynamics are captured by this nonlinear map. An initial approach to achieve one-sided projection matching the first two transfer functions of a quadratic-bilinear system has been discussed in [7]. This method has been enhanced in [8] by introducing a left projection subspace matrix to ensure the interpolation of the first two subsystems more effectively. A quadratic-bilinear DAE was approximated as a bilinear DAE using Carleman bilinearization in [2], adopting an $\mathcal{H}_2$ optimal model order reduction strategy for deriving a reduced-order system. An equivalent representation, simplifying the structure of the generalized transfer functions and extending the idea to two-sided interpolation of higher subsystems, was introduced in [90]. The application of this methodology to a specific class of quadratic-bilinear descriptor systems, akin to Navier–Stokes type equations, is discussed in [91], while another interpolation projection framework based on error bounds is proposed in [92]. These approaches preserve the first two or higher multivariate transfer functions and their first derivatives in the reduced-order models. Similar findings for multi-input multi-output (MIMO) quadratic-bilinear systems employing tangential interpolation have been reported in [93]. Additionally, a data-driven approach for quadratic-bilinear (QB) systems, extending the Loewner framework to linear and bilinear systems, has been introduced in [94]. A novel reduction technique, capturing higher-order information and leveraging a simplified structure of the multivariate transfer functions, has been proposed recently in [95].

Meanwhile, time-delay systems (see the monographs [96–98]) naturally arise in real-world

scenarios since, as a matter of fact, every system presents delays to some degree. Consequently, extensions of model order reduction techniques to time-delay systems have been intensively studied in recent years. We mention a few, namely [99], [100], [101], but note that the literature on model order reduction for quadratic-bilinear time-delay systems is scarce. A related work is [102] which considered bilinear systems with a single delay on the linear term.

1.3 Thesis Outline

The organization of the thesis is as follows.

In Chapter 2 we review the notation and background material related to the interconnection-based model order reduction method for general nonlinear systems. This includes discussions on two-sided interconnection, data-driven implementation, and extensions to differential-algebraic and time-delay systems. Unlike the extensive literature on interpolation/Krylov methods (also known as moment matching), which are based on the linear notion of moments (i.e., linked to the transfer function), the method introduced here is based on the nonlinear notion of moments (i.e., based on the steady-state response).

In Chapter 3 an interconnection-based moment matching method for quadratic-bilinear systems is developed. Our contribution lies in utilizing the special structure of quadratic-bilinear systems to provide easily computable approximations of the nonlinear moment and reduced-order models that preserve the quadratic-bilinear structure. This is not possible with the general nonlinear framework which is based on the solutions of PDEs, which are difficult to compute, and cannot be used to preserve the quadratic-bilinear structure.

In Chapter 4 we apply the interconnection-based method to Navier-Stokes type quadratic-bilinear descriptor systems to address the model order reduction problem for incompressible flows. Based on the model-based strategy, we then develop a data-driven algorithm to achieve reduced-order models by moment matching, using input and output data. This category of descriptor systems is directly formulated from the Navier–Stokes equations. We present three examples to illustrate the results.

In Chapter 5 the focus is on employing two-sided interconnection to simultaneously match the direct moments and the swapped moments. We construct two distinct families of reduced-order models: the first is based on results for general nonlinear systems, while the second is specially designed to preserve the quadratic-bilinear structure. The resulting reduced-order models match moments at 2-ν (distinct) interpolation points, effectively doubling the number of matching conditions.

In Chapter 6 we present the extension of moment matching results to quadratic-bilinear time-delay systems. Given the scarcity of the literature on model order reduction for such systems, we demonstrate that the (nonlinear) moment of these systems can still be characterized as the solution of an infinite-dimensional system of Sylvester-like equations, facilitating the approximations for the moment and the associated reduced-order models.

In Chapter 7 a summary of the contributions in this thesis is stated and some important directions for further research are given.

1.4 Publications

The interconnection-based moment matching method for quadratic-bilinear systems, given in Chapter 3, is based on the conference paper [103]. The application of this method to Navier-Stokes type quadratic-bilinear descriptor systems, including both the model-based and the data-driven approach, given in Chapter 4, is based on journal paper under preparation [104]. The enhancement of the two-sided framework for quadratic-bilinear systems, given in Chapter 5, are based upon the conference paper [105]. The extension to quadratic-bilinear time-delay systems, given in Chapter 6, is based upon the conference paper [106].

Chapter 2

Preliminaries

In order to lay the foundation for the following chapters of the thesis, preliminary definitions and results regarding nonlinear model order reduction by moment matching are reviewed.

The structure of this chapter is as follows. Section 2.1 introduces frequently used notation. Section 2.2 revisits some foundational concepts associated with nonlinear model order reduction by moment matching. In Section 2.3 we review data-driven estimation techniques. The interconnection-based moment matching method for general nonlinear differential-algebraic equations is discussed in Section 2.4, while Section 2.5 studies general nonlinear time-delay systems. Section 2.6 discusses some properties of the Kronecker product and the solvability of Sylvester equation that are essential in this thesis.

2.1 Notation

Standard notation is used throughout the thesis. This is briefly reviewed in what follows for the reader's benefit.

$\mathbb{R}$ and $\mathbb{C}$ denote the sets of real numbers and complex numbers respectively. $\mathbb{R}_{\geq 0}$ ($\mathbb{R}_{>0}$) denotes the set of non-negative (positive) real numbers. $\mathbb{C}_0$ ($\mathbb{C}_{<0}$) denotes the set of complex numbers with zero (negative) real part. The set of positive integers is denoted by $\mathbb{Z}_{>0}$. The symbol I_ν

and 0_ν denotes the identity and zero matrix of dimension $\nu \in \mathbb{R}$, respectively. I_A represents the identity matrix with dimension $\max(m, n)$ for any matrix $A \in \mathbb{R}^{n\times m}$. The symbol $\otimes$ indicates the Kronecker product and $\oplus$ indicates the Kronecker sum. A^{-1} indicates the inverse of the matrix A and the superscript $\top$ denotes the transposition operator. For square matrices A and B, $\mathrm{diag}(A, B)$ indicates a block diagonal matrix with A and B on the main diagonal. $\sigma(A)$ represents the set of all the eigenvalues of the matrix A. The operator $\mathrm{vec}(A)$ indicates the vectorization of the matrix $A \in \mathbb{R}^{n\times m}$, which is the $nm \times 1$ vector obtained by stacking the columns of the matrix A one on top of the other. $\mathcal{B}_{(a,r)}$ represents a ball centered at a of radius r and $\lambda_{\min}(A)$ represents the minimum eigenvalue of matrix A.

The subscript attached to a signal denotes the translation operator, *e.g.*, x_τ and u_λ indicates $x(t-\tau)$ and $u(t-\lambda)$, respectively. $\mathcal{T}_x = \{\tau_i \in \mathbb{R}_{\geq 0}\}$, with $\tau_0 = 0$ and $\mathcal{T}_u = \{\lambda_j \in \mathbb{R}_{>0}\}$, are sets of delays for states and inputs, respectively. Given a set of delays $\{\tau_i\}$, the symbol $\mathfrak{R}^n_T = \mathfrak{R}^n_T([-T, 0], \mathbb{R}^n)$, with $T = \max_i\{\tau_i\}$, indicates the set of continuous functions mapping the interval $[-T, 0]$ into $\mathbb{R}^n$ with the topology of uniform convergence. Given two sets X and Y , $X \setminus Y$ indicates the set of elements in X but not in Y. Given two functions, $f : Y \to Z$ and $g : X \to Y$, we denote with $f \circ g : X \to Z$ the composite function $(f \circ g)(x) = f(g(x))$ that maps all $x \in X$ to $f(g(x)) \in Z$.

2.2 Moment Matching for Nonlinear Input-affine Systems

Consider a nonlinear, minimal[1], single-input, single-output (SISO), system described by the equation

$$\dot{x} = f(x) + g(x)u, \qquad y = h(x), \tag{2.1}$$

where $x(t) \in \mathbb{R}^n$ is the state, $u(t) \in \mathbb{R}$ is the input, $y(t) \in \mathbb{R}$ is the output, and f, g and h are smooth mappings such that $f(0) = 0$, $g(0) = 0$, and $h(0) = 0$. Furthermore, we consider the

[1]See [107, Definition 2.12].

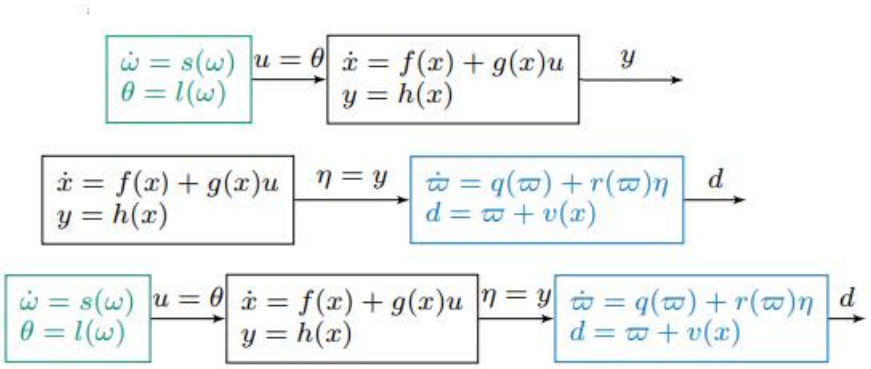

Figure 2.1: Diagrammatic illustration of the direct (top), the swapped (middle) and the two-sided (bottom) interconnections [1].

signal generator

$$\dot{\omega} = s(\omega), \qquad \theta = l(\omega), \tag{2.2}$$

with $\omega(t) \in \mathbb{R}^\nu$, $\theta(t) \in \mathbb{R}$, s and l smooth mappings such that $s(0) = 0$ and $l(0) = 0$, and the interconnection (with $u = \theta$) between this generator and system (2.1), namely

$$\dot{\omega} = s(\omega), \qquad \dot{x} = f(x) + g(x)l(\omega), \qquad y = h(x), \tag{2.3}$$

as represented at the top of Fig 2.1.

Assumption 1. The partial differential equation

$$\frac{\partial \pi}{\partial \omega} s(\omega) = f(\pi(\omega)) + g(\pi(\omega))l(\omega) \tag{2.4}$$

has a unique solution π.

Assumption 2. The signal generator (2.2) is observable, i.e. for any pair of initial conditions $\omega_a(0)$ and $\omega_b(0)$, such that $\omega_a(0) \neq \omega_b(0)$, the corresponding output trajectories $l(\omega_a(t))$ and $l(\omega_b(t))$ are such that $l(\omega_a(t)) - l(\omega_b(t)) \not\equiv 0$.

The moment of system (2.1) related to the generator (2.2) is defined as follows.

Definition 1. Consider the system (2.1) and the signal generator (2.2). Suppose that Assumptions 1 and 2 hold. We call the mapping $h \circ \pi$ the (direct) moment of system (2.1) at (s, l).

The signal generator captures the requirement that one is interested in studying the behaviour of the system (2.1) only in specific circumstances: a reduced-order model by moment matching is a model that matches the steady-state output response (if exists) of the system for the same class of inputs of interest. We now recall the definition of the "swapped moment". Consider the nonlinear filter

$$\dot{\varpi} = q(\varpi) + r(\varpi)\eta, \tag{2.5}$$

with $\varpi(t) \in \mathbb{R}^\nu$, $\eta(t) \in \mathbb{R}$, q and r smooth mappings such that $q(0) = 0$ and $r(0) = 0$, and the interconnection (with $\eta = y$) between this filter and system (2.1), namely

$$\dot{x} = f(x) + g(x)u, \quad \dot{\varpi} = q(\varpi) + r(\varpi)h(x), \tag{2.6}$$

as represented in the middle of Fig 2.1.

Assumption 3. The partial differential equation

$$\frac{\partial v}{\partial x} f(x) + r(-v(x))h(x) + q(-v(x)) = 0 \tag{2.7}$$

has a unique solution v.

Assumption 4. The filter (2.5) is observable.

The moment of system (2.1) related to the filter (2.5) is defined as follows.

Definition 2. Consider the system (2.1) and the filter (2.5). Suppose that Assumption 3 and 4 hold. We call the mapping $\frac{\partial v}{\partial x} g$ the (swapped) moment of system (2.1) at (q, r).

Consider the reduced-order model described by

$$\dot{\xi} = \phi(\xi) + \delta(\xi)u, \quad \psi = \kappa(\xi). \tag{2.8}$$

where $\xi(t) \in \mathbb{R}^\nu$, $\psi(t) \in \mathbb{R}$, $\nu < n$, $\phi(0) = 0$, $\delta(0) = 0$, and $\kappa(0) = 0$. System (2.8) matches the

moment $h \circ \pi$ at (s, l), if ϕ, δ and κ satisfy

$$\frac{\partial p}{\partial \omega} s(\omega) = \phi(p(\omega)) + \delta(p(\omega)) l(\omega) \tag{2.9}$$

and

$$\kappa(p(\omega)) = h(\pi(\omega)) \tag{2.10}$$

for all ω and some mapping p. These equations are satisfied by the selection $\phi(\xi) = s(\xi) - \delta(\xi) l(\xi)$, $\kappa(\xi) = h(\pi(\xi))$, with δ a free mapping[2], for the mapping $p(\omega) = \omega$. Thus, the model

$$\dot{\xi} = s(\xi) - \delta(\xi) l(\xi) + \delta(\xi) u, \qquad \psi = h(\pi(\xi)), \tag{2.11}$$

is a reduced-order model that matches the moment of system (2.1) at (s, l).

Moreover, this model matches also the moment $\frac{\partial v}{\partial x} g$ at (q, r), if δ is such that

$$-q(-\chi(\xi)) = \frac{\partial \chi}{\partial \xi} \phi(\xi) + r(-\chi(\xi)) \kappa(\xi) \tag{2.12}$$

and

$$\left[\frac{\partial \chi}{\partial \omega} \delta(\omega) \right]_{\xi = \omega} = \left[\frac{\partial v}{\partial x} g(x) \right]_{x = \pi(\omega)}, \tag{2.13}$$

for all ω and some mapping χ. This is achieved with the selection

$$\delta(\xi) = \left[\left(\frac{\partial v}{\partial x} \frac{\partial \pi}{\partial \xi} \right)^{-1} \frac{\partial v}{\partial x} g(x) \right]_{x = \pi(\xi)}, \tag{2.14}$$

which gives $\chi(\xi) = v(\pi(\xi))$. Thus, system (2.11) with (2.14) is a reduced-order model of system (2.1) matching the moments at (s, l) and (q, r), simultaneously. Note that this model, in addition to satisfying the matching conditions (2.10) and (2.13), also satisfies the additional matching condition

$$\chi(p(\omega)) = v(\pi(\omega)) \tag{2.15}$$

for all ω.

[2]As long as the solution of (2.9) is unique.

2.3 On-line Moment Estimation from Data

This Section is based on the results in [65].

In order to relate the moment of a system to the steady-state response of system (2.3), the following assumption is needed.

Assumption 5. The zero equilibrium of system (2.1) is locally exponentially stable and the signal generator (2.2) is neutrally stable[3].

Note that if Assumptions 2 and 5 hold, then (2.4) has a solution π and Assumption 1 is not explicitly required.

Theorem 1. Consider system (2.1) and the signal generator (2.2). Assume Assumptions 2 and 5 hold. Then the moment $h \circ \pi$ computed along a particular trajectory ω coincides with the steady-state output response of system (2.3).

Note that given the exponential stability hypothesis on the system and Theorem 1, the equation

$$y(t) = h(\pi(\omega(t))) + \iota(t), \tag{2.16}$$

where $\iota(t)$ is a transient term which decays to zero, holds. To what follows we need the following assumption.

Assumption 6. The mapping $h \circ \pi$ belongs to the function space identified by the family of continuous basis functions $\varphi_i : \mathbb{R}^\nu \to \mathbb{R}$, with $i = 1, \cdots K$, where $K \in \mathbb{Z}_{>0}$, i.e. for any ω, there exists constants $\gamma_i \in \mathbb{R}$ such that $h(\pi(\omega)) = \sum_{i=1}^{K} \gamma_i \varphi_i(\omega)$.

The assumption that the mapping to be approximated can be represented by a family of basis functions is standard, see [109]. For some families of basis functions, e.g. radial basis functions, there exist results of "universal" approximation, see [110]. Consider now the approximation

$$y(t) \approx \sum_{i=1}^{N} \widetilde{\gamma}_i \varphi_i(\omega(t)) = \widetilde{\Gamma}\Omega(\omega(t)), \tag{2.17}$$

[3]See [108, Chapter 8] for the definition of neutral stability.

where $N \leq K$, $\Gamma = [\gamma_1 \quad \gamma_2 \quad \cdots \quad \gamma_N]$ and $\Omega(\omega(t)) = [\varphi_1(\omega(t)) \quad \varphi_2(\omega(t)) \quad \cdots \quad \varphi_N(\omega(t))]^\top$. This approximation neglects the error e resulting by terminating the summation at N, namely $e(t) = \sum_{N+1}^{K} \gamma_i \varphi_i(\omega(t))$ and the transient error ι. Therefore we define $\widetilde{\Gamma}_j$ in (2.17) as an approximate on-line estimate of the matrix Γ computed at T_j^w, i.e. computed at the time t_j using the last w samples. Thus, we have the following

Theorem 2. Define the time-snapshots matrices $\widetilde{U}_j \in \mathbb{R}^{w \times N}$ and $\widetilde{Y}_j \in \mathbb{R}^w$ with, $w \geq N$, as

$$\widetilde{U}_j = [\Omega(t_{j-w+1} \quad \cdots \quad \Omega(t_{j-1}) \quad \Omega(t_j)]^T \tag{2.18}$$

and

$$\widetilde{Y}_j = [y(t_{j-w+1} \quad \cdots \quad y(t_{j-1}) \quad y(t_j)]^T. \tag{2.19}$$

If $\widetilde{U}_j$ is full column rank, then

$$\mathrm{vec}(\widetilde{\Gamma}_j) = (\widetilde{U}_j^T \widetilde{U}_j)^{-1} \widetilde{U}_j^T \widetilde{Y}_j \tag{2.20}$$

is an approximation of the estimate Γ_j.

To guarantee the convergence of the estimated moment, we introduce the following assumption.

Assumption 7. The initial condition $\omega(0)$ of the signal generator (2.2) is almost periodic[4] and all the solutions of the system are analytic. In addition, system (2.2) satisfies the excitation rank condition[5] at $\omega(0)$.

Theorem 3. Suppose Assumption 2, 5, 6 and 7 hold. Then

$$\lim_{t \to \infty} (h(\pi(\omega(t))) - \lim_{N \to K} \widetilde{\Gamma}_j \Omega(\omega(t))) = 0. \tag{2.21}$$

Until now, we have exclusively focused on a single trajectory ω. Although this suffices in a linear setting, where local properties extend globally, it might be limiting in nonlinear scenarios.

[4]See [111] for the definition of almost periodic point.
[5]See [111] for the definition of excitation rank condition.

Therefore, it becomes necessary to extend the theorem by substituting the matrices $\widetilde{U}_j$ and $\widetilde{Y}_j$ with the matrices

$$\begin{aligned} U &= [\widetilde{U}_j^{1\top} \quad \widetilde{U}_j^{2\top} \quad \cdots \quad \widetilde{U}_j^{q\top}], \\ Y &= [\widetilde{Y}_j^{1\top} \quad \widetilde{Y}_j^{2\top} \quad \cdots \quad \widetilde{Y}_j^{q\top}], \end{aligned} \tag{2.22}$$

for $q \geq 1$, with $\widetilde{U}_j^i$ and $\widetilde{Y}_j^i$ are the matrices defined by (2.18) and (2.19) sampled from different signal generator initial condition $\omega(0) = \omega_0^i$.

2.4 Moment Matching for General Nonlinear DAEs

Herein, we recall some preliminaries about this interconnection-based moment matching method for general nonlinear DAEs as presented in [68].

Consider a nonlinear, SISO continuous-time descriptor system

$$E\dot{x} = f(x, u), \quad y = h(x), \tag{2.23}$$

where $E \in \mathbb{R}^{n\times n}$, and $\text{rank}(E) = r < n$ with $E = \text{diag}(I, 0)$. Note that $x(t) \in \mathbb{R}^n$, $u(t) \in \mathbb{R}$ and, $y(t) \in \mathbb{R}^m$, and $f : \mathbb{R}^n \times \mathbb{R} \to \mathbb{R}^n$ and $h : \mathbb{R}^n \to \mathbb{R}^m$ are smooth mappings. Consider also a signal generator described by the equations

$$\dot{\omega} = s(\omega), \quad \theta = l(\omega), \tag{2.24}$$

with $\omega(t) \in \mathbb{R}^v$, $\theta(t) \in \mathbb{R}$, $s : \mathbb{R}^v \to \mathbb{R}^v$ and $l : \mathbb{R}^v \to \mathbb{R}$ smooth mappings, and the interconnected system

$$\dot{\omega} = s(\omega), \quad E\dot{x} = f(x, l(\omega)), \quad y = h(x). \tag{2.25}$$

Suppose that $f(0, 0) = 0$, $s(0) = 0$, $l(0) = 0$, $h(0) = 0$ and that the following standard assumptions for DAEs hold.

Assumption 8. The initial condition $x(0)$ is consistent, i.e., the initial value problem associated

with (2.23) has at least one solution [112].

Assumption 9. The pair (E, A), with $A = \frac{\partial f(x,0)}{\partial x}\Big|_{x=0}$, is strongly stable[6].

Without loss of generality, we assume that the generator has been constructed with the following properties.

Assumption 10. The signal generator (2.24) is observable and neutrally stable. Finally, $\omega(0)$ is almost periodic and such that (2.24) satisfies the excitation rank condition at $\omega(0)$.

Lemma 1. Consider the system (2.23) and the signal generator (2.24). Suppose the Assumptions 8, 9 and 10 hold. Then, there is a sufficiently smooth mapping π, with $\pi(0) = 0$, locally defined in a neighbourhood of $\omega(0)$, which solves the partial differential-algebraic equation (DAE)

$$E\frac{\partial \pi}{\partial \omega}s(\omega) = f(\pi(\omega), l(\omega)). \tag{2.26}$$

In addition, for any sufficiently small $x(0)$ and $\omega(0)$, the solution $x(t)$, $\omega(t)$ of (2.25) exists, is bounded for all $t \geq 0$, and satisfies $\lim_{t\to\infty} x(t) - \pi(\omega(t)) = 0$.

Remark 1. Observability and neutral stability of the generator (2.24) are the only conditions (from Assumption 10) required to prove Lemma 1. However, we want to exclude some "pathological" situations in which the components of the steady-state may be identically zero for selected initial conditions $\omega(0)$ (e.g., we want to exclude the initial condition $\omega(0) \neq 0$). For this reason, we require the excitability rank condition to be satisfied at an almost periodic $\omega(0)$. This condition guarantees persistence of excitation of the signal u [111]. For an in-depth discussion of the relation between this condition and the problem of model order reduction, see [113].

Definition 3. Consider the system (2.23) and the signal generator (2.24). Suppose Assumptions 8 holds. The mapping $h \circ \pi$, with π solution to (2.26), is the moment of system (2.23) at (s, l).

The moment $h \circ \pi$ computed along a particular trajectory ω of system (2.24) coincides with the steady-state response of the system (2.25) [68]. Thus, matching the moment of a system

[6]The pair (E, A) is strongly stable if for all $\bar{\lambda} \in \mathbb{C}$ such that $\det(\bar{\lambda}E - A) = 0$, $\bar{\lambda} \in \mathbb{C}_{<0}$ and $\deg(\det(\bar{\lambda}E - A)) = r$.

captures the requirement that one is interested in studying the *behavior* of the system under specific circumstances (e.g. when excited by specific frequencies of interest).

Consider then a model described by the equations

$$\Xi\dot{\xi} = \varphi(\xi, u), \quad \psi = \kappa(\xi), \tag{2.27}$$

where $\xi(t) \in \mathbb{R}^v$, $\psi(t) \in \mathbb{R}^m$, $\Xi \in \mathbb{R}^{v\times v}$ has $\text{rank}(\Xi) = \bar{r} \leq r$, with $\Xi = \text{diag}(I, 0)$. Assuming addition that $\varphi : \mathbb{R}^v \times \mathbb{R} \to \mathbb{R}^v$ and $\kappa : \mathbb{R}^v \to \mathbb{R}^m$ are smooth mappings.

Definition 4. System (2.27) is a *model* of system (2.23) at (s, l) if system (2.27) has the same moment at (s, l) as system (2.23). Furthermore, system (2.27) is a *reduced-order model* of system (2.23) at (s, l) if $v < n$.

Lemma 2. Consider system (2.23) and the signal generator 2.24. Suppose Assumptions 8, 9 and 10 hold. System (2.27) is a model of system (2.23) at (s, l) when the equation

$$\Xi\psi(p(\omega), l(\omega)) = \frac{\partial p}{\partial \omega} s(\omega) \tag{2.28}$$

has a unique solution p and the equation

$$h(\pi(\omega)) = \kappa(p(\omega)), \tag{2.29}$$

where π is the solution of (2.26) holds.
Note that selecting $\Xi = I_v$ results in the reduced-order model that is no longer a descriptor system. Thus in this case, the results in [107] could be directly applied.

2.5 Model Order Reduction for Nonlinear Time-Delay Systems

In this section we recall the notion of moment matching for general nonlinear time-delay, systems introduced in [101].

Consider a nonlinear, SISO, continuous-time, time-delay system described by equations of the form

$$\begin{aligned} \dot{x} &= f(x_{\tau_0}, \ldots, x_{\tau_\zeta}, u_{\lambda_0}, \ldots, u_{\lambda_\mu}), \qquad y = h(x), \\ x(\theta) &= q(\theta), \qquad -T \leq \theta \leq 0, \end{aligned} \tag{2.30}$$

with $x(t) \in \mathbb{R}^n$, $u(t) \in \mathbb{R}$, $y(t) \in \mathbb{R}$, $q \in \mathfrak{R}_T^n$, $\tau_i \in \mathcal{T}_x$, with $i = 0, \ldots, \zeta$, $\lambda_j \in \mathcal{T}_u$, with $j = 0, \ldots, \mu$, and f and h smooth mappings. Consider in addition a signal generator described by the equations

$$\dot{\omega} = s(\omega), \qquad \theta = l(\omega), \tag{2.31}$$

with $\omega(t) \in \mathbb{R}^\nu, \theta(t) \in \mathbb{R}$, and s and l smooth mappings, and the interconnected system

$$\begin{aligned} \dot{\omega} &= s(\omega), \\ \dot{x} &= f(x_{\tau_0}, \ldots, x_{\tau_\zeta}, l(\omega_{\lambda_0}), \ldots, l(\omega_{\lambda_\mu})), \\ y &= h(x). \end{aligned} \tag{2.32}$$

Suppose that $f(0, \ldots, 0, 0, \ldots, 0) = 0, s(0) = 0, l(0) = 0$, and $h(0) = 0$.

Assumption 11. There exists a unique mapping π, locally defined in a neighbourhood of $\omega = 0$, solving the partial differential equation

$$\frac{\partial \pi}{\partial \omega} s(\omega) = f\left(\pi\left(\bar{\omega}_{\tau_0}\right), \ldots, \pi\left(\bar{\omega}_{\tau_\varsigma}\right), l\left(\bar{\omega}_{\lambda_0}\right), \ldots, l\left(\bar{\omega}_{\lambda_\mu}\right)\right), \tag{2.33}$$

in which $\bar{\omega}_{\tau_i} = \Phi^s_{\tau_i}(\omega)$ and $\bar{\omega}_{\lambda_j} = \Phi^s_{\lambda_j}(\omega)$, with $i = 0, \ldots, \zeta$ and $j = 0, \ldots, \mu$, are the flows of the vector field s at $-\tau_i$ and $-\lambda_j$ [114], respectively.

Assumption 12. The signal generator (2.31) is observable.

We are now in a position to define the moment for system (2.30).

Definition 5. Consider the system (2.30) and the signal generator (2.31). Suppose Assumptions 11 and 12 hold. Then, the mapping $h \circ \pi$, with π the solution of (2.33), is the *moment* of system (2.31) at (s, l).

2.6 Kronecker Product and Sylvester Equation Basics

In the following chapters we consider power series representations which require the introduction of the Kronecker product notation. For any matrix A, we define

$$A^{(i)} = \underbrace{(A \otimes A \cdots \otimes A)}_{i-\text{factors}}, \quad A^{[i]} = \underbrace{(A \oplus A \cdots \oplus A)}_{i-\text{factors}}, \tag{2.34}$$

for all $i \geq 2$, with $A^{(1)} = A^{[1]} = A$ and $A^{(0)} = A^{[0]} = 1$, i.e. $A^{(0)}$ and $A^{[0]}$ are scalars. Then, we recall some properties of the Kronecker product. Let A, B, C and D be matrices of conformable dimensions, then [115]

P1) $(AB) \otimes (CD) = (A \otimes C)(B \otimes D)$,

P2) $A \oplus B = A \otimes I_B + I_A \otimes B$, where $A \in \mathbb{R}^{n \times n}$ and $B \in \mathbb{R}^{m \times m}$,

P3) $Ab = A \otimes b$ whereas b is a scalar.

For any matrix $A \in \mathbb{R}^{n \times m}$, note that the standard Kronecker sum is defined for square matrix and we define the Kronecker sum of same non-square matrices as follows

$$A \oplus A = A \otimes I_n + I_n \otimes A$$

The following lemma is a modified version of the results in [116, Lemma 4.6].

Lemma 3. Let $z \in \mathbb{R}^q$ and $M \in \mathbb{R}^{q \times q}$.

(i) For $k \geq 1$

$$\frac{\partial z^{(k)}}{\partial z} = \frac{\partial \overbrace{(z \otimes \cdots \otimes z)}^{k-\text{factors}}}{\partial z} = \sum_{i=1}^{k} z^{(i-1)} \otimes I_z \otimes z^{(k-i)}. \tag{2.35}$$

(ii) For $k \geq 1$

$$M^{[k]} = \sum_{i=1}^{k} (I_z^{(i-1)} \otimes M \otimes I_z^{(k-i)}). \tag{2.36}$$

(iii) For $k \geq 1$

$$\frac{\partial z^{(k)}}{\partial z} Mz = M^{[k]} z^{(k)}. \tag{2.37}$$

Proof. Equation (2.35) follows from the definition of the Kronecker product and an application of the chain rule.

To prove that (2.36) holds, note that for $k = 1$, $M^{[1]} = M$ which satisfies (2.36) trivially. Suppose that for $k = j - 1$, (2.36) holds. Then, when $k = j$,

$$\begin{aligned}
M^{[j]} &= M^{[j-1]} \oplus M \\
&= \sum_{i=1}^{j-1} (I_z^{(i-1)} \otimes M \otimes I_z^{(j-i-1)}) \oplus M \\
&= \sum_{i=1}^{j-1} (I_z^{(i-1)} \otimes M \otimes I_z^{(j-i-1)}) \otimes I_z + I_z^{(j-1)} \otimes M \\
&= \sum_{i=1}^{j-1} (I_z^{(i-1)} \otimes M \otimes I_z^{(j-i)}) + I_z^{(j-1)} \otimes M \\
&= \sum_{i=1}^{j} (I_z^{(i-1)} \otimes M \otimes I_z^{(j-i)}).
\end{aligned}$$

That is, (2.36) holds for $k \geq 1$ by induction. The condition (2.37) is demonstrated as follows

$$\begin{aligned}
\frac{\partial z^{(k)}}{\partial z} Mz &= \sum_{i=1}^{k} z^{(i-1)} \otimes I_z \otimes z^{(k-i)} Mz \\
&= \sum_{i=1}^{k} z^{(i-1)} \otimes (I_z \otimes z^{(k-i)})(Mz \otimes 1) \\
&\overset{P1}{=} \sum_{i=1}^{k} z^{(i-1)} \otimes (Mz) \otimes z^{(k-i)} \\
&= \sum_{i=1}^{k} (I_z^{(i-1)} z^{(i-1)}) \otimes (Mz) \otimes (I_z^{(k-i)} z^{(k-i)}) \\
&\overset{P1}{=} \sum_{i=1}^{k} (I_z^{(i-1)} \otimes M \otimes I_z^{(k-i)}) z^{(k)} \\
&= M^{[k]} z^{(k)}.
\end{aligned}$$

Note that M has the same dimension as I_z and we have repeatedly used P1 during the proof. □

The Sylvester equation is a classic problem in linear algebra, formulated as:

$$AX - XB = C \tag{2.38}$$

where A, B, and C are given matrices, and X is the matrix to be determined. Matrix A is $m \times m$, matrix B is $n \times n$, and both matrices C and X are $m \times n$. The existence of a solution to the Sylvester equation depends significantly on the eigenvalues of matrices A and B. Specifically, the equation has a unique solution for all C if and only if matrices A and B have no eigenvalues in common:

$$\sigma(A) \cap \sigma(B) = \emptyset \tag{2.39}$$

where $\sigma(A)$ and $\sigma(B)$ denote the eigenvalue sets of A and B, respectively. This condition ensures that the equation can be rearranged and treated effectively as a linear system by using the properties of the Kronecker product and vectorization [117]. Note that in the rest of paper, we assume that this holds for all the Sylvester equation we solve.

Chapter 3

Interconnection-based Model Order Reduction for Quadratic-bilinear Systems Using Nonlinear Moments

The results presented in this chapter are based on [103], in which the problem of model order reduction for quadratic-bilinear systems using the steady-state notion of moment has been addressed. It is important to note that, unlike the extensive literature on moment matching for quadratic-bilinear systems, which primarily relies on the linear notion of moment (i.e., linked to the transfer function), our work distinguishes itself by focusing on the nonlinear notion of moment (i.e., based on the steady state).

The structure of this chapter is as follows. Section 3.1 formulates the problem of model order reduction for quadratic-bilinear systems and defines the concept of direct moment for these systems. In Section 3.2, we introduce the first family of reduced-order models, which retains the quadratic-bilinear form. Section 3.3 develops the second family of reduced-order models, addressing enhancements in terms of stability properties and well-defined relative degree. Finally, Section 3.4 presents a numerical example to demonstrate the results discussed in this chapter.

3.1 Direct Moments for Quadratic-bilinear Systems

Consider a SISO quadratic-bilinear system described by the equations

$$\begin{aligned} \dot{x} &= f(x,u) = Ax + H(x \otimes x) + Nxu + Bu, \\ y &= h(x) = Cx, \end{aligned} \tag{3.1}$$

with $A \in \mathbb{R}^{n\times n}$, $N \in \mathbb{R}^{n\times n}$, $H \in \mathbb{R}^{n\times n^2}$, $B \in \mathbb{R}^n$, and $C^\top \in \mathbb{R}^n$. Consider a signal generator of the form

$$\dot{\omega} = s(\omega) = S\omega, \quad \theta = l(\omega) = L\omega, \tag{3.2}$$

with $S \in \mathbb{R}^{v\times v}$ and $L^\top \in \mathbb{R}^v$. Consider the interconnected system given by

$$\begin{aligned} \dot{\omega} &= S\omega, \\ \dot{x} &= Ax + H(x \otimes x) + NxL\omega + BL\omega, \\ y &= Cx. \end{aligned} \tag{3.3}$$

Note that for system (3.1) and the signal generator (3.2), Assumption 5 reduces to requiring local exponential stability of the zero equilibrium of (3.1) and that the eigenvalues of S are simple and belong to $\mathbb{C}_0$. We formulate these requirements in two Assumptions.

Assumption 13. The origin of the system (3.1) is locally exponentially stable.

Assumption 14. The signal generator (3.2) is observable and the eigenvalues of S are simple and belong to $\mathbb{C}_0$.

We now present a result that provides a way of computing the nonlinear moment of (3.1).

Theorem 4. Consider the system (3.1) and the signal generator (3.2), and suppose that Assumptions 13 and 14 hold. Then there is a mapping

$$\pi(\omega) = \sum_{i\geq 1} \Pi_i \omega^{(i)} \tag{3.4}$$

which formally solves the PDE

$$\frac{\partial \pi}{\partial \omega} S\omega = A\pi(\omega) + H(\pi(\omega) \otimes \pi(\omega)) + N\pi(\omega)L\omega + BL\omega, \tag{3.5}$$

where Π_i, $i \geq 1$, solve the infinite-dimensional system of Sylvester like equations

$$\begin{aligned} \Pi_1 S &= A\Pi_1 + BL, \\ \Pi_2 S^{[2]} &= A\Pi_2 + H(\Pi_1 \otimes \Pi_1) + N(\Pi_1 \otimes L), \\ \Pi_i S^{[i]} &= A\Pi_i + H(\Pi_1 \otimes \Pi_{i-1} + \Pi_2 \otimes \Pi_{i-2} + \cdots + \Pi_{i-1} \otimes \Pi_1) + N(\Pi_{i-1} \otimes L), \end{aligned} \tag{3.6}$$

for $i \geq 3$.

Proof. Under Assumptions 13 and 14, equation (3.5) has a solution π [107]. Moreover, Assumptions 13 and 14 are also sufficient to guarantee that system (3.6) has a unique solution, see [116, Lemma 4.13]. Consider the formal power series expansion of π, namely (3.4). Substituting (3.4) into (3.5) yields

$$\begin{aligned} &\frac{\partial(\Pi_1\omega + \Pi_2(\omega \otimes \omega) + \cdots)}{\partial \omega} S\omega = A(\Pi_1\omega + \Pi_2(\omega \otimes \omega) + \cdots) \\ &+ H(\Pi_1\omega + \Pi_2(\omega \otimes \omega) + \cdots) \otimes (\Pi_1\omega + \Pi_2(\omega \otimes \omega) + \cdots) \\ &+ N(\Pi_1\omega + \Pi_2(\omega \otimes \omega) + \cdots)L\omega + BL\omega. \end{aligned} \tag{3.7}$$

The equations in (3.6) can be obtained by matching the powers of $\omega^{(i)}$, $i = 1, 2, \cdots$. In particular, considering the linear terms in ω, it is easy to see that Π_1 must satisfy the Sylvester equation

$$A\Pi_1 + BL = \Pi_1 S. \tag{3.8}$$

Considering now the terms in $\omega \otimes \omega$, we have that

$$A\Pi_2(\omega \otimes \omega) + H(\Pi_1\omega) \otimes (\Pi_1\omega) + N(\Pi_1\omega)L\omega = \frac{\partial(\Pi_2(\omega \otimes \omega))}{\partial \omega} S\omega. \tag{3.9}$$

Applying the properties P1) and P3), and condition (iii) of Lemma 3, yields

$$\begin{aligned} &A\Pi_2(\omega\otimes\omega)+H(\Pi_1\otimes\Pi_1)(\omega\otimes\omega)+N(\Pi_1\otimes L)(\omega\otimes\omega)\\ &=\Pi_2\frac{\partial((\omega\otimes\omega))}{\partial\omega}S\omega=\Pi_2(S\oplus S)(\omega\otimes\omega), \end{aligned} \tag{3.10}$$

and it follows that Π_2 is the solution of the Sylvester-like equation

$$A\Pi_2+H(\Pi_1\otimes\Pi_1)+N(\Pi_1\otimes L)=\Pi_2(S\oplus S). \tag{3.11}$$

Following the same reasoning, it can be shown that Π_i, for $i\geq 3$, are solutions of

$$A\Pi_i+H\left(\Pi_1\otimes\Pi_{i-1}+\Pi_2\otimes\Pi_{i-2}+\cdots+\Pi_{i-1}\otimes\Pi_1\right)+(N\Pi_{i-1})\otimes L=\Pi_i S^{[i]}. \tag{3.12}$$

□

Remark 2. Theorem 4 is inspired and follows a similar approach to the derivations in [116, Chapter 4] for the problem of output regulation.

From a practical point of view, it is useful to define an approximate version of the (direct) moment which uses a finite number of terms Π_i, $i=1,2,\cdots,k$.

Definition 6. We call $C\bar{\pi}_k(\omega)=C\sum_{i=1}^{k}\Pi_i\omega^{(i)}$ the k-th approximate (direct) moment of system (3.1) at (S,L).

Note that if the convergence radius of (3.4) is positive, then (3.4) is an exact solution of (3.5) in power form and the k-th approximate moment of system (3.1) is such that

$$\lim_{k\to\infty} C\bar{\pi}_k(\omega)-C\pi(\omega)=0. \tag{3.13}$$

3.2 A First family of reduced-order models

In this section, we introduce a family of reduced-order models which has the same quadratic-bilinear form as the original system, namely

$$\begin{aligned} \dot{\xi} &= F\xi + G(\xi \otimes \xi) + M\xi u + Eu, \\ \psi &= \sum_{i \geq 1} D_i \xi^{(i)}, \end{aligned} \tag{3.14}$$

where $F \in \mathbb{R}^{v \times v}$, $M \in \mathbb{R}^{v \times v}$, $G \in \mathbb{R}^{v \times v^2}$, $E \in \mathbb{R}^v$ and $D_i^\top \in \mathbb{R}^{v^i}$. In the following statement we give conditions on F, Π_i, E and D_i such that (3.14) is indeed a reduced-order model by moment matching of (3.1).

Theorem 5. Consider the system (3.1), the signal generator (3.2), the model (3.14) and suppose that Assumptions 13 and 14 hold. System (3.14) is a reduced-order model by moment matching of system (3.1) at (S, L) if $v < n$ and the following equations hold

$$\begin{aligned} C\Pi_1 &= D_1 P_{(1,1)}, \\ C\Pi_i &= D_1 P_{(i,1)} + D_2 P_{(i,2)} + \cdots + D_{i-1} P_{(i,i-1)} + D_i P_{(i,i)}, \end{aligned} \tag{3.15}$$

for all $i > 1$, where

$$P_{(i,j)} = \begin{cases} P_i, & j = 1, \\ \sum_{k=1}^{i-j+1} P_k \otimes P_{(i-k,j-1)}, & j \geq 2, \end{cases} \tag{3.16}$$

for $i \geq 1$, $j \leq i$, and P_i are the solutions to the equations

$$\begin{aligned} P_1 S &= F P_1 + E L, \\ P_2 S^{[2]} &= F P_2 + G(P_1 \otimes P_1) + M(P_1 \otimes L), \\ P_i S^{[i]} &= F P_i + G(P_1 \otimes P_{i-1} + P_2 \otimes P_{i-2} + \cdots + P_{i-1} \otimes P_1) + M(P_{i-1} \otimes L), \end{aligned} \tag{3.17}$$

for $i \geq 3$.

Proof. To match the moment of the systems (3.14) and (3.1) at (S, L), there must exist a

mapping $p(\cdot)$ solving

$$\frac{\partial p(\omega)}{\partial \omega} S\omega = Fp(\omega) + G(p(\omega) \otimes p(\omega)) + Mp(\omega)(L\omega) + EL\omega. \tag{3.18}$$

Similar to the proof of Theorem 4, considering the formal power series

$$p(\omega) = \sum_{i \geq 1} P_i \omega^{(i)}, \tag{3.19}$$

yields the system of equations (3.17). Recall that p must also solve (2.10), which in this case becomes

$$C \sum_{i \geq 1} \Pi_i \omega^{(i)} = \sum_{i \geq 1} D_i P_i \omega^{(i)}. \tag{3.20}$$

This equation yields

$$\begin{aligned}
&C\Pi_1\omega + C\Pi_2(\omega \otimes \omega) + C\Pi_3(\omega \otimes \omega \otimes \omega) + \cdots \\
&= D_1P_1\omega + (D_1P_2 + D_2(P_1 \otimes P_1))(\omega \otimes \omega) + (D_3P_1 + D_2(P_1 \otimes P_2 + P_2 \otimes P_1) \\
&\quad + D_3(P_1 \otimes P_1 \otimes P_1))(\omega \otimes \omega \otimes \omega) + \cdots \\
&= D_1P_{(1,1)}\omega + (D_1P_{(2,1)} + D_2P_{(2,2)})(\omega \otimes \omega) + (D_3P_{(3,1)} + D_2P_{(3,2)} + D_3P_{(3,3)})(\omega \otimes \omega \otimes \omega) + \cdots .
\end{aligned} \tag{3.21}$$

By matching the power of $\omega^{(i)}$, the above implies that

$$C\Pi_i\omega^{(i)} = (D_1P_{(i,1)} + D_2P_{(i,2)} + \cdots + D_{i-1}P_{(i,i-1)} + D_iP_{(i,i)})\omega^{(i)} \tag{3.22}$$

which provides (3.15). Here, $P_{(i,j)}$ represents the coefficient matrix of $\omega^{(i)}$ corresponding to D_j. Then, it is easy to verify that $P_{(i,1)} = P_i$. Moreover, for $2 \leq j \leq i$

$$\begin{aligned}
P_{(i,j)}\omega^{(i)} &= (P_1\omega) \otimes (P_{(i-1,j-1)}\omega^{(i-1)}) + \cdots + (P_{(i-j+1)}\omega^{(i-j+1)}) \otimes (P_{(j-1,j-1)}\omega^{(j-1)}) \\
&= (P_1 \otimes P_{(i-1,j-1)} + P_2 \otimes P_{(i-2,j-1)} + \cdots + P_{(i-j+1)} \otimes P_{(j-1,j-1)})\omega^{(i)} \\
&= \left(\sum_{k=1}^{i-j+1} P_k \otimes P_{(i-k,j-1)} \right) \omega^{(i)},
\end{aligned} \tag{3.23}$$

which yields (3.16). This completes the proof. □

We now show that the equations in Theorem 5 can be simplified. In fact, note that selecting $P_1 = I_v$, yields

$$F = S - EL, \tag{3.24}$$

and from equation (3.16), when $i = j$,

$$P_{(i,i)} = I_{v^i} \tag{3.25}$$

for all $i \geq 1$. Now select any G and M, and determine $P_{(i,j)}$ from (3.16) by solving (3.17). It follows that the D_i's are determined by

$$\begin{aligned} D_1 &= C\Pi_1, \\ D_2 &= C\Pi_2 - D_1 P_{(2,1)}, \\ D_i &= C\Pi_i - D_1 P_{(i,1)} - D_2 P_{(i,2)} + \cdots - D_{i-1} P_{(i,i-1)}, \end{aligned} \tag{3.26}$$

for $i \geq 3$. Then, a family of reduced-order models of system (3.1) that match the k-th approximate moment is given by

$$\begin{aligned} \dot{\xi}(t) &= (S - EL)\xi(t) + G(\xi(t) \otimes \xi(t)) + M\xi(t)u(t) + Eu(t), \\ \bar{\psi}(t) &= \sum_{i=1}^{k} D_i \xi^{(i)}(t), \end{aligned} \tag{3.27}$$

where E, G and M are free parameters that can be used to impose additional properties on the model and the D_i's are selected as in (3.26) (computed for the specific selection of E, G and M from (3.16), (3.17), (3.24) and (3.25). For instance, in the next result we show how to ensure that the origin of (3.27) is an asymptotically stable equilibrium.

Theorem 6. Let $F = S - EL \in \mathbb{R}^{v \times v}$ and assume $F + F^\top$ is Hurwitz. Then there exist α and R such that

$$(F + \alpha I)^\top + (F + \alpha I) + R = 0, \tag{3.28}$$

with R a symmetric positive semidefinite matrix and $\alpha \in [0, \eta(F))$, where $\eta(F)$ represents the spectral abscissa of F. Then, $\xi^* = 0$ is a locally asymptotically stable equilibrium of system (3.27) of domain $\mathcal{B}_{(0,\bar{r})}$, with $\bar{r} = \frac{\lambda_{\min}(R)}{2\|G\|} + \frac{\alpha}{\|G\|}$.

Proof. First, we define the candidate Lyapunov function $V(\xi) = \xi^\top \xi$ which is positive definite. Since $F + F^\top$ is Hurwitz, (3.28) follows trivially and

$$F^\top + F = -R - 2\alpha I. \tag{3.29}$$

For $\xi \in \mathcal{B}_{(0,\bar{r})} \backslash \{0\}$, this implies that

$$\|\xi\| < \frac{\lambda_{\min}(R)}{2\|G\|} + \frac{\alpha}{\|G\|} \leq \frac{\xi^\top R \xi}{\xi^\top \xi} \cdot \frac{1}{2\|G\|} + \frac{\alpha}{\|G\|}. \tag{3.30}$$

Combining (3.29) and (3.30), we have

$$2\xi^\top G(\xi \otimes \xi) \leq 2\|G\|\|\xi\|^3 < \xi^\top R \xi + 2\alpha \xi^\top \xi. \tag{3.31}$$

Then, for $\xi \in \mathcal{B}_{(0,r)} \backslash \{0\}$

$$\begin{aligned} \dot{V}(\xi) &= \dot{\xi}^\top \xi + \xi^\top \dot{\xi} \\ &= \xi^\top (F^\top + F)\xi + (\xi \otimes \xi)^\top G^\top \xi + \xi^\top G(\xi \otimes \xi) \\ &= -\xi^\top (R + 2\alpha I)\xi + 2\xi^\top G(\xi \otimes \xi) < 0, \end{aligned} \tag{3.32}$$

and local asymptotic stability of the origin of the system (3.27) follows. □

Theorem 6 implies that we can design the eigenvalues of F by selecting the matrix E to guarantee that the reduced-order model inherits a certain property (i.e. local asymptotic stability of the origin) of the original system. In addition, the region of stability of the reduced-order model can be enlarged by selecting a matrix E that produces larger values of α and $\lambda_{\min}(R)$, or by selecting a matrix G with a small norm. The matrix M can then be used to assign some further properties of the reduced-order model.

3.3 A Second family of reduced-order models

The family of reduced-order models (3.27) that we have introduced in Section 3.2 has the same structure as the original quadratic-bilinear system (3.1). However, the output mapping is quite complicated. This causes some difficulties when we wish to assign the relative degree of the reduced-order model. In fact, one can show that it is impossible to assign the relative degree of models (3.27). To overcome this difficulty, we propose an alternative family of reduced-order models.

Consider now a different class of reduced-order models of the form

$$\begin{aligned} \dot{\xi} &= \sum_{i\geq 1} F_i \xi^{(i)} + \sum_{i\geq 1} M_i \xi^{(i)} u + Eu, \\ \psi &= D\xi, \end{aligned} \tag{3.33}$$

where $F_i \in \mathbb{R}^{v\times v^i}$, $M_i \in \mathbb{R}^{v\times v^i}$ and $D^\top \in \mathbb{R}^v$. We now give conditions on F_i, M_i, E and D such that (3.33) is a reduced-order model by moment matching of (3.1).

Theorem 7. Consider the system (3.1), the signal generator (3.2), the model (3.33) and suppose Assumptions 13 and 14 hold. System (3.33) is a reduced model by moment matching of system (3.1) at (S, L) if $v < n$ and the following equations hold

$$C\Pi_i = DP_i, \tag{3.34}$$

for all $i \geq 1$, where the P_i's solve the equations

$$\begin{aligned} P_1 S &= F_1 P_{(1,1)} + EL, \\ P_2 S^{[2]} &= F_1 P_{(2,1)} + F_2 P_{(2,2)} + (M_1 P_{(1,1)}) \otimes L, \\ P_i S^{[i]} &= F_1 P_{(i,1)} + F_2 P_{(i,2)} + \cdots + F_i P_{(i,i)} + (M_1 P_{(i-1,1)} + M_2 P_{(i-1,2)} + \cdots + M_{i-1} P_{(i-1,i-1)}) \otimes L, \end{aligned} \tag{3.35}$$

for $i \geq 3$, where the $P_{(i,j)}$'s are defined in (3.16).

Proof. The proof follows steps similar to the proof of Theorem 5, hence it is omitted. □

In the same way as we proceeded for the first family of reduced-order models, we now determine a simplified parametrization. Let $P_1 = I_v$. This yields

$$D = C\Pi_1 \tag{3.36}$$

and, from equation (3.16), when $i = j$,

$$P_{(i,i)} = I_{v^i}, \tag{3.37}$$

for all $i \geq 1$. The other P_i, with $i \geq 1$, are determined as full-rank solutions of (3.34). Thus,

$$\begin{aligned} F_1 =& S - EL, \\ F_2 =& P_2 S^{[2]} - (M_1 P_{(1,1)}) \otimes L - F_1 P_{(2,1)}, \\ F_i =& P_i S^{[i]} - F_1 P_{(i,1)} - F_2 P_{(i,2)} - \cdots - F_{i-1} P_{(i,i-1)} - \\ & (M_1 P_{(i-1,1)} + M_2 P_{(i-1,2)} + \cdots + M_{i-1} P_{(i-1,i-1)}) \otimes L \end{aligned} \tag{3.38}$$

for $i \geq 3$.

By matching the k-th approximate moment of system (3.1) and system (3.33), a new class of reduced-order models of system (3.1) can be obtained as

$$\begin{aligned} \dot{\xi}(t) &= \sum_{i=1}^{k} F_i \xi^{(i)} + \sum_{i=1}^{k-1} M_i \xi^{(i)} u(t) + E u(t), \\ \bar{\psi}(t) &= D\xi(t), \end{aligned} \tag{3.39}$$

where the matrices F_i are selected as in (3.38) and D is chosen as in (3.36). Note that we still have k free matrices M_i and E which can be used to assign some specific properties of the reduced-order model.

3.3.1 Asymptotic Stability

Consider the problem of achieving order reduction by moment matching with a reduced-order model described by equations of the form (3.39), such that $\xi^* = 0$ is a locally asymptotically stable equilibrium point. A solution to this problem is provided in the following statement.

Theorem 8. Let $F_1 = S - EL \in \mathbb{R}^{v\times v}$ and assume $F_1 + F_1^\top$ is Hurwitz. Then there exist α and R such that

$$(F_1 + \alpha I)^\top + (F_1 + \alpha I) + R = 0, \tag{3.40}$$

with R a symmetric positive semidefinite matrix and $\alpha \in [0, \eta(F_1))$, where $\eta(F_1)$ represents the spectral abscissa of F_1. Then, $\xi^* = 0$ is a locally asymptotically stable equilibrium of system (3.39) in the region $\mathcal{B}_{(0,\bar{r})}$ with

$$\bar{r} = \min\left(\sqrt[i]{\frac{\lambda_{\min}(R)}{2(k-1)\|F_{i+1}\|} + \frac{\alpha}{(k-1)\|F_{i+1}\|}}\right),$$

where $i = 1, \cdots, k-1$.

Proof. Define the candidate Lyapunov function $V(\xi) = \xi^\top\xi$, which is positive definite. According to (3.40), we have

$$F_1^\top + F_1 = -R - 2\alpha I. \tag{3.41}$$

For $\xi \in \mathcal{B}_{(0,\bar{r})}\backslash\{0\}$, this implies that

$$\|\xi\|^i < \frac{\lambda_{\min}(R)}{2(k-1)\|F_{i+1}\|} + \frac{\alpha}{(k-1)\|F_{i+1}\|} \leq \frac{\xi^\top R\xi}{\xi^\top\xi}\cdot\frac{1}{2(k-1)\|F_{i+1}\|} + \frac{\alpha}{(k-1)\|F_{i+1}\|}, \tag{3.42}$$

where $i = 1, \cdots, k-1$.

Combining (3.41) and (3.42), we have

$$2\xi^\top F_{i+1}\xi^{(i)} \leq 2\|F_{i+1}\|\|\xi\|^i < \frac{\xi^\top R\xi + 2\alpha\xi^\top\xi}{k-1}. \tag{3.43}$$

Then, for $\xi \in \mathcal{B}_{(0,\bar{r})} \backslash \{0\}$,

$$\begin{aligned} &2\xi^\top F_2(\xi \otimes \xi) + 2\xi^\top F_3(\xi \otimes \xi \otimes \xi) + \cdots + 2\xi^\top F_k \xi^{(k-1)} \\ &< (k-1)\frac{\xi^\top R\xi + 2\alpha\xi^\top \xi}{k-1} = \xi^\top R\xi + 2\alpha\xi^\top \xi. \end{aligned} \tag{3.44}$$

Finally,

$$\begin{aligned} \dot{V}(\xi) &= \dot{\xi}^\top \xi + \xi^\top \dot{\xi} \\ &= \xi^\top (F_1^\top + F_1)\xi + 2\xi^\top F_2(\xi \otimes \xi) + 2\xi^\top F_3(\xi \otimes \xi \otimes \xi) + \cdots + 2\xi^\top F_k \xi^{(k-1)} \\ &= -\xi^\top (R + 2\alpha I)\xi + \xi^\top (R + 2\alpha I)\xi < 0 \end{aligned} \tag{3.45}$$

holds and local asymptotic stability of the origin follows. □

3.3.2 Relative Degree

Consider the problem of selecting the free matrices M_i in system (3.39) such that the reduced order model has a given relative degree $r \geq 1$ at $\bar{\xi} = 0$.

Theorem 9. Let $M_0 = E$, then system (3.39) has relative degree $r \geq 1$, at $\bar{\xi}$ if the following equations hold for all $i \in [0, k-1]$

$$\begin{aligned} &DM_i = 0, \\ &D\sum_{j=1}^{i+1} F_{(1,j)} M_{i-j+1}^{[j]} = 0, \\ &\quad\vdots \\ &D\sum_{j=1}^{i+1} F_{(r-2,j)} M_{i-j+1}^{[j]} = 0, \end{aligned} \tag{3.46}$$

and

$$D\sum_{l=0}^{k-1}\sum_{j=1}^{l+1} F_{(r-1,j)} M_{l-j+1}^{[j]} \bar{\xi}_0^{(l)} \neq 0, \tag{3.47}$$

where

$$F_{(i,j)} = \begin{cases} F_j, & i = 1, \\ \sum_{l=1}^{j} F_{(i-1,l)} F_{j+1-l}^{[l]}, & 2 \le i \le k-1. \end{cases}$$

Proof. Consider a general nonlinear systems of the form

$$\begin{aligned} \dot{x} &= f(x) + g(x)u, \\ y &= h(x). \end{aligned} \tag{3.48}$$

By definition, its relative degree is r at $\bar{x}$ if

$$L_g h(x) = L_g L_f h(x) = \cdots = L_g L_f^{r-2} h(x) = 0, \tag{3.49}$$

for all x in some neighborhood of $x = \bar{x}$ and

$$L_g L_f^{r-1} h(\bar{x}) \neq 0. \tag{3.50}$$

For system (3.39), $f(\xi) = \sum_{i=1}^{k} F_i \xi^{(i)}$, $g(\xi) = \sum_{i=0}^{k-1} M_i \xi^{(i)}$ (recall that $M_0 \xi^{(0)} = E$) and $h(\xi) = D\xi$. By replacing these into (3.49) and (3.50), we obtain (3.46) and (3.47) directly by matching the coefficients of the same powers of $\xi^{(i)}$, $i = 0, 1, \cdots, k-1$.

□

Note that, while for the second family we can assign the relative degree, the resulting system dynamics is more complex than for the first family. In particular, the second family is a general polynomial system, as opposed to a quadratic-bilinear system.

3.4 Simulation Results

We now illustrate the results of this section by means of a numerical example. Consider the system (3.1) with $n = 106$, where $A = \text{diag}(A_1, A_2, A_3, A_4)$, with

$$A_1 = \mathrm{diag}(-1, -2, \cdots, -100), \quad A_2 = \begin{bmatrix} -1 & 5 \\ -5 & -1 \end{bmatrix},$$

$$A_3 = \begin{bmatrix} -1 & 10 \\ -10 & -1 \end{bmatrix}, \qquad A_4 = \begin{bmatrix} -1 & 15 \\ -15 & -1 \end{bmatrix},$$

$B^\top = C = \begin{bmatrix} 1 & 1 & 0 & \cdots & 0 & 1 & 1 \end{bmatrix}$ and the remaining matrices H and N generated randomly. We wish to obtain a reduced-order model of order $v = 7$. The signal generator (3.2) has been selected with $S = \mathrm{diag}(0, S_2, S_3, S_4)$, with $S_2 = A_2 + I_2$, $S_3 = A_3 + I_2$, $S_4 = A_4 + I_2$, and $L = \begin{bmatrix} 1 & 1 & 0 & 1 & 0 & 1 & 0 \end{bmatrix}$. For both the first and the second family of reduced-order models, the matrix E has been selected as

$$E^\top = \begin{bmatrix} 84.4 & 4.7 & 32.8 & -0.5 & 16.8 & -2.6 & 10.8 \end{bmatrix},$$

so that the eigenvalues of F (F_1 in the second family) is a subset of the spectrum of A. As we do not have any other property to assign in this simulation, all the other free matrices in the reduced-order models are randomly generated.

In the simulation, we obtain reduced-order models which matches the k-th approximate moment for $k = 1$, 2 and 3. We plot the time histories of the outputs of the first family of reduced-order models in Figure 3.1 and of the second family of reduced-order models in Figure 3.2. Both the output response and the error between the reduced-order models and the original system are displayed. The black (solid) line indicates the output of the original model, while the yellow (dashed), blue (dotted) and red (dash-dotted) lines indicate the output of the reduced-order model, when $k = 1, 2$ and 3, respectively.

As shown in the figures, both families of reduced-order models provide good approximations of the output response. When the order of the approximate moment k increases, the accuracy of the approximation improves as well, i.e. the error becomes smaller.

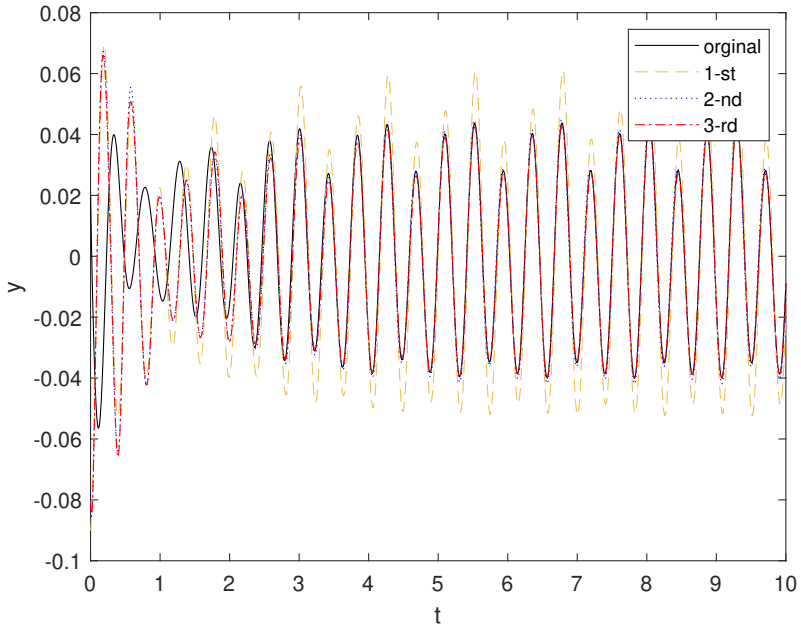

(a) Time histories of the output of the original model (black/solid) and of the reduced-order model when k =1 (yellow/dashed), k =2 (blue/dotted) and k =3 (red/dash-dotted).

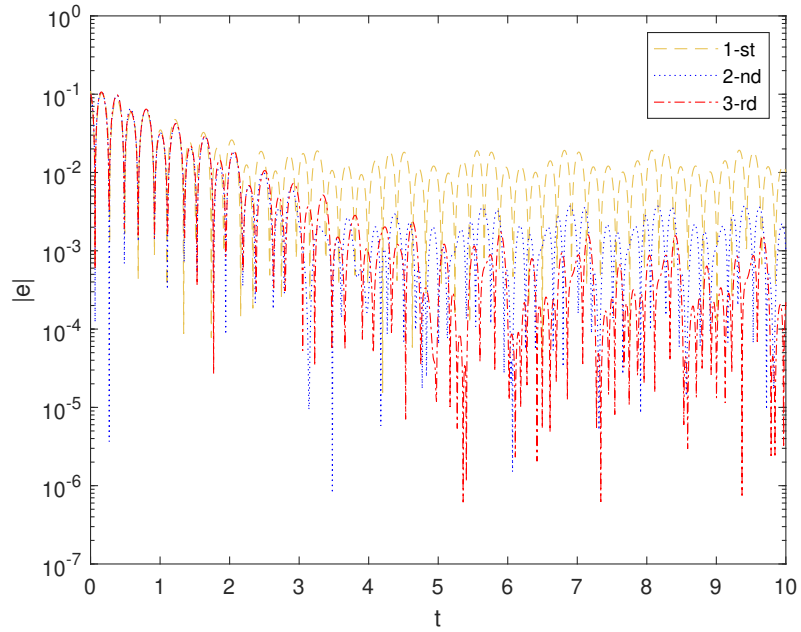

(b) Time histories of the errors between the original and the reduced-order model when k =1 (yellow/dashed), k =2 (blue/dotted) and k =3 (red/dash-dotted).

Figure 3.1: Output response of the first family of reduced-order models.

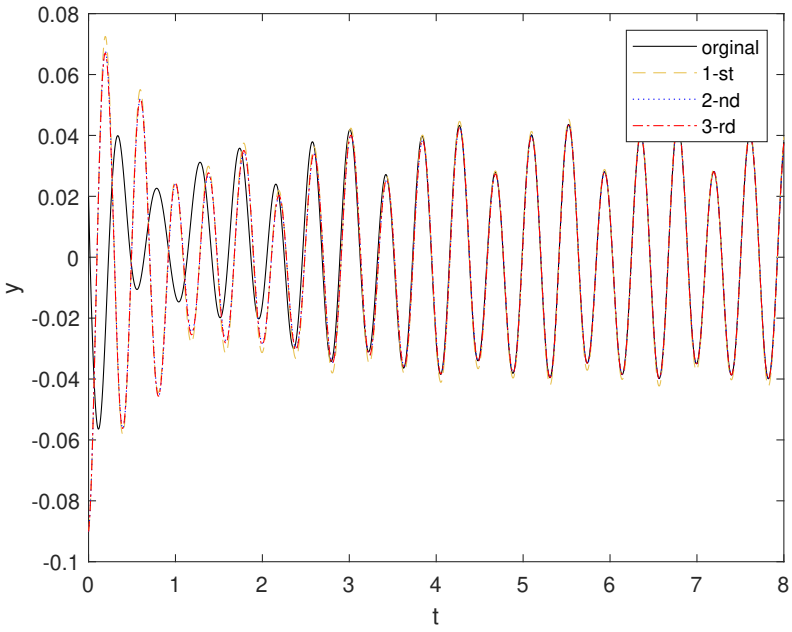

(a) Time histories of the output of the original model (black/solid) and of the reduced-order model when k =1 (yellow/dashed), k =2 (blue/dotted) and k =3 (red/dash-dotted).

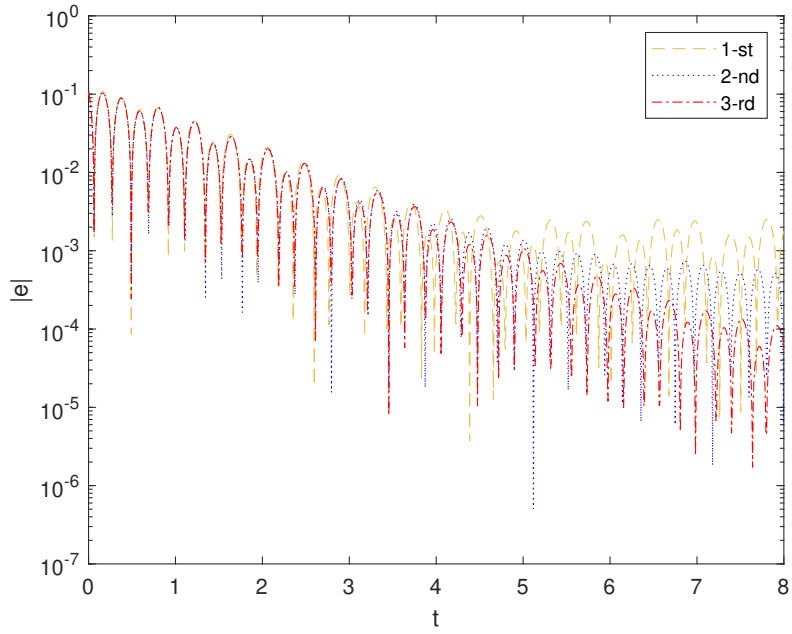

(b) Time histories of the errors between the original and the reduced-order model when k =1 (yellow/dashed), 2 (blue/dotted) and 3 (red/dash-dotted).

Figure 3.2: Output response of the second family of reduced-order models.

Chapter 4

Interconnection-based Model Order Reduction for Navier-Stokes Type Quadratic-bilinear Systems

In this chapter our focus is on addressing the model order reduction problem for single-input Navier–Stokes type quadratic-bilinear systems [104]. These systems are directly formulated from the Navier–Stokes equations, utilizing the vorticity-stream form [8]. Our primary objective is to develop and apply interconnection-based moment matching methods specifically tailored for the model order reduction of incompressible flows, demonstrating their effectiveness in fluid scenarios.

The structure of this chapter is as follows. In Section 4.1 we define the nonlinear moments for Navier-Stokes type quadratic-bilinear systems and provide both model-based and data-driven implementations for computing these moments. Section 4.2 is dedicated to developing a family of reduced-order models that emphasize stability. Finally, in Section 4.3 we demonstrate the proposed methods on three applications: the 1D Burgers' equation, the lid-driven cavity, and the lid-driven polar cavity.

4.1 Nonlinear moments for Navier-Stokes DAEs

In this section we provide methods to compute the nonlinear moments for a class of Navier-Stokes DAEs. In Section 4.1.1 we present a model-based method, whereas in Section 4.1.2 we present a data-driven method.

4.1.1 Model-based approach

Consider the Navier-Stokes type quadratic-bilinear DAEs (see [2]), with vorticity ϵ and stream function ζ, described by the followings

$$\begin{aligned} \dot{\epsilon} =& A_{11}\epsilon + A_{12}\zeta + H_1(\epsilon \otimes \zeta) + H_2(\zeta \otimes \zeta) + N_2\zeta u + B_1 u, \\ 0 =& \epsilon + A_{22}\zeta, \\ y =& C_2\zeta, \quad \epsilon(0) = \zeta(0) = 0, \end{aligned} \tag{4.1}$$

where $A_{11}, A_{12}, A_{22}, N_2 \in \mathbb{R}^{n\times n}$, $H_1, H_2 \in \mathbb{R}^{n\times n^2}$, $B_1, C_2^\top \in \mathbb{R}^n$, ϵ and $\zeta \in \mathbb{R}^n$. $u(t) \in \mathbb{R}$ is the external input and $y(t) \in \mathbb{R}$ is the output.

System (4.1) can be rewritten in the form

$$\begin{aligned} E\dot{x}(t) =& Ax(t) + H(x(t) \otimes x(t)) + Nx(t)u(t) + Bu(t), \\ y(t) =& Cx(t), \quad x(0) = 0, \end{aligned} \tag{4.2}$$

where $x(t) = [\epsilon \quad \zeta]^\top \in \mathbb{R}^{2n}$ is the state vector, and

$$E = \begin{bmatrix} I_n & 0 \\ 0 & 0 \end{bmatrix}, \quad A = \begin{bmatrix} A_{11} & A_{12} \\ I_n & A_{22} \end{bmatrix}, \quad N = \begin{bmatrix} 0 & N_2 \\ 0 & 0 \end{bmatrix} \in \mathbb{R}^{2n\times 2n},$$

$$B = [B_1 \quad 0]^\top \in \mathbb{R}^{2n}, \quad C^\top = [0 \quad C_2]^\top \in \mathbb{R}^{2n}.$$

$H \in \mathbb{R}^{2n\times 4n^2}$ is obtained as follows. H_1 and H_2 can be divided into n square matrices, namely

$$H_1 = \begin{bmatrix} H_{11} & H_{12} & \cdots & H_{1n} \end{bmatrix}$$

$$H_2 = \begin{bmatrix} H_{21} & H_{22} & \cdots & H_{2n} \end{bmatrix}.$$

Then $H = \begin{bmatrix} \widetilde{H_1} & \widetilde{H_2} \\ 0_{n\times n^2} & 0_{n\times n^2} \end{bmatrix}$ where

$$\widetilde{H_1} = \begin{bmatrix} 0_n & H_{11} & 0_n & H_{12} & \cdots & 0_n & H_{1n} \end{bmatrix}$$

and

$$\widetilde{H_2} = \begin{bmatrix} 0_n & H_{21} & 0_n & H_{22} & \cdots & 0_n & H_{2n} \end{bmatrix}.$$

Consider now a signal generator described by the equations

$$\dot{\omega} = S\omega, \quad \theta = L\omega, \tag{4.3}$$

with $\omega(t) \in \mathbb{R}^\nu$, and $S \in \mathbb{R}^{\nu\times\nu}$ and the interconnected system

$$\begin{gathered} \dot{\omega} = S\omega, \quad E\dot{x} = Ax + H(x\otimes x) + Nxu + BL\omega, \\ y = Cx, \end{gathered} \tag{4.4}$$

Note that for the signal generator (4.3), Assumption 10 reduces to its linear version, namely the pair (S, L) is observable and the eigenvalues of S are simple and belong to $\mathbb{C}_0$. We now present a result that provides a way of computing the nonlinear moment of (4.2) through this system interconnection.

Theorem 10. Consider the system (4.2), the signal generator (4.3) and suppose that Assumptions 8, 9 and 10 hold. Then there is a mapping

$$\pi(\omega) = \sum_{i=1}^{+\infty} \Pi_i \omega^{(i)}. \tag{4.5}$$

which formally solves the partial differential equation

$$E\frac{\partial \pi}{\partial \omega}S\omega = A\pi(\omega) + H(\pi(\omega)\otimes\pi(\omega)) + N\pi(\omega)L\omega + BL\omega, \tag{4.6}$$

where the Π_i's solve the infinite-dimensional system of Sylvester-like equations

$$\begin{aligned} E\Pi_1 S &= A\Pi_1 + BL, \\ E\Pi_2 S^{[2]} &= A\Pi_2 + H(\Pi_1\otimes\Pi_1) + N(\Pi_1\otimes L), \\ E\Pi_i S^{[i]} &= A\Pi_i + H(\Pi_1\otimes\Pi_{i-1} + \Pi_2\otimes\Pi_{i-2} \\ &\quad + \cdots + \Pi_{i-1}\otimes\Pi_1) + N(\Pi_{i-1}\otimes L), \end{aligned} \tag{4.7}$$

for $i \geq 3$.

Proof. By Assumptions 8, 9 and 10 and Lemma 1, equation (4.6) has a solution π defined around $\omega = 0$. Consider the formal power series expansion of π, namely (4.5). Substituting (4.5) into (4.6) yields

$$\begin{aligned} E\frac{\partial(\Pi_1\omega+\Pi_2(\omega\otimes\omega)+\cdots)}{\partial\omega}S\omega &= A(\Pi_1\omega + \Pi_2(\omega\otimes\omega) + \cdots) \\ &+ H(\Pi_1\omega + \Pi_2(\omega\otimes\omega)+\cdots)\otimes(\Pi_1\omega + \Pi_2(\omega\otimes\omega) + \cdots) \\ &+ N(\Pi_1\omega + \Pi_2(\omega\otimes\omega) + \cdots)L\omega + BL\omega. \end{aligned} \tag{4.8}$$

The equations (4.7) can then be obtained by matching the powers of $\omega^{(i)}$, $i = 1, 2, \cdots$. In particular, considering the linear terms in ω, it is easy to see that Π_1 must satisfy the Sylvester-like equation

$$E\Pi_1 S = A\Pi_1 + BL. \tag{4.9}$$

Considering now the terms in $\omega\otimes\omega$, we have that

$$E\frac{\partial(\Pi_2(\omega\otimes\omega))}{\partial\omega}S\omega = A\Pi_2(\omega\otimes\omega) + H(\Pi_1\omega)\otimes(\Pi_1\omega) + N(\Pi_1\omega)L\omega. \tag{4.10}$$

Applying the properties P1) and P3), and condition (iii) of Lemma 3, yields

$$\begin{aligned} E\Pi_2\frac{\partial((\omega\otimes\omega))}{\partial\omega}S\omega &= E\Pi_2(S\oplus S)(\omega\otimes\omega)\\ =&A\Pi_2(\omega\otimes\omega)+H(\Pi_1\otimes\Pi_1)(\omega\otimes\omega)\\ &+N(\Pi_1\otimes L)(\omega\otimes\omega) \end{aligned} \tag{4.11}$$

and it follows that Π_2 is the solution of the Sylvester-like equation

$$E\Pi_2(S\oplus S)=A\Pi_2+H(\Pi_1\otimes\Pi_1)+N(\Pi_1\otimes L). \tag{4.12}$$

Following the same reasoning, it can be shown that Π_i, for $i\geq 3$, are solutions of

$$E\Pi_i S^{[i]}=A\Pi_i+H(\Pi_1\otimes\Pi_{i-1}+\Pi_2\otimes\Pi_{i-2}+\cdots+\Pi_{i-1}\otimes\Pi_1)+(N\Pi_{i-1})\otimes L. \tag{4.13}$$

□

Remark 3. The conditions $\sigma(S)\in\mathbb{C}_0$ and $\sigma(A)\in\mathbb{C}_{<0}$ imply that equations (4.7) have unique solution that can be computed by solving the linear equations

$$\begin{aligned} (S^\top\otimes E-I_\nu\otimes A)\mathrm{vec}(\Pi_1)&=\mathrm{vec}(BL),\\ ((S\oplus S)^\top\otimes E-I_{\nu^2}\otimes A)\mathrm{vec}(\Pi_2)&=\mathrm{vec}\big(H(\Pi_1\otimes\Pi_1)+N(\Pi_1\otimes L)\big),\\ (S^{[i]\top}\otimes E-I_{\nu^i}\otimes A)\mathrm{vec}(\Pi_i)&=\mathrm{vec}\big(H(\Pi_1\otimes\Pi_{i-1}+\Pi_2\otimes\Pi_{i-2}+\cdots+\Pi_{i-1}\otimes\Pi_1)+N(\Pi_{i-1}\otimes L)\big), \end{aligned} \tag{4.14}$$

for $i\geq 3$ [118].

The matrices in system (4.2), derived from the discretization of the Navier-Stokes equations, have special structures as shown above. We will demonstrate that, by exploiting the structure of these matrices, together with the assumption that A_{22} is invertible (which holds in practice), the equations in Theorem 10 can be simplified.

Note, in fact, that rewriting the first equation of (4.7) with block matrices, we obtain

$$\begin{bmatrix} I_n & 0 \\ 0 & 0 \end{bmatrix} \begin{bmatrix} \Pi_{1a} \\ \Pi_{1b} \end{bmatrix} S = \begin{bmatrix} A_{11} & A_{12} \\ I_n & A_{22} \end{bmatrix} \begin{bmatrix} \Pi_{1a} \\ \Pi_{1b} \end{bmatrix} + \begin{bmatrix} B_1 \\ 0 \end{bmatrix} L. \tag{4.15}$$

Let $A_p := A_{11} - A_{12}A_{22}^{-1}$. This yields

$$\begin{aligned} \Pi_{1a} S &= A_p \Pi_{1a} + B_1 L, \\ \Pi_{1b} &= -A_{22}^{-1} \Pi_{1a}. \end{aligned} \tag{4.16}$$

Similar to (4.15), defining

$$Q_2 := \begin{bmatrix} Q_{2a} \\ Q_{2b} \end{bmatrix} = H(\Pi_1 \otimes \Pi_1) + N(\Pi_1 \otimes L) \quad \text{and} \quad \Pi_2 := \begin{bmatrix} \Pi_{2a} \\ \Pi_{2b} \end{bmatrix}$$

yields $Q_{2b} = 0$ and

$$\begin{aligned} \Pi_{2a} S^{[2]} &= A_p \Pi_{2a} + Q_{2a}, \\ \Pi_{2b} &= -A_{22}^{-1} \Pi_{2a}. \end{aligned} \tag{4.17}$$

Following the same reasoning, define

$$Q_i := \begin{bmatrix} Q_{ia} \\ 0 \end{bmatrix} = H(\Pi_1 \otimes \Pi_{i-1} + \Pi_2 \otimes \Pi_{i-2} + \cdots + \Pi_{i-1} \otimes \Pi_1) + N(\Pi_{i-1} \otimes L), \tag{4.18}$$

and note that $\Pi_i = \begin{bmatrix} \Pi_{ia} \\ \Pi_{ib} \end{bmatrix}$ with $\Pi_{ib} = -A_{22}^{-1}\Pi_{ia}$ and Π_{ia} the solution of

$$\Pi_{ia} S^{[i]} = A_p \Pi_{ia} + Q_{ia}. \tag{4.19}$$

Note that the resulting equations (4.19) are of dimensions reduced to half of those compared with (4.7). Moreover, (4.19) falls into the form of a standard Sylvester equation which can be solved directly with a variety of methods, e.g., the function *Sylvester* in MATLAB.

Remark 4. The approach presented in Theorem 10 can be directly applied to systems with multiple outputs (i.e. $C_2 \in \mathbb{R}^{m\times n}$ with $m \geq 1$).

From a practical point of view, it is useful to define an approximate version of the moment which uses a finite number of terms Π_i, $i = 1, 2, \cdots, k$.

Definition 7. We call $C\bar{\pi}_k(\omega) = C\sum_{i=1}^{k} \Pi_i \omega^{(i)}$ the k-th approximate moment of system (4.2) at (S, L).

Note that if the convergence radius of (4.5) is positive, then (4.5) is an exact solution of (4.6) in power form and the k-th approximate moment of system (4.2) is such that

$$\lim_{k\to\infty} C\bar{\pi}_k(\omega) - C\pi(\omega) = 0. \tag{4.20}$$

Remark 5. Finding the solutions to the nested Sylvester-like equations (4.7) (or (4.19)) is generally a computationally demanding task: solving the first equation of (4.7) (or (4.19)) has complexity of $\mathcal{O}(\nu^3 n^3)$ and the complexity for the k-th equation grows as $\mathcal{O}(\nu^{3k} n^3)$. The dependence on n^3 significantly degrades the applicability of this computation in some fluid mechanics problems in which spacial discretization gives rise to a large number of ODEs (i.e. an extremely large n).

As mentioned in Remark 5, the model-based approach hinges on the computation of the Π_i's (up to a certain k) that results in major bottleneck in computation. Note, however, that to construct the approximate moment in Definition 7, the information of the matrices $\Pi_1, \ldots, \Pi_k$ is not necessarily required as long as we know the vectors $C\Pi_1, \ldots, C\Pi_k$. Note that the size of $C\Pi_i$ is smaller than the size of Π_i by a factor of n. As a consequence these can be much more efficiently estimated using a data-driven procedure which we introduce in the following subsection.

4.1.2 Data-driven Approach

We now propose a data-driven algorithm inspired by [65] for general nonlinear systems. Different from the model-based approach introduced in the previous section, the data-driven approach proposed here has the advantage of not requiring any other information from the system except for the signal generator (which is selected by the user and, consequently, known) and the output data.

Exploiting the power expansion developed in the previous section, we can write the output of the system as

$$y(t) = C\pi(\omega) + \iota(t) = \sum_{i=1}^{+\infty} C\Pi_i \omega^{(i)} + \iota(t), \tag{4.21}$$

where ι is the transient error, which decays to zero at steady state. Consider the set of polynomial basis function

$$\bar{\Omega} := [\omega \quad \omega^{(2)} \quad \cdots \quad \omega^{(k)} \quad \cdots]^\top. \tag{4.22}$$

The goal is to estimate the coefficients

$$\bar{\Gamma} := [C\Pi_1 \quad C\Pi_2 \quad \cdots \quad C\Pi_i \quad \cdots]. \tag{4.23}$$

However, when $i \geq 2$, we note that $\omega^{(i)}$ contains duplicated terms (e.g. both $\omega_1\omega_2$ and $\omega_2\omega_1$ appears in $\omega^{(2)}$). Thus, without loss of generality, we can introduce the following vector which contains all elements in $\omega^{(i)}$ without repetition, see [116, Chapter 4]. For $\omega = [\omega_1, \omega_2, \cdots, \omega_\nu]^\top$, let $\omega^{\{i\}}$ denotes the vector

$$\omega^{\{i\}} := [\omega_1^i, \omega_1^{i-1}\omega_2, \cdots, \omega_1^{i-1}\omega_\nu, \omega_1^{i-2}\omega_2^2, \omega_1^{i-2}\omega_2\omega_3, \cdots, \omega_1^{i-2}\omega_2\omega_\nu, \cdots, \omega_\nu^i]^\top, \tag{4.24}$$

which contains all monomials of order i. Note that $\omega^{(i)}$ and $\omega^{\{i\}}$ have ν^i and $\frac{\nu(\nu+1)\cdots(\nu+i-1)}{i(i-1)\cdots 1}$ ($\leq \nu^i$) elements, respectively, and that there exists matrices X_i such that

$$\omega^{\{i\}} = X_i \omega^{(i)}. \tag{4.25}$$

For example, when $\nu = 2$,

$$\omega^{(2)} = \begin{bmatrix} \omega_1^2 \\ \omega_1\omega_2 \\ \omega_2\omega_1 \\ \omega_2^2 \end{bmatrix}, \qquad \omega^{\{2\}} = \begin{bmatrix} \omega_1^2 \\ \omega_1\omega_2 \\ \omega_2^2 \end{bmatrix}, \qquad X_2 = \begin{bmatrix} 1 & 0 & 0 & 0 \\ 0 & 1 & 0 & 0 \\ 0 & 0 & 0 & 1 \end{bmatrix}.$$

Using the vector $\omega^{\{i\}}$ defined above, the approximation problem can be rewritten compactly as

$$y(t) \approx C\bar{\pi}_k(\omega) = \sum_{i=1}^{k} \widetilde{C\Pi_i}\omega^{(i)} = \sum_{i=1}^{k} \widetilde{Z}_i X_i \omega^{(i)} = \sum_{i=1}^{k} \widetilde{Z}_i \omega^{\{i\}} = \widetilde{\Gamma}^k \widetilde{\Omega}^k, \tag{4.26}$$

where $\widetilde{\Gamma}^k = [\widetilde{Z}_1 \quad \widetilde{Z}_2 \quad \cdots \quad \widetilde{Z}_k]$ and $\widetilde{\Omega}^k = [\omega \quad \omega^{\{2\}} \quad \cdots \quad \omega^{\{k\}}]^\top$. This approximation neglects the error e resulting by terminating the summation at k, namely $e(t) = \sum_{i>k} C\Pi_i\omega^{(i)}$, and the transient error ι. In this way, we define $\widetilde{\Gamma}_j^k$ as an on-line estimate of the coefficient matrix $\widetilde{\Gamma}^k$ (in (4.26)) using samples collected from time instants T_j^w, namely computed at the time t_j using the last w samples. The computation is given by the following result.

Theorem 11. Define the time-snapshots matrices $\widetilde{U}_j \in \mathbb{R}^{w\times N}$ and $\widetilde{Y}_j \in \mathbb{R}^w$ with, $w \geq N$, as

$$\widetilde{U}_j := [\Omega^k(t_{j-w+1}) \quad \cdots \quad \Omega^k(t_{j-1}) \quad \Omega^k(t_j)]^\top \tag{4.27}$$

and

$$\widetilde{Y}_j := [y(t_{j-w+1}) \quad \cdots \quad y(t_{j-1}) \quad y(t_j)]^\top. \tag{4.28}$$

If $\widetilde{U}_j$ is full column rank, then

$$\mathrm{vec}(\widetilde{\Gamma}_j^k) = (\widetilde{U}_j^\top \widetilde{U}_j)^{-1} \widetilde{U}_j^\top \widetilde{Y}_j, \tag{4.29}$$

and the estimation $\widetilde{C\Pi_i}$ are given as

$$\widetilde{C\Pi_i} = \widetilde{Z}_i X_i, \tag{4.30}$$

for $i = 1, 2, \cdots, k$.

The convergence of the estimated moment is guaranteed by the next result.

Theorem 12. Suppose Assumptions 8, 9 and 10 hold. Then

$$\lim_{t_j \to \infty} \left(C\pi(\omega) - \lim_{k \to \infty} (\widetilde{\Gamma}_j^k \widetilde{\Omega}^k) \right) = 0. \tag{4.31}$$

Proof. By Theorem 10, the mapping π can be defined as a power series expansion of ω. Assumption 10 guarantees that the approximation $\widetilde{\Gamma}_j^k$ is well-defined for all j. The transient error ι vanishes as $t \to \infty$ by Assumption 9, i.e. $\lim_{t_j \to \infty} \widetilde{\Gamma}_j^k = \widetilde{\Gamma}^k$. Then, by (4.20) and (4.26), $\lim_{k \to \infty, t_j \to \infty} (\widetilde{\Gamma}_j^k \widetilde{\Omega}^k)$ converges to y, thus $C\pi(\omega)$. □

Up to this point, what we have considered is only one trajectory ω of the signal generator. This is restrictive in the nonlinear setting. Thus, in practice we can construct the new snapshots matrices U and Y with multiple trajectories, namely

$$\begin{aligned} U &= [\widetilde{U}_j^{1\top} \quad \widetilde{U}_j^{2\top} \quad \cdots \quad \widetilde{U}_j^{q\top}]^\top, \\ Y &= [\widetilde{Y}_j^{1\top} \quad \widetilde{Y}_j^{2\top} \quad \cdots \quad \widetilde{Y}_j^{q\top}]^\top, \end{aligned} \tag{4.32}$$

for $q \geq 1$, with $\widetilde{U}_j^i$ and $\widetilde{Y}_j^i$ the data matrices (defined in (4.27) and (4.28)) sampled from different signal generator initial condition $\omega(0) = \omega_0^i$.

An online implementation of the proposed data-driven approach is given in the following Algorithm 1.

Remark 6. Obtaining the least-squares solution (4.29) constitutes the most costly operation in this data-driven procedure. This step involves computing the pseudo-inverse of a $w \times N$ matrix with $w \geq N$, hence having complexity[1] $\mathcal{O}(N^3)$. As N is bounded by $\sum_{i=1}^{k} \nu^i$, the complexity is bounded by $\mathcal{O}(\nu^{3k})$, which is significantly better than the complexity $\mathcal{O}(\nu^{3k} n^3)$ of the model-based approach (as discussed in Remark 5) since now the computational cost no longer scales with the original problem size n, that could be extremely large in practice.

Remark 7. The data-driven method does not rely on the knowledge of the system matrices E, A, N, B and C, and hence opens the possibility of exploiting directly the data from the

[1]This is the computational cost using the standard Gaussian elimination.

Algorithm 1 On-Line Approximation of $\widetilde{C\Pi}_1, \cdots, \widetilde{C\Pi}_k$

1: **Input:** the approximation order k; sufficiently large $j \in \mathbb{Z}$; $w \geq N$; sufficiently small tolerance e_Γ; a proper $q \in \mathbb{Z}$
2: construct matrix $\widetilde{U}_j$ and $\widetilde{Y}_j$ in (4.27) and (4.28)
3: construct U and Y in (4.32) by repeating step 2 for q times with different initial condition $\omega(0)$
4: **if** $U^\top U$ is full rank **then**
5: compute $\widetilde{\Gamma}_j^k$ solving (4.29)
6: **else**
7: increase w **go to** 2
8: **if** $\|\widetilde{\Gamma}_j^k - \widetilde{\Gamma}_{j-1}^k\| > (t_k - t_{k-1})e_\Gamma$ **then**
9: $j = j + 1$ **go to** 2
10: **else**
11: obtain $\widetilde{\Gamma}_j^k$
12: obtain $\widetilde{Z}_i$ from $\widetilde{\Gamma}_j^k$
13: **Return:** $\widetilde{C\Pi}_i$ for $i = 1, 2, \cdots, k$ ▷ see (4.30)

original fluids model. In other words, one could possibly bypass the use of certain system discretization techniques which are typically expensive *per se*.

4.2 A family of reduced-order models

We now introduce a family of reduced-order models which is in a quadratic-bilinear form, namely in the form

$$\begin{aligned} \dot{\xi} &= F\xi + G(\xi \otimes \xi) + M\xi u + Ru, \\ \psi &= \sum_{i \geq 1} D_i \xi^{(i)}, \end{aligned} \tag{4.33}$$

where $F \in \mathbb{R}^{\nu \times \nu}$, $M \in \mathbb{R}^{\nu \times \nu}$, $G \in \mathbb{R}^{\nu \times \nu^2}$, $R \in \mathbb{R}^\nu$ and $D_i^\top \in \mathbb{R}^{\nu^i}$. In the following statement we give conditions on F, Π_i, R and D_i such that (4.33) is indeed a reduced-order model by moment matching of (4.2).

Theorem 13. Consider the system (4.2), the signal generator (4.3), the model (4.33) and suppose that Assumption 8, 9 and 10 hold. System (4.33) is a reduced-order model by moment

matching of system (4.2) at (S, L) if $\nu < n$ and the following equations hold

$$\begin{aligned} C\Pi_1 =& D_1 P_{(1,1)}, \\ C\Pi_i =& D_1 P_{(i,1)} + D_2 P_{(i,2)} + \cdots + D_{i-1} P_{(i,i-1)} + D_i P_{(i,i)}, \end{aligned} \tag{4.34}$$

for all $i > 1$, where

$$P_{(i,j)} = \begin{cases} P_i, & j = 1, \\ \sum_{k=1}^{i-j+1} P_k \otimes P_{(i-k,j-1)}, & j \geq 2, \end{cases} \tag{4.35}$$

for $i \geq 1$, $j \leq i$, and P_i are the solutions to the equations

$$\begin{aligned} P_1 S &= F P_1 + RL, \\ P_2 S^{[2]} &= F P_2 + G(P_1 \otimes P_1) + M(P_1 \otimes L), \\ P_i S^{[i]} &= F P_i + G(P_1 \otimes P_{i-1} + P_2 \otimes P_{i-2} + \cdots + P_{i-1} \otimes P_1) + M(P_{i-1} \otimes L), \end{aligned} \tag{4.36}$$

for $i \geq 3$.

Proof. By Lemma 1, to match the moment of the systems (4.33) and (4.2) at (S, L), there must exist a unique mapping $p(\cdot)$ solving

$$\frac{\partial p(\omega)}{\partial \omega} S\omega = F p(\omega) + G(p(\omega) \otimes p(\omega)) + M p(\omega)(L\omega) + RL\omega. \tag{4.37}$$

Similar to the proof of Theorem 1, considering the formal power series

$$p(\omega) = \sum_{i \geq 1} P_i \omega^{(i)}, \tag{4.38}$$

yields the system of equations (4.36). Recall that p must also solve (2.29), which in this case becomes

$$C \sum_{i \geq 1} \Pi_i \omega^{(i)} = \sum_{i \geq 1} D_i P_i \omega^{(i)}. \tag{4.39}$$

This equation yields

$$\begin{aligned}
&C\Pi_1\omega + C\Pi_2(\omega\otimes\omega) + C\Pi_3(\omega\otimes\omega\otimes\omega) + \cdots \\
&= D_1P_1\omega + (D_1P_2 + D_2(P_1\otimes P_1))(\omega\otimes\omega) \\
&\quad + (D_3P_1 + D_2(P_1\otimes P_2 + P_2\otimes P_1) \\
&\quad + D_3(P_1\otimes P_1\otimes P_1))(\omega\otimes\omega\otimes\omega) + \cdots \\
&= D_1P_{(1,1)}\omega + (D_1P_{(2,1)} + D_2P_{(2,2)})(\omega\otimes\omega) \\
&\quad + (D_3P_{(3,1)} + D_2P_{(3,2)} + D_3P_{(3,3)})(\omega\otimes\omega\otimes\omega) + \cdots .
\end{aligned} \tag{4.40}$$

By matching the power of $\omega^{(i)}$, the above implies that

$$\begin{aligned}
C\Pi_i\omega^{(i)} =&(D_1P_{(i,1)} + D_2P_{(i,2)} + \cdots \\
&+ D_{i-1}P_{(i,i-1)} + D_iP_{(i,i)})\omega^{(i)},
\end{aligned} \tag{4.41}$$

which yields (4.34). Here, $P_{(i,j)}$ represents the coefficient matrix of $\omega^{(i)}$ corresponding to D_j. Then, it is easy to verify that $P_{(i,1)} = P_i$. Moreover, for $2 \le j \le i$,

$$\begin{aligned}
P_{(i,j)}\omega^{(i)} =&(P_1\omega)\otimes(P_{(i-1,j-1)}\omega^{(i-1)}) + (P_2\omega^{(2)})\otimes(P_{(i-2,j-1)}\omega^{(i-2)}) + \cdots \\
&+ (P_{(i-j+1)}\omega^{(i-j+1)})\otimes(P_{(j-1,j-1)}\omega^{(j-1)}) \\
=&(P_1\otimes P_{(i-1,j-1)} + P_2\otimes P_{(i-2,j-1)} + \cdots + P_{(i-j+1)}\otimes P_{(j-1,j-1)})\omega^{(i)} \\
=&\left(\sum_{k=1}^{i-j+1} P_k\otimes P_{(i-k,j-1)}\right)\omega^{(i)},
\end{aligned} \tag{4.42}$$

which yields (4.35). This completes the proof. □

We now show that the reduced-order system (4.33) can be simplified. In fact, note that selecting $P_1 = I_\nu$, yields

$$F = S - RL, \tag{4.43}$$

and from equation (4.35), when $i = j$,

$$P_{(i,i)} = I_{\nu^i} \tag{4.44}$$

for all $i \geq 1$. Now select any G and M, and determine $P_{(i,j)}$ from (4.35) by solving (4.36). It follows that the D_i's are determined by the model-based approach (data-driven approach, respectively) as

$$\begin{aligned} D_1 &= C\Pi_1(\widetilde{C\Pi}_1), \\ D_2 &= C\Pi_2(\widetilde{C\Pi}_2) - D_1P_{(2,1)}, \\ D_i &= C\Pi_i(\widetilde{C\Pi}_i) - D_1P_{(i,1)} - D_2P_{(i,2)} + \cdots - D_{i-1}P_{(i,i-1)}, \end{aligned} \tag{4.45}$$

for $i \geq 3$. For data-driven approach, it suffers to replace $C\Pi_i$ with the estimation $\widetilde{C\Pi}_i$ obtained from Algorithm 1.

Then, a family of reduced-order models of system (4.2) that match the k-th approximate moment is given by

$$\begin{aligned} \dot{\xi}(t) &= (S-RL)\xi(t)+G(\xi(t)\otimes\xi(t))+M\xi(t)u(t)+Eu(t), \\ \bar{\psi}(t) &= \sum_{i=1}^{k} D_i\xi^{(i)}(t), \end{aligned} \tag{4.46}$$

where R, G and M are free parameters that can be used to impose additional properties of the model and the D_i's are selected as in (4.45) (computed for the specific selection of R, G and M from (4.36) and (4.35)). Note that for the obtained reduced-order system, we can easily write it back to the DAEs form by properly designing an invertible matrix F_{22} as we want. The stability analysis is the same as Theorem 6.

4.3 Simulations

In this section, we first consider a one-dimension Burgers' equation which is a general quadratic-bilinear system and then apply it to models that describe fluid flows in two types of cavity: a lid-driven (square) cavity flow and a lid-driven polar cavity flow. Both model-based approach and data-driven approach are implemented. We examine the performance of the proposed moment matching model reduction methods for Navier-Stokes type quadratic-bilinear systems

by comparing the output response between the original system and the reduced-order model. A comparison is given between the proposed method and the two-sided projection method in [8].

4.3.1 Burgers' equation

The Burgers' equation is a PDE that models many physical phenomena and provides the simplest model for diffusive waves in fluid dynamics. It has been extensively used to numerically test nonlinear model reduction techniques [119]. Consider the one-dimension Burgers' equation of the form

$$\begin{aligned} v\frac{\partial v(x,t)}{\partial x} + \gamma\frac{\partial^2 v(x,t)}{\partial x^2} &= \frac{\partial v(x,t)}{\partial t}, \\ \alpha v(0,t) + \beta\frac{\partial v(x,t)}{\partial x}|_{x=0} &= u(t), \\ \frac{\partial v(x,t)}{\partial x}|_{x=1} &= 0, \end{aligned} \tag{4.47}$$

with boundary condition $v(x,0) = v_0(x)$. This set of equations describes the diffusive wave in a one-dimensional space $x \in \Omega = [0,1]$. To the left boundary ($x = 0$), we implement the Dirichlet boundary control with $\alpha = 1, \beta = 0$ and $\gamma = 0.1$. The output of interest is the response of x at the right boundary ($x = 1$).

We discretize the above PDE using the central difference method [120] which leads to a quadratic-bilinear system of order 1500 of the form

$$\dot{v} = f(v,u) = Av + H(v \otimes v) + Nvu + Bu. \tag{4.48}$$

The primary purpose of the 1D Burgers' equation is not to directly simulate a physical phenomenon but to serve as a simplified model of the homogeneous incompressible Navier-Stokes equation. It captures essential mathematical characteristics, including the nonlinear convection term and the second-order derivative representing viscous forces [121]. The original intention behind introducing the 1D Burgers' equation was to facilitate a deeper understanding of the

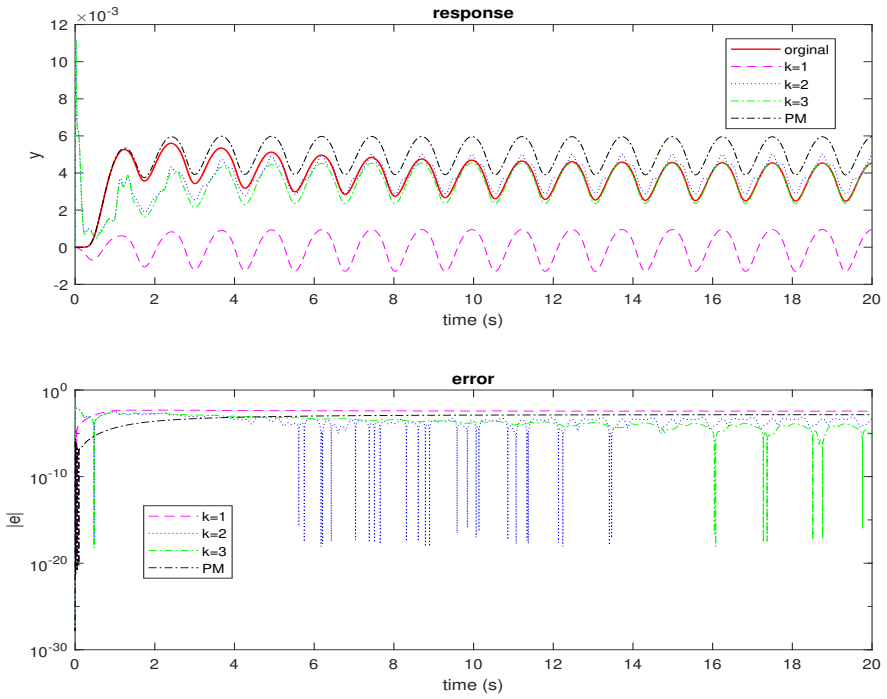

(a) Model-based approach

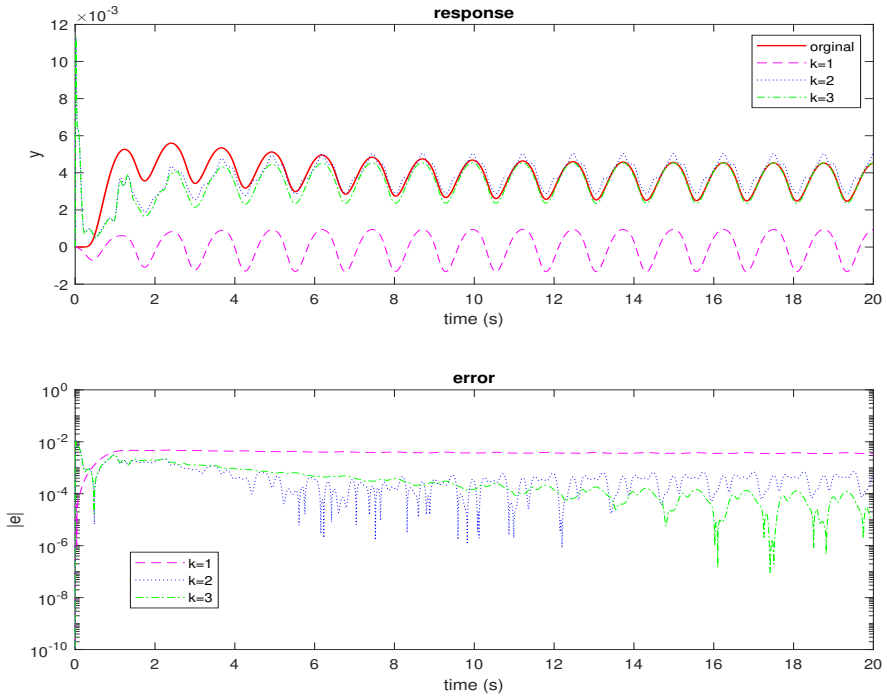

(b) Data-driven approach

Figure 4.1: Simulation for 1D burgers' equation

mathematical complexities present in the Navier-Stokes equation, especially under conditions of

low viscosity (high Reynolds numbers).

The signal generator (4.3) has been selected as $S = \text{diag}(5S_0, 10S_0, 15S_0, 20S_0)$, with $S_0 = [0, 1; -1, 0]$, and $L = [1, 0, 1, 0, 1, 0, 1, 0]$, which leads to a reduced-order model of order 8. We select the eigenvalues of F randomly and guarantee stability by selecting the matrix R. Algorithm 1 has been applied with $q = 20$, $e_\Gamma = 10^{-6}$, and the initial conditions w_0^i randomly sampled from the normal distribution $\mathcal{N}(0, 10^{-4})$. For both model-based and data-driven methods, we have investigated the matching for 1-st, 2-nd and 3-rd approximate moments. For the two-sided projection method, to ensure the same dimension of the reduced-order systems, we have only considered the first two interpolation points to construct the projection matrix.

Figure 4.1 (a) (top) displays the time history of the output response obtained from the model-based approach, while the associated absolute error is shown in Figure 4.1 (a) (bottom). The black/solid line indicates the output response of the original model, while the yellow/dashed, blue/dotted and red/dash-dotted lines indicate the output response of the reduced-order model for $k = 1, 2$ and 3, respectively. We have also compared this interconncection -based method with the two-sided projection method (purple/dash-dotted) in Figure 4.1(a). Figure 4.1(b) dislpays the analogous quantities for the use of the data-driven approach.

While matching the 1-st approximate moment ($k = 1$) is still unsatisfactory, observe that both the reduced-order models (obtained by the model-based and data-driven approaches) provide a sufficiently good approximation as the steady-state responses *almost* coincide when the 2-nd ($k = 2$) and 3-rd ($k = 3$) approximate moments are matched. When the order of the approximate moment k increases, the accuracy of the approximation improves accordingly as the error becomes smaller. For comparison, the two-sided projection method has better performance at transient, whilst at steady-state it performs better than the case $k = 1$ but noticeably falls behind for $k = 2$ and $k = 3$. It is worth mentioning that, as G and M are randomly selected, these are free for the enforcement of some extra properties.

4.3.2 Lid driven cavity

The lid-driven flow in a square cavity is a typical steady separated flow which has been examined experimentally and numerically in detail [122, 123]. So far, some accurate numerical results are available for this case over a certain range of Reynolds numbers. Therefore, it has also been used to test numerical solutions of the Navier-Stokes equations [124].

The considered lid-driven cavity is shown in Figure 4.2. It has a square domain $(x, y) \in \Omega = [0, L] \times [0, L]$ with the boundary that consists of three rigid walls and a moving top lid with velocity U. This flow dynamics modelled by the Navier-Stokes equations using vorticity ϵ and stream function ζ are given as

$$\begin{aligned} \frac{\partial \epsilon}{\partial t} &= -u\frac{\partial \epsilon}{\partial x} - v\frac{\partial \epsilon}{\partial y} + \frac{1}{Re}\nabla^2 \epsilon, \\ 0 &= \epsilon + \nabla^2 \zeta, \end{aligned} \tag{4.49}$$

where Re is the Reynolds number and ∇^2 is the Laplacian operator. u and v are the x and y components of the velocity,

$$u = \frac{\partial \zeta}{\partial y}, v = -\frac{\partial \zeta}{\partial x} \tag{4.50}$$

A velocity profile $u_{top} = U(t)$ is imposed on the upper lid as the system input and the boundary conditions are set to mixed Dirichlet and Neumann conditions. We collect the boundary conditions and summarize them as follows

$$\begin{aligned} x = 0, \quad 0 \le y \le L: &\qquad u = v = 0, \quad \zeta = 0, \quad \epsilon = -\frac{\partial^2 \zeta}{\partial x^2}; \\ x = L, \quad 0 \le y \le L: &\qquad u = v = 0, \quad \zeta = 0, \quad \epsilon = -\frac{\partial^2 \zeta}{\partial x^2}; \\ y = 0, \quad 0 \le x \le L: &\qquad u = v = 0, \quad \zeta = 0, \quad \epsilon = -\frac{\partial^2 \zeta}{\partial y^2}; \\ y = 0, \quad 0 \le x \le L: &\qquad u = U, \quad v = 0, \quad \zeta = 0, \quad \epsilon = -\frac{\partial^2 \zeta}{\partial y^2}. \end{aligned} \tag{4.51}$$

We apply the central difference method to (4.49) on the $p \times p$ unit square mesh with the nodes

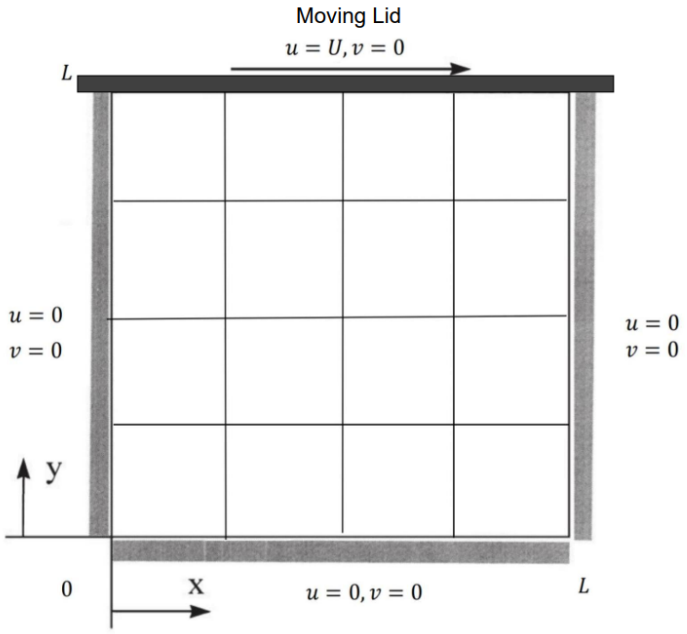

Figure 4.2: Lid-driven cavity [2].

$\epsilon_{i,j}$ and $\zeta_{i,j}$ inside the cavity, leading to the set of equations

$$\begin{aligned}\frac{\mathrm{d}\epsilon_{i,j}}{\mathrm{d}t} &= \frac{\epsilon_{i+1,j} + \epsilon_{i-1,j} + \epsilon_{i,j+1} + \epsilon_{i,j-1} - 4\epsilon_{i,j}}{Re \cdot h^2} \\ &\quad + \frac{(\zeta_{i+1,j} - \zeta_{i-1,j})(\epsilon_{i,j+1} - \epsilon_{i,j-1}) - (\zeta_{i,j+1} - \zeta_{i,j-1})(\epsilon_{i+1,j} - \epsilon_{i-1,j})}{4h^2}, \\ 0 &= \epsilon_{i,j} + \frac{\zeta_{i+1,j} + \zeta_{i-1,j} + \zeta_{i,j+1} + \zeta_{i,j-1} - 4\zeta_{i,j}}{h^2}.\end{aligned} \tag{4.52}$$

for $2 \leq i \leq p$ and $2 \leq j \leq p$, with $h = \frac{L}{p}$. The boundary condition can be rewritten as

$$\begin{aligned} i = 1, 2 \leq j \leq p &: \zeta_{1,j} = 0, \epsilon_{1,j} = -\frac{2}{h^2}\zeta_{2,j}; \\ i = p+1, 2 \leq j \leq p &: \zeta_{p+1,j} = 0, \epsilon_{p+1,j} = -\frac{2}{h^2}\zeta_{p,j}; \\ j = 1, 2 \leq i \leq p &: \zeta_{i,1} = 0, \epsilon_{i,1} = -\frac{2}{h^2}\zeta_{i,2}; \\ j = p+1, 2 \leq i \leq p &: \zeta_{i,p+1} = 0, \\ &\quad \epsilon_{i,p+1} = -\frac{2}{h^2}\zeta_{i,p} - \frac{2}{h}U. \end{aligned} \tag{4.53}$$

Let ϵ (ζ, respectively) be a vector that contains the elements $\epsilon_{i,j}$ ($\zeta_{i,j}$, respectively) at all nodes. Combining system (4.52) and the boundary conditions (4.53) yields a DAE quadratic-bilinear system in the form of (4.1). The output of the system is the stream function at the centre of the

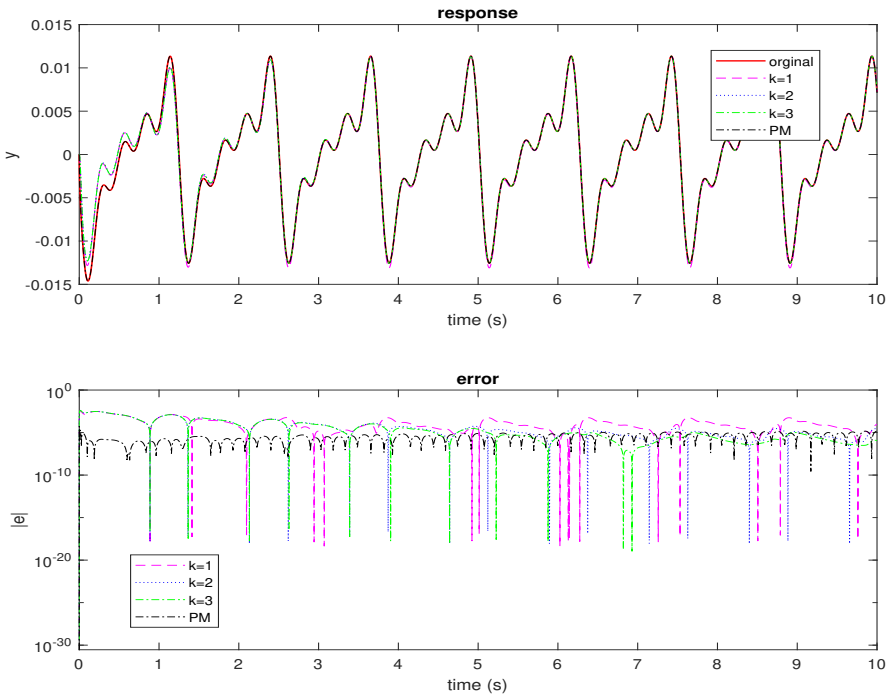

(a) Model-based approach

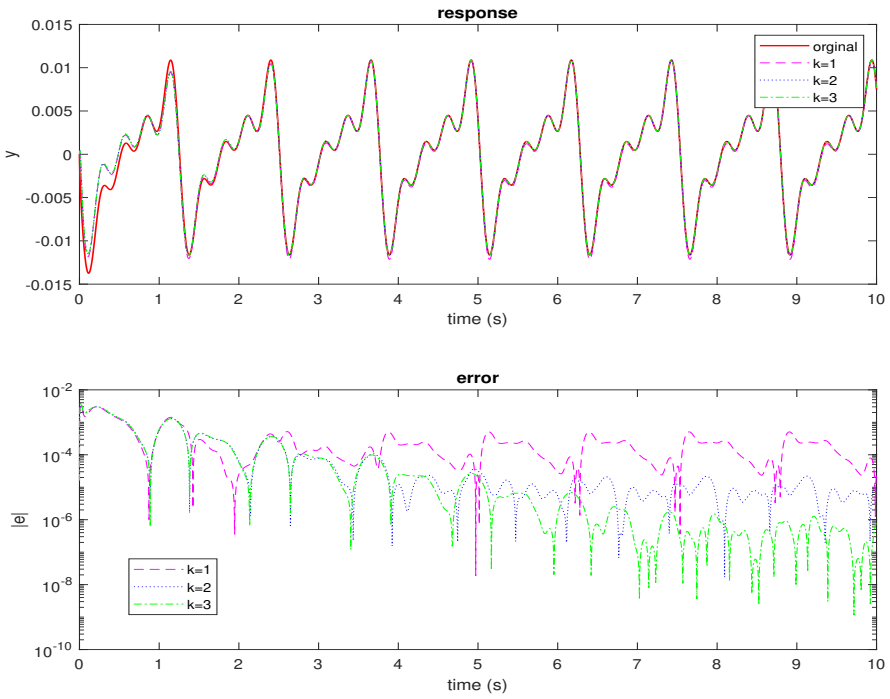

(b) Data-driven approach

Figure 4.3: Simulation for lid-driven cavity.

cavity. Let $p = 31$ and set the Reynolds number to 10. The discretized DAE quadratic-bilinear

system has order $2(p-1)^2 = 1800$. The reduced-order model is configured with a dimension $\nu = 8$, i.e., it utilizes 8 interpolation points. These points consist of 4 complex conjugates pairs. The signal generator, represented by the matrices S and L, remains the setup described in Section 4.3.1. The settings of the data-driven and two-sided projection approaches are the same as in Section 4.3.1. All the other free matrices in the reduced-order models are randomly selected as part of the original system matrices.

Figure 4.3 (a) (top) displays the time histories of the stream function at the centre point obtained from the model-based approach, while the respective absolute error is shown in Figure 4.3 (a) (bottom). The black/solid line indicate the output response of the original model ,while the yellow/dashed, blue/dotted and red/dash-dotted lines indicate the output response of the reduced-order models for $k = 1, 2$ and 3, respectively. We have also compared this interconnection-based method with the two-sided projection method (purple/dash-dotted) in Figure 4.3(a). Figure 4.3(b) displays the analogous quantities for the used data-driven approach.

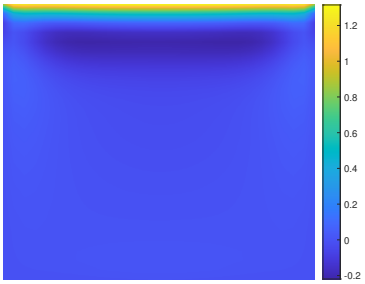

(a) ϵ obtained from original model

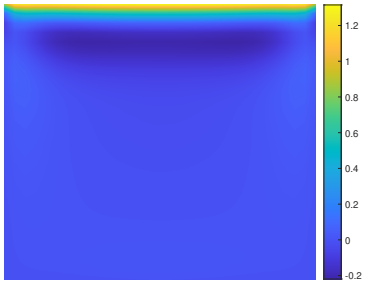

(b) ϵ obtained from the reduced-order model when $p = 3$

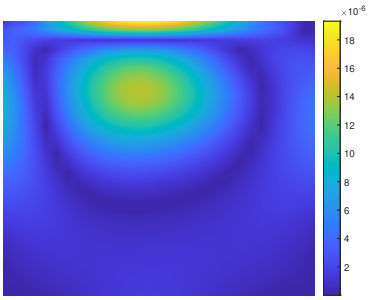

(c) error between full and reduced-order model

Figure 4.4: A visualization of the vorticities of the original model (a), the reduced-order model (b) and of the respective error (c) at $t = 8s$ in the cavity.

It can be observed that both the model-based and the data-driven approaches result in reduced-order models that well approximate the steady-state response of the original system, even with $k = 1$. Compared with the two-sided projection method, our proposed approaches also present competitive performance in terms of approximation error.

We plot the vorticity ϵ at each point by selecting $C_2 = I_n$ with the same input at time $t = 8s$ when $k = 3$. In Figure 4.4, we compare the response of the reduced-order model with that of the original system and the errors are visualized in the cavity. The states of the reduced-order model do not have any physical meaning and we also keep the possibility that we can select some key points as the output instead of the full states to reduce the computational complexity. For example, as in the lid-driven cavity we know the information that the top lid is moving, we can focus more on the top half and reduce the output points at the bottom. Note that for the obtained reduced-order system, we can easily write it back to the DAEs form by properly designing an invertible matrix F_{22} without any change on the output response.

4.3.3 Lid driven polar cavity

As a third case study, we solve the lid-driven cavity flow in cylindrical (polar) coordinates [3]. The lid-driven polar cavity flow is another test case which has been frequently used to validate numerical algorithms [125, 126]. Compared with the square cavity flow problem studied in Section 4.3.2, due to the special geometry, it is more challenging to present a numerical scheme for the flow in this polar cavity. The features of the flow in a lid-driven polar cavity have been investigated in [127], both experimentally and numerically.

The schematic view of polar cavity geometry is shown in Figure 4.5 with $r = 1$, $R = e$ and $\theta = 1$. We assume that the polar cavity is driven from the inside wall, such that the wall with smaller radius is moving with a constant velocity and the other three walls are stationary. The governing equations for a two-dimensional flow in terms of the stream function and the scalar

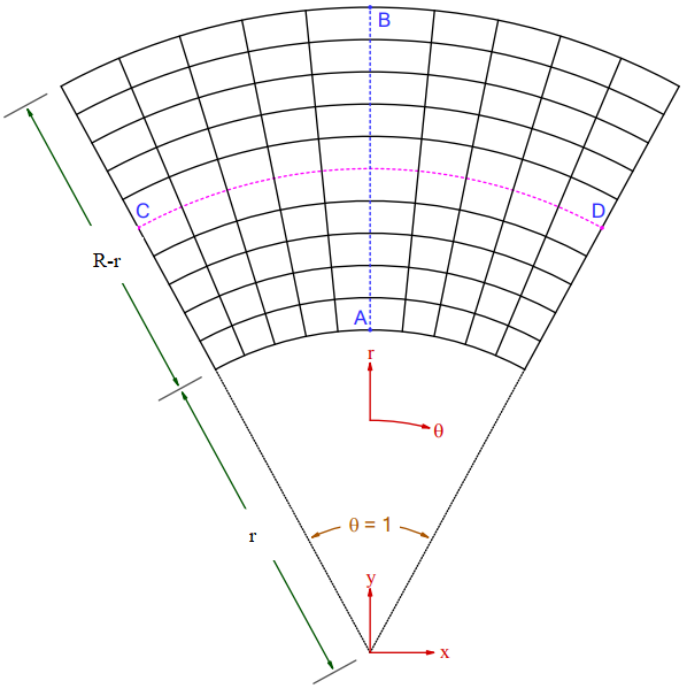

Figure 4.5: Schematic view of polar cavity geometry [3].

vorticity field are given by

$$\begin{aligned} \frac{\partial \epsilon}{\partial t} &= -\frac{1}{r}\left(\frac{\partial \epsilon}{\partial r}\frac{\partial \zeta}{\partial \theta} - \frac{\partial \epsilon}{\partial \theta}\frac{\partial \zeta}{\partial r}\right) + \frac{2}{Re}\nabla^2 \epsilon, \\ 0 &= \epsilon + \nabla^2 \zeta. \end{aligned} \tag{4.54}$$

The factor $r\frac{\partial}{\partial r}$ in the polar coordinate Laplacian is awkward to discretize and we theredore introduce a change of variables $r = r(\rho)$. We define the function

$$r = r(\rho) = e^{\rho} \tag{4.55}$$

so that $r\frac{\partial}{\partial r} = \frac{\partial}{\partial \rho}$ and we take as our boundary condition $\rho = 0$ when $r = 1$, corresponding to points lying on the boundary of the circular cylinder. Then, the governing equations (4.54) become

$$\begin{aligned} \frac{\partial \epsilon}{\partial t} &= -e^{-2\rho}\left(\frac{\partial \epsilon}{\partial \rho}\frac{\partial \zeta}{\partial \theta} - \frac{\partial \epsilon}{\partial \theta}\frac{\partial \zeta}{\partial \rho}\right) + \frac{2}{Re}e^{-2\rho}\left(\frac{\partial^2 \epsilon}{\partial \rho^2} + \frac{\partial^2 \epsilon}{\partial \theta^2}\right), \\ 0 &= \epsilon + e^{-2\rho}\left(\frac{\partial^2 \zeta}{\partial \rho^2} + \frac{\partial^2 \zeta}{\partial \theta^2}\right), \end{aligned} \tag{4.56}$$

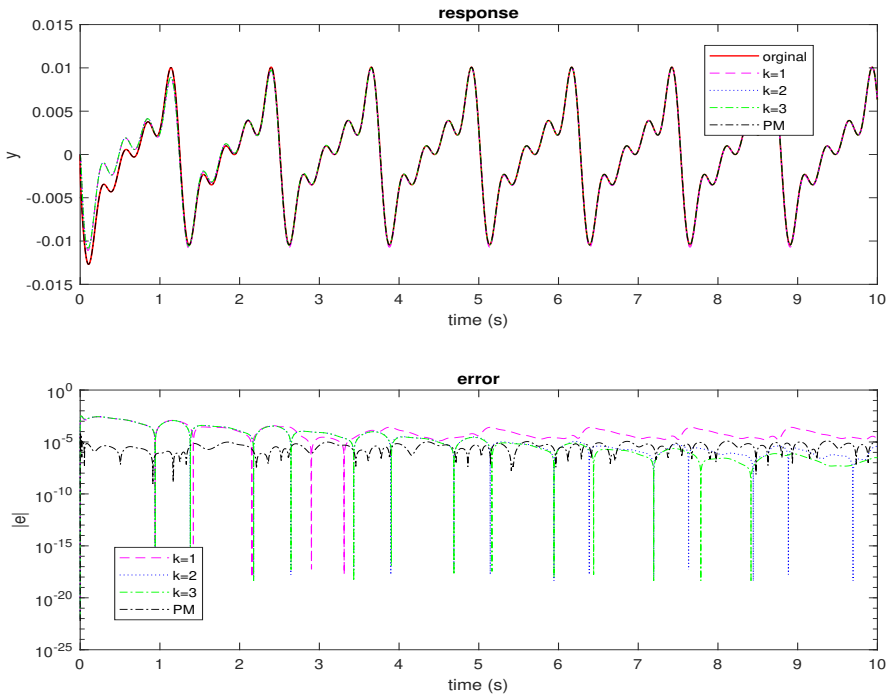

(a) Model-based approach

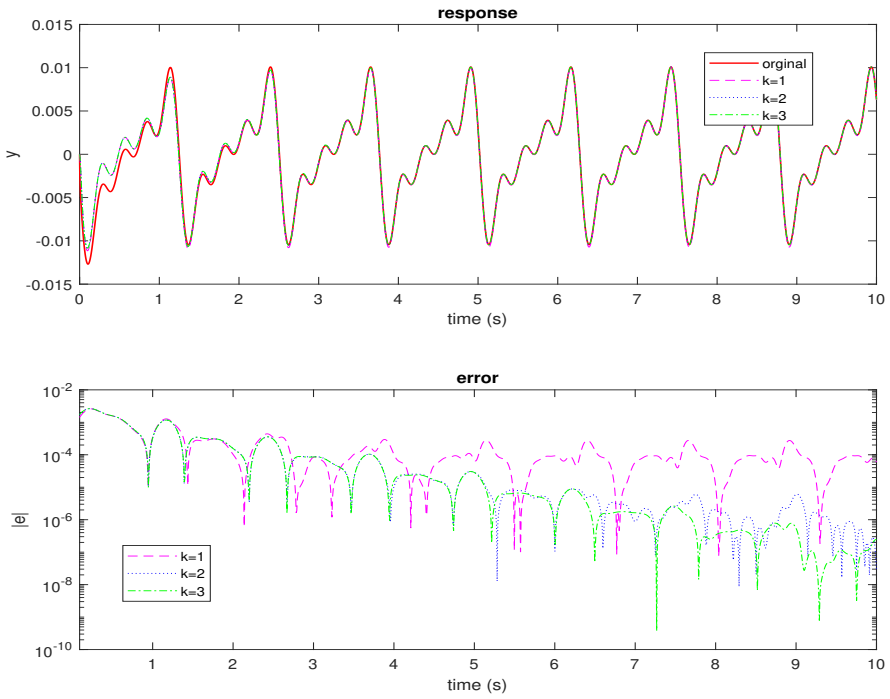

(b) Data-driven approach

Figure 4.6: Simulation for lid-polar cavity.

By the central difference method, (4.56) has been transformed into

$$\begin{aligned}\frac{\mathrm{d}\epsilon_{i,j}}{\mathrm{d}t} &= \frac{2e^{-2\rho_i}}{Re\cdot h^2}(\epsilon_{i+1,j}+\epsilon_{i-1,j}+\epsilon_{i,j+1}+\epsilon_{i,j-1}-4\epsilon_{i,j})\\ &\quad+\frac{e^{-2\rho_i}}{4h^2}[(\zeta_{i+1,j}-\zeta_{i-1,j})(\epsilon_{i,j+1}-\epsilon_{i,j-1})-(\zeta_{i,j+1}-\zeta_{i,j-1})(\epsilon_{i+1,j}-\epsilon_{i-1,j})],\\ 0 &= \epsilon_{i,j}+\frac{\zeta_{i+1,j}+\zeta_{i-1,j}+\zeta_{i,j+1}+\zeta_{i,j-1}-4\zeta_{i,j}}{h^2e^{2\rho_i}},\end{aligned} \tag{4.57}$$

for $2\le i\le p$ and $2\le j\le p$. Here, $h=\frac{1}{p}$ and $\rho_i=(i-1)h$. The boundary conditions are given as

$$\begin{aligned} i=1,2\le j\le p:&\quad \zeta_{1,j}=0,\epsilon_{1,j}=(1-\frac{2}{h})u-\frac{2\zeta_{2,j}}{h^2};\\ i=p+1,2\le j\le p:&\quad \zeta_{p+1,j}=0,\epsilon_{p+1,j}=-\frac{2\zeta_{p,j}}{h^2};\\ j=1,2\le i\le p:&\quad \zeta_{i,1}=0,\epsilon_{i,1}=-e^{-2\rho_i}\frac{2\zeta_{i,2}}{h^2};\\ j=p+1,2\le i\le p:&\quad \zeta_{i,p+1}=0,\epsilon_{i,p+1}=-e^{-2\rho_i}\frac{2\zeta_{i,p}}{h^2}.\end{aligned} \tag{4.58}$$

Similar to the lid-driven cavity, we obtain the DAE quadratic-bilinear system in the form of (4.1) by combing system (4.57) and the boundary condition (4.58). We consider the original DAE system with order 1800 and reduce it to a general quadratic-bilinear system of order 8. The simulation settings remains as in Section 4.3.2.

Figure 4.6 illustrates similar results as those Figure 4.3 for the lid-driven polar cavity. The reduced-order models provide good approximations of the output and the performance will be better if the higher approximate moments are matched. Compared with the two-sided projection method, we have similar accuracy at steady-state and some free parameters can be easily used to enforce some additional properties. Note that for the obtained reduced-order system, it can easily be written in DAEs form.

Chapter 5

Two-sided Interconnection-Based Model Order Reduction for Quadratic-Bilinear Systems

In the preceding chapters, we have focused on what are termed "direct" moments, where the signal generator is connected in front of the system. An alternative time-domain concept of nonlinear moments, based on the swapped interconnection, was introduced in [75]. This concept achieves matching on an arbitrary manifold that might lack practical significance. To address this, we consider a two-sided interconnection approach, which promises to provide a manifold at steady-state that aids in resolving the challenge of matching "swapped" moments. In this chapter, we develop a two-sided method aimed at enhancing model order reduction through moment matching for quadratic-bilinear systems. The resulting reduced-order models, of order ν, match moments at 2-ν (distinct) interpolation points, effectively doubling the matched conditions compared to those discussed in Chapter 3. The findings presented in this chapter draw upon the foundational work in [105].

The structure of this chapter is as follows. Section 5.1 characterizes the swapped nonlinear moment for quadratic-bilinear systems, leveraging the solution of a system of Sylvester-like equations. Section 5.2 introduces two families of reduced-order models. Finally, Section 5.3

demonstrates the applicability of these models through a numerical example based on the 1-D Burgers' equation.

5.1 Swapped Moments for Quadratic-Bilinear Systems

In this section we provide a characterization of "swapped" moment for quadratic-bilinear systems.

Consider again system (3.1) together with the linear filter

$$\dot{\varpi} = q(\varpi) + r(\varpi)\eta = Q\varpi + R\eta. \tag{5.1}$$

To define the swapped moments for system (3.1), we introduce the following assumption.

Assumption 15. The filter (5.1) is controllable and the eigenvalues of Q are simple and belong to $\mathbb{C}_0$.

The following result provides a formula to compute the moment of system (3.1) at (Q, R).

Theorem 14. Consider the system (3.1) and the filter (5.1). Suppose that Assumptions 15 and 13 hold. Then the mapping

$$v(x) = \sum_{i\geq 1} \Upsilon_i x^{(i)} \tag{5.2}$$

formally solves the partial differential equation

$$Qv(x) = \frac{\partial v}{\partial x}(Ax + H(x \otimes x)) + RCx, \tag{5.3}$$

where Υ_i, $i \geq 1$, solve the Sylvester-like equations

$$\begin{aligned} Q\Upsilon_1 &= \Upsilon_1 A + RC, \\ Q\Upsilon_2 &= \Upsilon_2(A \oplus A) + \Upsilon_1 H, \\ Q\Upsilon_i &= \Upsilon_i A^{[i]} + \Upsilon_{i-1} H^{[i-1]}, \end{aligned} \tag{5.4}$$

for $i \geq 3$. Moreover, the (swapped) moment of system (3.1) at (Q, R) is given by $\sum_{i\geq 1}(\Upsilon_i B^{[i]} + \Upsilon_{i-1} N^{[i-1]})x^{(i-1)}$ (with $\Upsilon_0 = 0$).

Proof. Consider the formal power series expansion (5.2) of v. Substituting (5.2) into (5.3) yields

$$Q(\Upsilon_1 x + \Upsilon_2 x^{(2)} + \cdots) = \frac{\partial(\Upsilon_1 x + \Upsilon_2 x^{(2)} + \cdots)}{\partial x}(Ax + Hx^{(2)}) + RCx. \tag{5.5}$$

Then the equations in (5.4) are obtained by matching the powers of $x^{(i)}$. According to Definition 2, since $g(x) = Nx + B$, the swapped moment of system (3.1) is given by $\sum_{i\geq 1}(\Upsilon_i B^{[i]} + \Upsilon_{i-1} N^{[i-1]})x^{(i-1)}$. To see this, note that, for instance,

$$\frac{\partial \Upsilon_2(x \otimes x)}{\partial x} B = \Upsilon_2(x \oplus x)B = \Upsilon_2(B \oplus B)x = \Upsilon_2 B^{[2]} x.$$

This completes the proof. □

From a practical point of view, it is useful to define an approximate version of the moment which uses a finite number of terms Υ_i, $i = 1, 2, \cdots, k$.

Definition 8. We call

$$\overline{\left(\frac{\partial v}{\partial x} g\right)}_k = \sum_{i=1}^{k} (\Upsilon_i B^{[i]} + \Upsilon_{i-1} N^{[i-1]})x^{(i-1)}$$

the k-th approximate (swapped) moment of system (3.1) at (Q, R).

Note that if the convergence radius of (5.2) is positive, then (5.2) is an exact solution of (5.3) in power form and the k-th approximate moment of system (3.1) is such that

$$\lim_{k\to\infty} \overline{\left(\frac{\partial v}{\partial x} g\right)}_k = \frac{\partial v}{\partial x} g. \tag{5.6}$$

5.2 Two sided moment matching for quadratic-bilinear systems

As explained in detail in [1], for nonlinear systems the one-sided swapped moment matching loses practical meaning: since the swapped moment is a function of the state. Therefore matching between the full-order and the reduced-order models must be done on a manifold $x = \alpha(\xi)$, for some arbitrary α. However, when the two-sided moment matching is considered, the mapping α is uniquely characterized because both x and ξ are restricted at steady state on a manifold induced by ω.

In this section, we construct two families of reduced-order models that achieve approximate two-sided moment matching for quadratic-bilinear systems. The first family is a specialisation of (2.11). We show that the drawback of this family is that it does not preserve the polynomial structure of the system. This motivates us to introduce a second family which instead preserves the quadratic-bilinear structure of the original system.

Note that in this chapter we mainly focus on matching the first two approximate moments to design the reduced-order model for the following reasons. First, as shown in our simulations, the approximation of moments is very accurate, i.e. the error of the output response between the original system and the reduced-order model is less than 10^{-5}. Moreover, as the original system is in quadratic-bilinear form, we want to preserve this structure (especially in the second family). Finally, in the computation of higher order approximate moments, the complexity increases as well.

5.2.1 First family of reduced-order models

The first family of two-sided reduced-order models is a direct consequences of the results in Section 2.2. Consider the system (2.11) written for the linear signal generator (3.2) with the

moment at (S, L) written exploting the polynomial expansion (3.4), namely

$$\begin{aligned}\dot{\xi} &= S\xi - \delta(\xi)L\xi + \delta(\xi)u,\\ \psi &= \sum_{i\geq 1} C\Pi_i \xi^{(i)},\end{aligned} \tag{5.7}$$

where the Π_i's are defined as in (3.6). We know that this model matches the (direct) moment of (3.1) at (S, L), and that if δ is selected as in (2.14), then the model also matches the (swapped) moment of system (3.1) at (Q, R). Such a δ can be computed explicitly as shown in the next result.

Theorem 15. Consider the system (3.1), the signal generator (3.2) and the filter (5.1). Suppose Assumptions 13, 14 and 15 hold and that both (3.4) and (5.2) are convergent series. System (5.7) with the selection

$$\delta(\xi) := \lim_{j\to\infty} \delta_j(\xi), \tag{5.8}$$

where

$$\delta_j(\xi) = \left[\left(\frac{\partial \bar{v}_j}{\partial x}\frac{\partial \bar{\pi}_j}{\partial \xi}\right)^{-1}\frac{\partial \bar{v}_j}{\partial x}(Nx+B)\right]_{x=\bar{\pi}_j(\xi)=\sum_{i=1}^{j}\Pi_i\xi^{(i)}}^{\bar{v}_j(x)=\sum_{i=1}^{j}\Upsilon_i x^{(i)}}, \tag{5.9}$$

matches the moments of system (3.1) at (S, L) and (Q, R), simultaneously.

Proof. Now we recall that at steady state $x = \pi(\omega)$ and $\xi = p(\omega) = \omega$ which leads to the dynamic properties of two-sided interconnection

$$d_{ss} - \omega_{ss} = v(\pi(\omega)) = \chi(\omega). \tag{5.10}$$

Then, according to equation (2.13), δ is designed to satisfy

$$\left[\frac{\partial v}{\partial x}(Nx+B)\right]_{x=\pi(\omega)} = \left[\frac{\partial \chi}{\partial \xi}\delta(\xi)\right]_{\xi=\omega}, \tag{5.11}$$

with $\chi(\xi) = v(\pi(\xi))$ which gives

$$\frac{\partial \chi}{\partial \xi} = \frac{\partial v}{\partial x}\frac{\partial \pi}{\partial \xi}. \tag{5.12}$$

By substituting (5.12) into (5.11), δ is derived as (2.14). When we use the j-th approximate moment, the corresponding v and π are replaced by the approximation $\bar{v}_j$ and $\bar{\pi}_j$, which yields (5.9). The mapping χ satisfy (2.12) when we rewrite equation (2.12) at steady state and combine equation (3.5) and (5.3), that is

$$\begin{aligned}
&\frac{\partial \chi}{\partial \xi}(S\xi - \delta(\xi)L\xi) + RC\pi(\omega) - Q\chi(\xi) \\
=&\frac{\partial v}{\partial x}\frac{\partial \pi}{\partial \omega}S\omega - \frac{\partial v}{\partial x}(N\pi(\omega)+B)L\xi + RC\pi(\omega) - Qv(\pi(\omega)) \\
=&\frac{\partial v}{\partial x}(Ax + Hx^{(2)}) + RCx - \frac{\partial v}{\partial x}(Ax + Hx^{(2)}) - RCx \\
=&0.
\end{aligned} \tag{5.13}$$

By Theorem 4, $\bar{\pi}_j$ converges to π and, by Theorem 14, $\bar{v}_j$ converges to v. Thus, δ_j approaches (2.14) as $j \to \infty$. □

The advantage of writing δ as in Theorem 15 is that this provides formulas to compute an approximation of the two-sided reduced-order model up to an arbitrary order of accuracy of the power series expansions.

Example 1. For $j = 1$, we have

$$\delta_1(\xi) = (\Upsilon_1\Pi_1)^{-1}\Upsilon_1(N\Pi_1\xi + B). \tag{5.14}$$

Note that this expression involves a polynomial in ξ of order 1. Ignoring higher order terms yields

$$\delta_1(\xi) = (\Upsilon_1\Pi_1)^{-1}\Upsilon_1 B, \tag{5.15}$$

which is the δ of the linearised reduced-order model, see [78]. For $j = 2$, we have

$$\begin{aligned}
\delta_2(\xi) = &\Bigg[\left((\Upsilon_1 + \Upsilon_2 x^{[2]})(\Pi_1 + \Pi_2\xi^{[2]})\right)^{-1} \\
&(\Upsilon_1 + \Upsilon_2 x^{[2]})(Nx + B)\Bigg]_{x=\Pi_1\xi+\Pi_2\xi^{[2]}}.
\end{aligned} \tag{5.16}$$

Note that this expression involves polynomials in ξ of order above 1. In general, δ_j involves

polynomials in ξ of order above j. These higher-than-j-polynomials can be used or ignored (the latter produces a coarser approximation). In both cases, as $j \to \infty$, both expressions converge to (2.14).

5.2.2 A Second Family of reduced-order models

In the previous section we have provided a family of reduced-order models of order ν that match moments at $\sigma(S)$ and $\sigma(Q)$, simultaneously. However, the resulting model does not preserve the quadratic-bilinear structure. Moreover, no free parameter is left in the resulting two-sided reduced-order model and, thus, no further property can be imposed. In this section we propose an alternative family of reduced-order models that preserve the polynomial structure of the system and maintain some free parameters to be used for further design.

Consider a class of polynomial models described by the equations

$$\begin{aligned} \dot{\xi} &= F\xi + G(\xi \otimes \xi) + \sum_{i \geq 1} M_i \xi^{(i-1)} u, \\ \psi &= \sum_{i \geq 1} D_i \xi^{(i)}, \end{aligned} \tag{5.17}$$

where $M_i \in \mathbb{R}^{\nu \times \nu^i}$, while F, G and D_i have the same size as the matrices in (3.14).

Consider the problem of matching only the 1-st approximate direct and swapped moments. This problem is solved by the family of models described by

$$\begin{aligned} \dot{\xi} &= F\xi + G(\xi \otimes \xi) + M_0 u, \\ \psi &= D_1 \xi, \end{aligned} \tag{5.18}$$

where

$$F = S - M_0 L, \qquad M_0 = (\Upsilon_1 \Pi_1)^{-1} \Upsilon_1 B, \qquad D_1 = C\Pi_1$$

and G free. Π_1, Υ_1 are defined by the first equations of (3.6) and (5.4), respectively. System (5.18) describes a family of reduced-order models parameterised in G that match the 1-st approximate direct and swapped moments. The parameter G can be used to enforce additional properties. If

$G = 0$, then the resulting system is the standard two-sided linear(ised) reduced-order model by moment matching, see [78] for more details.

Consider now the problem of matching the 2-nd approximate direct and swapped moments. For this problem, we want to determine the parameters of

$$\begin{aligned} \dot{\xi} &= F\xi + G(\xi \otimes \xi) + M_1 \xi u + M_0 u, \\ \psi &= D_1 \xi + D_2(\xi \otimes \xi), \end{aligned} \tag{5.19}$$

such that the given approximate matching is achieved. Note that system (5.19) has a quadratic-bilinear dynamics with a quadratic output map. The problem is solved by the next result.

Theorem 16. Consider the system (3.1), the signal generator (3.2) and the filter (5.1). Suppose that Assumptions 13, 14 and 15 hold. Then system (5.19) describes a family of reduced-order models of system (3.1) that match the 2-nd approximate moments at $\sigma(S)$ and $\sigma(Q)$, simultaneously, for the selection

$$\begin{aligned} &F = S - M_0 L, \quad M_0 = (\Upsilon_1 \Pi_1)^{-1} \Upsilon_1 B, \\ &D_1 = C\Pi_1, \qquad D_2 = C\Pi_2 - D_1 P_2 \\ &M_1 = Y_1^{-1}[Z - Y_2 M_0^{[2]}] \end{aligned} \tag{5.20}$$

where

$$\begin{aligned} Z &= (\Upsilon_1 N + \Upsilon_2 B^{[2]})\Pi_1, \quad Y_1 = \Upsilon_1 \Pi_1, \\ X &= \Upsilon_1 \Pi_2 + \Upsilon_2 \Pi_1^{(2)}, \qquad Y_2 = X - Y_1 P_2, \end{aligned} \tag{5.21}$$

and P_2 is the unique solution of the Sylvester equation

$$P_2(S^{[2]} - M_0^{[2]}(I_\nu \otimes L)) = FP_2 + G + Y_1^{-1}(Z - XM_0^{[2]})(I_\nu \otimes L), \tag{5.22}$$

while G is free, and Π_1, Π_2, Υ_1, and Υ_2 are given by (3.6) and (5.4), respectively, if and only if $\sigma(S) \cap \sigma(S - M_0 L) = \emptyset$ and $\sigma(S^{[2]} - M_0^{[2]}(I_\nu \otimes L)) \cap \sigma(S - M_0 L) = \emptyset$.

Proof. Using the notation for general nonlinear systems introduced in Section 2.2, to satisfy the

direct moment matching condition (2.10) up to the second order, we need to solve

$$C(\Pi_1\omega + \Pi_2\omega^{(2)}) + \mathcal{O}(\omega^{(3)}) = \\ D_1(P_1\omega + P_2\omega^{(2)}) + D_2(P_1\omega + P_2\omega^{(2)})^{(2)} + \mathcal{O}(\omega^{(3)})$$

where $\mathcal{O}(\omega^{(3)})$ indicates terms of order higher than $\omega^{(2)}$ that can be disregarded. The condition above induces the equations

$$C\Pi_1 = D_1P_1$$

for ω and

$$C\Pi_2 = D_1P_2 + D_2P_1^{(2)}$$

for $\omega^{(2)}$. Recall from Section 3.2 that P_1 is defined as the solution of

$$P_1S = FP_1 + M_0L \tag{5.23}$$

while P_2 is defined as the solution of

$$P_2S^{[2]} = FP_2 + G + M_1(P_1 \otimes L). \tag{5.24}$$

Select $P_1 = I_\nu$ and $F = S - M_0L$. This selection solves equation (5.23) and yields $D_1 = C\Pi_1$ and $D_2 = C\Pi_2 - D_1P_2$. These matrices, as expected, are the same as those given in Section 3.2 for the one-sided direct family of reduced-order models (3.14). Next, consider that according to Section 2.2, two-sided moment matching requires that the condition (2.15) holds for all ω. Similarly to v, let

$$\chi(\xi) = \sum_{i\geq 1} Y_i\xi^{(i)} \tag{5.25}$$

be the formal power series expansion of χ. Then, condition (2.15) written for the 2-nd approximate moments yields

$$\Upsilon_1\Pi_1\omega + (\Upsilon_1\Pi_2 + \Upsilon_2\Pi_1^{(2)})\omega^{(2)} = \\ Y_1P_1\omega + (Y_1P_2 + Y_2P_1^{(2)})\omega^{(2)}$$

which gives the conditions

$$\Upsilon_1 \Pi_1 = Y_1 P_1$$

for $\omega^{(1)}$ and

$$\Upsilon_1 \Pi_2 + \Upsilon_2 \Pi_1^{(2)} = Y_1 P_2 + Y_2 P_1^{(2)}$$

for $\omega^{(2)}$. Thus, the selections $Y_1 = \Upsilon_1 \Pi_1$ and $Y_2 = X - Y_1 P_2$ with $X = \Upsilon_1 \Pi_2 + \Upsilon_2 (\Pi_1 \otimes \Pi_1)$ solve the matching

$$v(\pi(\omega)) = \chi(p(\omega))$$

up to second order. Finally, to satisfy the swapped moment matching condition (2.13) up to second order, we have to satisfy

$$\begin{aligned} \Upsilon_1 B + (\Upsilon_1 B^{[2]} + \Upsilon_1 N)\Pi_1 \omega = \\ Y_1 M_0 + (Y_1 M_1 + Y_2 M_0^{[2]})\omega. \end{aligned}$$

This equation yields the conditions

$$\Upsilon_1 B = Y_1 M_0$$

for $\omega^{(1)}$ and

$$(\Upsilon_2 B^{[2]} + \Upsilon_1 N)\Pi_1 = Y_1 M_1 + Y_2 M_0^{[2]}$$

for $\omega^{(2)}$. Thus, the selections $M_0 = Y_1^{-1}(\Upsilon_1 B)$ and $M_1 = Y_1^{-1}[Z - Y_2 M_0^{[2]}]$ with $Z = (\Upsilon_1 N + \Upsilon_2 B^{[2]})\Pi_1$ solve the matching condition

$$\left(\frac{\partial v}{\partial x}(Nx + B) \right)_{x=\pi(\omega)} = \left(\frac{\partial \chi}{\partial \xi}(M_1 \xi + M_0) \right)_{\xi=\omega}, \tag{5.26}$$

up to the 2-nd approximate moment. Substituting the matrices M_1 and Y_2 in (5.24), yields (5.22). All quantities are now uniquely defined, as long as I_ν is the unique solution of (5.23) and (5.24) has a unique solution P_2. This is the case if and only if $\sigma(S) \cap \sigma(S - M_0 L) = \emptyset$ and $\sigma(S^{[2]} - M_0^{[2]}(I_\nu \otimes L)) \cap \sigma(S - M_0 L) = \emptyset$, respectively. Finally, Y_1 and Y_2 obtained from the

selections above also satisfy the Sylvester equations

$$Y_1 F = QY_1 - RD_1$$

and

$$Y_2 F^{[2]} = QY_2 - Y_1 G - RD_2,$$

which arise from the PDE (2.12). The proof is now complete. □

The family of reduced-order models given in Theorem 16 and parameterized in G has a quadratic output map, while the full-order model (3.1) has a linear output map. If the quadratic output is undesired, this can be removed setting $D_2 = 0$ in (5.19) and using the parameter G to achieve two-sided moment matching of the 2-nd approximate moment. In this way, what we obtain as the reduced-order (5.19) has the same structure as the original system (3.1).

Corollary 16.1. Consider the system (3.1), the signal generator (3.2) and the filter (5.1). Suppose Assumptions 13, 14 and 15 hold. Then system (5.19) is a family of reduced-order models of system (3.1) that match the 2-nd approximate moments at $\sigma(S)$ and $\sigma(Q)$, simultaneously, for the selection

$$\begin{aligned} &F = S - M_0 L, \quad M_0 = (\Upsilon_1 \Pi_1)^{-1} \Upsilon_1 B, \\ &D_1 = C\Pi_1, \qquad D_2 = 0, \\ &M_1 = Y_1^{-1}[Z - Y_2 M_0^{[2]}], \quad G = P_2 S^{[2]} - M_1 \otimes L - F P_2, \end{aligned} \tag{5.27}$$

where

$$\begin{aligned} Z &= (\Upsilon_1 N + \Upsilon_2 B^{[2]})\Pi_1, \quad Y_1 &= \Upsilon_1 \Pi_1, \\ X &= \Upsilon_1 \Pi_2 + \Upsilon_2 \Pi_1^{(2)}, \qquad Y_2 &= X - Y_1 P_2, \end{aligned} \tag{5.28}$$

P_2 is the solution of the equation

$$C\Pi_2 = D_1 P_2, \tag{5.29}$$

and Π_1, Π_2, Υ_1, and Υ_2 are given by (3.6) and (5.4), respectively.

5.3 Simulations Results for the 1D Burgers' Equation

We illustrate the results of this section on the one-dimension Burgers' equation discussed in Section 4.3.1.

We consider the system (4.48) with order $n = 100$. The signal generator (3.2) and the filter (5.1) have been selected as $S = \text{diag}(0.7S_0, 5S_0, 33S_0)$, $Q = \text{diag}(34Q_0, 70Q_0, 90Q_0)$, with $S_0 = Q_0 = [0, 1; -1, 0]$ and $L = R^\top = [1, 0, 1, 0, 1, 0]$. This selection results in two-sided reduced-order models of order $\nu = 6$.

We have constructed both families of reduced-order models that match the first and second approximate moment by using Theorems 15 and 16. Fig. 5.1 (a) (top) shows the time histories of the output of the full-order model (blue/solid line) and of the output of the reduced-order model from Theorem 15 when $k = 1$ (red/dashed line) and $k = 2$ (black/dotted line). Fig. 5.1 (a) (bottom) shows the respective absolute errors. Fig. 5.1 (b) (top) shows the time histories of the 4-th component[1] of ϖ for the full-order model (blue/solid) and for the reduced-order model from Theorem 7 when $k = 1$ (red/dashed) and $k = 2$ (black/dotted). Fig. 5.1 (a) (bottom) shows the respective absolute errors. Fig. 5.2 shows the same quantities for the family from Theorem 16 with G randomly selected.

As shown in the figures, both reduced-order models provide good approximations of the steady-state responses of interest. It is also clear that when we consider the matching of higher approximate moments (compare the case $k = 2$ with the case $k = 1$), the accuracy of the approximation improves, i.e. the error becomes smaller. Note that, while the two families of reduced-order models have similar steady-state performances, simulations with the model from Theorem 15 are several times slower than simulations with the model from Theorem 16, indicating that in practice the second model is less complex.

[1]Note that this component is randomly selected and all other components have similar behaviour.

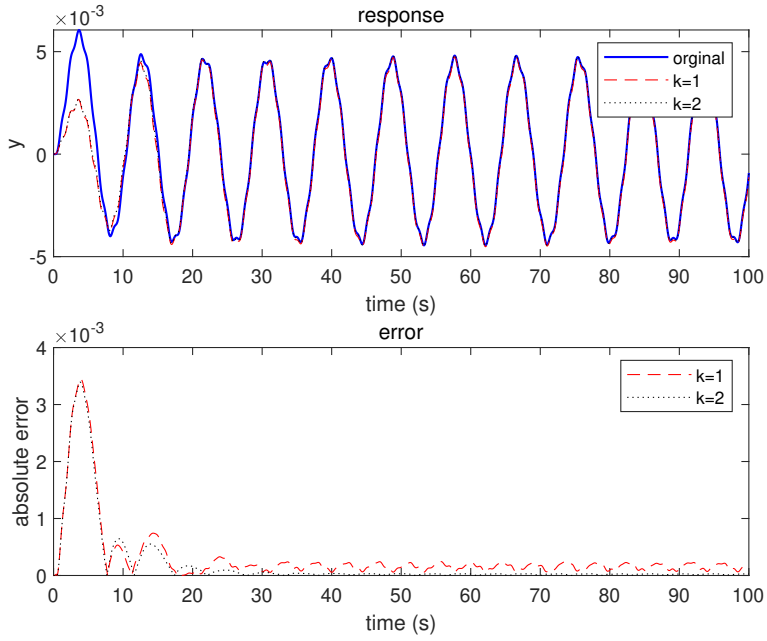

(a) Top: time histories of the output of the full-order model (blue/solid) and of the output of the reduced-order model when $k = 1$ (red/dashed), $k = 2$ (black/dotted). Bottom: respective absolute errors.

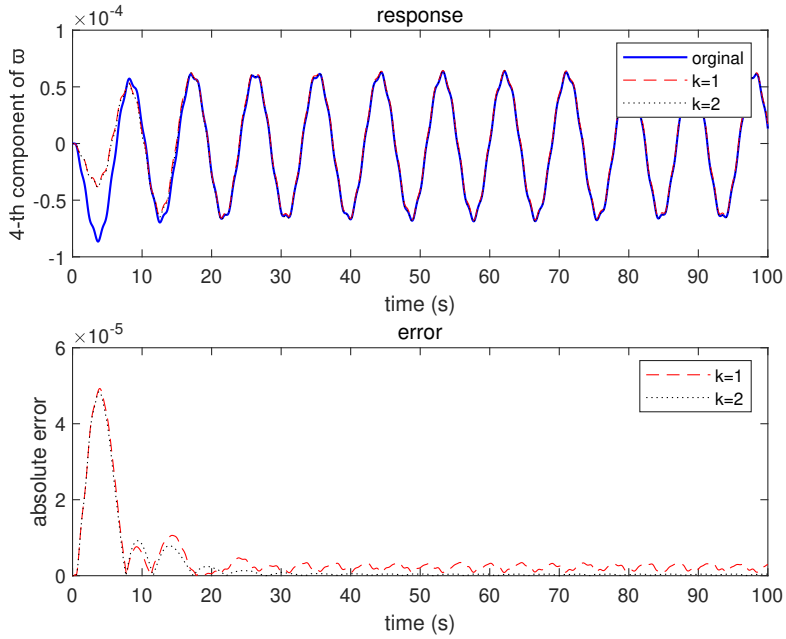

(b) Top: time histories of the 4-th component of ϖ for the full-order model (blue/solid) and for the reduced-order model when $k = 1$ (red/dashed), $k = 2$ (black/dotted). Bottom: respective absolute errors.

Figure 5.1: Simulations for the first family of reduced-order models.

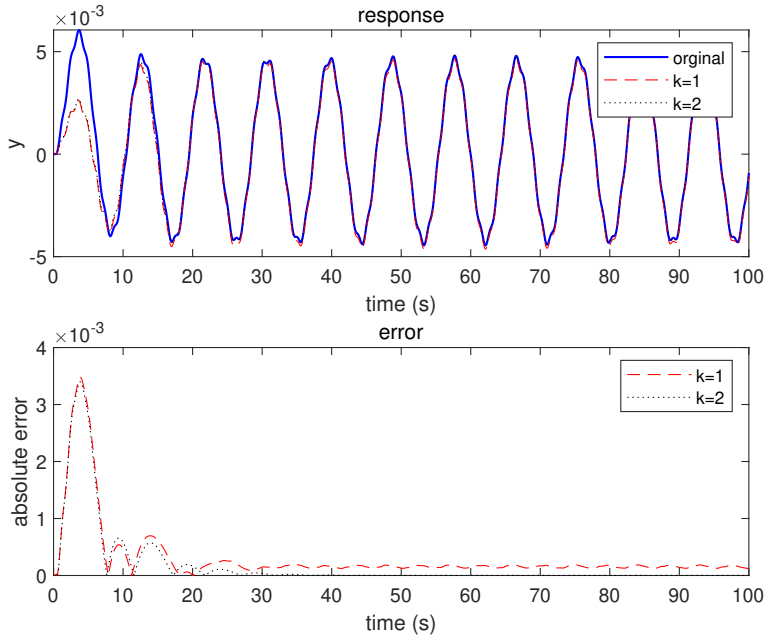

(a) Top: time histories of the output of the full-order model (blue/solid) and of the output of the reduced-order model when $k = 1$ (red/dashed), $k = 2$ (black/dotted). Bottom: respective absolute errors.

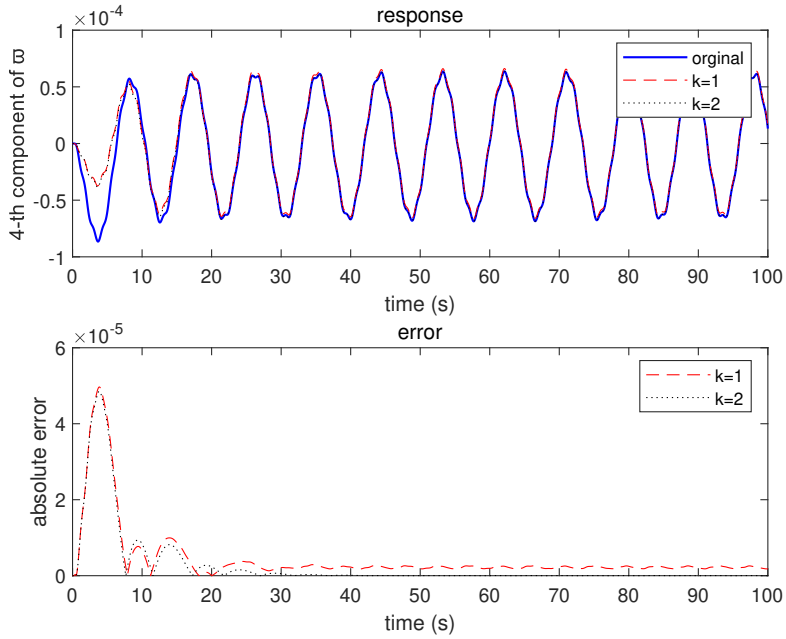

(b) Top: time histories of the 4-th component of ϖ for the full-order model (blue/solid) and for the reduced-order model when $k = 1$ (red/dashed), $k = 2$ (black/dotted). Bottom: respective absolute errors.

Figure 5.2: Simulations for the second family of reduced-order models.

Chapter 6

Interconncection-based Model Order Reduction for Quadratic-Bilinear Time-Delay Systems

The results of this chapter are based on [106]. In this chapter we propose an enhanced method that, exploiting the special structure of quadratic-bilinear systems, allows to easily compute approximations of the nonlinear moment and obtain reduced-order models which preserve the quadratic-bilinear time-delay structure.

The remainder of this chapter is organized as follows. Section 6.1 characterizes the nonlinear moment for quadratic-bilinear time-delay systems by solving a system of Sylvester-like equations, based on which a family of reduced-order models is presented in Section 6.2. In Section 6.3, the results are demonstrated by via numerical example.

6.1 Moments for Quadratic-Bilinear Systems with Delays

Consider the quadratic-bilinear, SISO, continuous-time, time-delay system described by the equations

$$\begin{aligned} \dot{x} &= \sum_{\tau_i \in \mathcal{T}_x} A_i x_{\tau_i} + \sum_{\tau_i \in \mathcal{T}_x} H_i (x_{\tau_i} \otimes x_{\tau_i}) + \sum_{\lambda_j \in \mathcal{T}_u} B_j u_{\lambda_j} + \sum_{\tau_i \in \mathcal{T}_x} \sum_{\lambda_j \in \mathcal{T}_u} N_{ij} x_{\tau_i} u_{\lambda_j}, \\ y &= Cx, \qquad\qquad x(\theta) = q(\theta), \qquad\qquad -T \leq \theta \leq 0, \end{aligned} \tag{6.1}$$

where $x(t) \in \mathbb{R}^n$, $u(t) \in \mathbb{R}$, $y(t) \in \mathbb{R}$, $q \in \mathfrak{R}_T^n$, $A_i \in \mathbb{R}^{n \times n}$, $N_{ij} \in \mathbb{R}^{n \times n}$, $H_i \in \mathbb{R}^{n \times n^2}$, $B_j \in \mathbb{R}^n$, $C^\top \in \mathbb{R}^n$.

Consider a linear signal generator (3.2). In the context of system (6.1) we can provide a series of simple conditions that ensure that the mapping in Assumption 11 exists (in virtue of the center manifold theory for time-delay systems, see [96]). In virtue of their simplicity, we replace Assumption 11 with the following.

Assumption 16. The zero equilibrium of system (6.1) is locally exponentially stable and the matrix S has simple eigenvalues with $\sigma(S) \subset \mathbb{C}_0$.

In addition, since the linear signal generator (3.2) is considered, Assumption 12 reduces to its linear version.

Assumption 17. The pair (S, L) is observable.

We now present a result that allows computing the nonlinear moment of (6.1) by solving a series of linear equations recursively.

Theorem 17. Consider the system (6.1) and the signal generator (3.2), and suppose that Assumptions 16 and 17 hold. Then there is a mapping

$$\pi(\omega) = \sum_{k \geq 1} \Pi_k \omega^{(k)} \tag{6.2}$$

which formally solves the partial differential equation

$$\begin{aligned}\frac{\partial \pi}{\partial \omega} S\omega = &\sum_{\tau_i \in \mathcal{T}_x} A_i \pi(\omega_{\tau_i}) + \sum_{\tau_i \in \mathcal{T}_x} H_i(\pi(\omega_{\tau_i}) \otimes \pi(\omega_{\tau_i})) \\ &+ \sum_{\lambda_j \in \mathcal{T}_u} B_j L\omega_{\lambda_j} + \sum_{\tau_i \in \mathcal{T}_x} \sum_{\lambda_j \in \mathcal{T}_u} N_{ij} \pi(\omega_{\tau_i}) L\omega_{\lambda_j}\end{aligned} \tag{6.3}$$

where the Π_k's, $k \geq 1$, are the solutions of the following system of Sylvester-like equations

$$\begin{aligned}\Pi_1 S =& \sum_{\tau_i \in \mathcal{T}_x} A_i \Pi_1 e^{-S\tau_i} + \sum_{\lambda_j \in \mathcal{T}_u} B_j L e^{-S\lambda_j}, \\ \Pi_2 S^{[2]} =& \sum_{\tau_i \in \mathcal{T}_x} A_i \Pi_2 (e^{-S\tau_i})^{(2)} + \sum_{\tau_i \in \mathcal{T}_x} H_i(\Pi_1 \otimes \Pi_1)(e^{-S\tau_i})^{(2)} \\ &+ \sum_{\tau_i \in \mathcal{T}_x} \sum_{\lambda_j \in \mathcal{T}_u} N_{ij}(\Pi_1 \otimes L)(e^{-S\tau_i} \otimes e^{-S\lambda_j}), \\ \Pi_k S^{[k]} =& \sum_{\tau_i \in \mathcal{T}_x} A_i \Pi_k (e^{-S\tau_i})^{(k)} + \sum_{\tau_i \in \mathcal{T}_x} H_i(\Pi_1 \otimes \Pi_{k-1} \\ &+ \Pi_2 \otimes \Pi_{k-2} + \cdots + \Pi_{k-1} \otimes \Pi_1)(e^{-S\tau_i})^{(k)} \\ &+ \sum_{\tau_i \in \mathcal{T}_x} \sum_{\lambda_j \in \mathcal{T}_u} N_{ij}(\Pi_{k-1} \otimes L)((e^{-S\tau_i})^{(k-1)} \otimes e^{-S\lambda_j}),\end{aligned} \tag{6.4}$$

for $k \geq 3$.

Proof. By Assumptions 16 and 17, equation (6.3) has a solution π [101]. Consider the formal power series expansion of π, that is (6.2). Substituting (6.2) into (6.3) yields

$$\begin{aligned}&\frac{\partial(\Pi_1\omega + \Pi_2(\omega \otimes \omega) + \cdots)}{\partial \omega} S\omega \\ &= \sum_{\tau_i \in \mathcal{T}_x} A_i(\Pi_1 e^{-S\tau_i}\omega + \Pi_2(e^{-S\tau_i})^{(2)}(\omega \otimes \omega) + \cdots) \\ &+ \sum_{\tau_i \in \mathcal{T}_x} H_i(\Pi_1 e^{-S\tau_i}\omega + \Pi_2(e^{-S\tau_i})^{(2)}(\omega \otimes \omega) + \cdots)^{(2)} \\ &+ \sum_{\tau_i \in \mathcal{T}_x} \sum_{\lambda_j \in \mathcal{T}_u} N_{ij}(\Pi_1 e^{-S\tau_i}\omega + \Pi_2(e^{-S\tau_i}) L e^{-S\lambda_j}\omega \\ &+ \sum_{\lambda_j \in \mathcal{T}_u} B_j L e^{-S\lambda_j}\omega.\end{aligned} \tag{6.5}$$

The equations in (6.4) can be obtained by matching the powers of $\omega^{(k)}$, $k = 1, 2, \cdots$. In particular,

considering the linear terms in ω, it is easy to see that Π_1 must satisfy the Sylvester-like equation

$$\Pi_1 S = \sum_{\tau_i \in \mathcal{T}_x} A_i \Pi_1 e^{-S\tau_i} + \sum_{\lambda_j \in \mathcal{T}_u} B_j L e^{-S\lambda_j}. \tag{6.6}$$

Considering now the terms in $\omega \otimes \omega$, we have that

$$\begin{aligned} \frac{\partial(\Pi_2(\omega \otimes \omega))}{\partial \omega} S\omega = & \sum_{\tau_i \in \mathcal{T}_x} A_i \Pi_2 (e^{-S\tau_i}\omega \otimes e^{-S\tau_i}\omega) + \\ & \sum_{\tau_i \in \mathcal{T}_x} H_i (\Pi_1 e^{-S\tau_i}\omega) \otimes (\Pi_1 e^{-S\tau_i}\omega) + \\ & \sum_{\tau_i \in \mathcal{T}_x} \sum_{\lambda_j \in \mathcal{T}_u} N_{ij} (\Pi_1 e^{-S\tau_i}\omega) L e^{-S\lambda_j}\omega. \end{aligned} \tag{6.7}$$

Applying the properties P1) and P3), and condition (iii) of Lemma 3, it follows that Π_2 is the solution of the Sylvester-like equation

$$\begin{aligned} \Pi_2 S^{[2]} = & \sum_{\tau_i \in \mathcal{T}_x} A_i \Pi_2 (e^{-S\tau_i})^{(2)} + \sum_{\tau_i \in \mathcal{T}_x} H_i (\Pi_1 \otimes \Pi_1)(e^{-S\tau_i})^{(2)} \\ & + \sum_{\tau_i \in \mathcal{T}_x} \sum_{\lambda_j \in \mathcal{T}_u} N_{ij} (\Pi_1 \otimes L)(e^{-S\tau_i} \otimes e^{-S\lambda_j}). \end{aligned} \tag{6.8}$$

Following the same reasoning, it can be shown that Π_k, for $k \geq 3$, are solutions of (6.4). □

Based on Definition 5, the moment of this kind of system at (S, L) can be obtained as $\sum_{k \geq 1} C \Pi_k \omega^{(k)}$.

Remark 8. It is possible that the original system has a time-delay output mapping, *i.e.*, $y = \sum_{\tau_i \in \mathcal{T}_x} C_i x_{\tau_i}$. In this case, the moment can be generalized as $\sum_{k \geq 1} \sum_{\tau_i \in \mathcal{T}_x} C_i \Pi_k \left(e^{-S\tau_i}\right)^{(k)} \omega^{(k)}$. This follows trivially from

$$\begin{aligned} \sum_{\tau_i \in \mathcal{T}_x} C_i \pi(\omega_{\tau_i}) &= \sum_{\tau_i \in \mathcal{T}_x} C_i \sum_{k \geq 1} \Pi_k \omega_{\tau_i}^{(k)} \\ &= \sum_{\tau_i \in \mathcal{T}_x} C_i \sum_{k \geq 1} \Pi_k \left(e^{-S\tau_i}\right)^{(k)} \omega^{(k)} \\ &= \sum_{k \geq 1} \sum_{\tau_i \in \mathcal{T}_x} C_i \Pi_k \left(e^{-S\tau_i}\right)^{(k)} \omega^{(k)}. \end{aligned} \tag{6.9}$$

In order to simplify the discussion, we consider delay-free output mapping in the rest of the

thesis.

From a practical point of view, it is useful to define an approximate version of the moment which uses a finite number of terms Π_k, $k = 1, 2, \cdots, m$.

Definition 9. We call $\sum_{k=1}^{m} C\Pi_k\omega^{(k)}$ the m-th approximate moment of system (6.1) at (S, L), with the following asymptotic property for all ω

$$\lim_{m\to\infty} \sum_{k=1}^{m} C\Pi_k\omega^{(k)} - C\pi(\omega) = 0. \tag{6.10}$$

6.2 A Family of Reduced-Order Models

In this section a family of reduced-order models is introduced to match the k-th approximate moment of system (6.1). We guarantee that the reduced-order model is a quadratic-bilinear time-delay system with a nonlinear delay-free output mapping, namely it is described by the equations

$$\begin{aligned} \dot{\xi} &= \sum_{\chi_i\in\mathcal{T}_\xi} F_i\xi_{\chi_i} + \sum_{\chi_i\in\mathcal{T}_\xi} G_i(\xi_{\chi_i}\otimes\xi_{\chi_i}) + \sum_{\gamma_j\in\mathcal{T}_{\bar{u}}} E_j u_{\gamma_j} + \sum_{\chi_i\in\mathcal{T}_x}\sum_{\gamma_j\in\mathcal{T}_{\bar{u}}} M_{ij}\xi_{\chi_i}u_{\gamma_j}, \\ \psi &= \sum_{k\geq 1} D_k\xi^{(k)} \end{aligned} \tag{6.11}$$

where $F_i \in \mathbb{R}^{v\times v}$, $M_{ij} \in \mathbb{R}^{v\times v}$, $G_i \in \mathbb{R}^{v\times v^2}$, $E_j \in \mathbb{R}^{v}$, $D_k^\top \in \mathbb{R}^{v^k}$,and $\mathcal{T}_\xi = \{\chi_i \in \mathbb{R}_{\geq 0}\}$, with $\chi_0 = 0$ and $\mathcal{T}_{\bar{u}} = \{\gamma_j \in \mathbb{R}_{>0}\}$ are sets of delays for states and inputs, respectively. In the following statement we give conditions on F_i, Π_k, E_j and D_k such that (6.11) is indeed a reduced-order model by moment matching of (6.1).

Definition 10. System (6.11) is a reduced-order model by moment matching of system (6.1) at (S, L) if it has the same moments at (S, L).

Lemma 4. Consider the system (6.1), the signal generator (3.2), the model (6.11) and suppose that Assumptions 16 and 17 hold. System (6.11) is a reduced-order model by moment matching

of system (6.1) at (S, L) if $v < n$ and the equations

$$\begin{aligned} C\Pi_1 e^{-S\tau_i} &= D_1 P_{(1,1)}, \\ C\Pi_k (e^{-S\tau_i})^{(k)} &= D_1 P_{(k,1)} + D_2 P_{(k,2)} + \cdots \\ &\quad + D_{k-1} P_{(k,k-1)} + D_k P_{(k,k)}, \end{aligned} \tag{6.12}$$

for all $k > 1$, hold, where

$$P_{(i,j)} = \begin{cases} P_i, & j = 1, \\ \sum_{k=1}^{i-j+1} P_k \otimes P_{(i-k,j-1)}, & j \geq 2, \end{cases} \tag{6.13}$$

for $i \geq 1$, $j \leq i$ and P_k are the solutions to the equations

$$\begin{aligned} P_1 S &= \sum_{\chi_i \in \mathcal{T}_\xi} F_i P_1 e^{-S\chi_i} + \sum_{\gamma_j \in \mathcal{T}_{\bar{u}}} E_j L e^{-S\gamma_j}, \\ P_2 S^{[2]} &= \sum_{\chi_i \in \mathcal{T}_\xi} F_i P_2 (e^{-S\chi_i})^{(2)} + \sum_{\chi_i \in \mathcal{T}_\xi} G_i (P_1 \otimes P_1)(e^{-S\chi_i})^{(2)} \\ &\quad + \sum_{\chi_i \in \mathcal{T}_\xi} \sum_{\gamma_j \in \mathcal{T}_{\bar{u}}} M_{ij} (P_1 \otimes L)(e^{-S\chi_i} \otimes e^{-S\gamma_j}), \\ P_k S^{[k]} &= \sum_{\chi_i \in \mathcal{T}_\xi} F_i P_k (e^{-S\chi_i})^{(k)} + \sum_{\chi_i \in \mathcal{T}_\xi} G_i (P_1 \otimes P_{k-1} \\ &\quad + P_2 \otimes P_{k-2} + \cdots \quad + P_{k-1} \otimes P_1)(e^{-S\chi_i})^{(k)} \\ &\quad + \sum_{\chi_i \in \mathcal{T}_\xi} \sum_{\gamma_j \in \mathcal{T}_{\bar{u}}} M_{ij} (P_{k-1} \otimes L)((e^{-S\chi_i})^{(k-1)} \otimes e^{-S\gamma_j}), \end{aligned} \tag{6.14}$$

for $k \geq 3$.

Proof. Applying Theorem 17 to system (6.11), the moment of the systems (6.11) at (S, L) is characterized by a mapping p solving

$$\begin{aligned} \frac{\partial p(\omega)}{\partial \omega} S\omega &= \sum_{\chi_i \in \mathcal{T}_\xi} F_i p(\omega_{\chi_i}) + \sum_{\chi_i \in \mathcal{T}_\xi} G_i (p(\omega_{\chi_i}) \otimes p(\omega_{\chi_i})) \\ &\quad + \sum_{\gamma_j \in \mathcal{T}_{\bar{u}}} E_j L \omega_{\gamma_j} + \sum_{\chi_i \in \mathcal{T}_\xi} \sum_{\gamma_j \in \mathcal{T}_{\bar{u}}} M_{ij} p(\omega_{\chi_i}) L \omega_{\gamma_j}. \end{aligned} \tag{6.15}$$

Considering the formal power series

$$p(\omega) = \sum_{k\geq 1} P_k \omega^{(k)}, \tag{6.16}$$

yields the system of equations (6.14). Recall that p must also solve the moment matching condition, namely

$$C \sum_{k\geq 1} \Pi_k \omega^{(k)} = \sum_{j\geq 1} D_j \sum_{k\geq 1} P_k \omega^{(k)}. \tag{6.17}$$

This equation yields

$$\begin{aligned}
&C\Pi_1\omega + C\Pi_2(\omega\otimes\omega) + C\Pi_3(\omega\otimes\omega\otimes\omega) + \cdots \\
&= D_1P_1\omega + (D_1P_2 + D_2(P_1\otimes P_1))(\omega\otimes\omega) + (D_3P_1 + D_2(P_1\otimes P_2 + P_2\otimes P_1) \\
&\quad + D_3(P_1\otimes P_1\otimes P_1))(\omega\otimes\omega\otimes\omega) + \cdots \\
&= D_1P_{(1,1)}\omega + (D_1P_{(2,1)} + D_2P_{(2,2)})(\omega\otimes\omega) \\
&\quad + (D_3P_{(3,1)} + D_2P_{(3,2)} + D_3P_{(3,3)})(\omega\otimes\omega\otimes\omega) + \cdots .
\end{aligned} \tag{6.18}$$

By matching the power of $\omega^{(k)}$, the above implies that

$$C\Pi_k\omega^{(k)} = (D_1P_{(k,1)} + D_2P_{(k,2)} + \cdots + D_{k-1}P_{(k,k-1)} + D_kP_{(k,k)})\omega^{(k)} \tag{6.19}$$

which provides (6.12). Here, $P_{(i,j)}$ represents the coefficient matrix of $\omega^{(i)}$ corresponding to D_j. Then, it is easy to verify that $P_{(i,1)} = P_i$. Moreover, for $2 \leq j \leq i$

$$\begin{aligned}
P_{(i,j)}\omega^{(i)} &= (P_1\omega)\otimes(P_{(i-1,j-1)}\omega^{(i-1)}) \\
&\quad + (P_2\omega^{(2)})\otimes(P_{(i-2,j-1)}\omega^{(i-2)}) + \cdots \\
&\quad + (P_{(i-j+1)}\omega^{(i-j+1)})\otimes(P_{(j-1,j-1)}\omega^{(j-1)}) \\
&= (P_1\otimes P_{(i-1,j-1)} + P_2\otimes P_{(i-2,j-1)} + \cdots \\
&\quad + P_{(i-j+1)}\otimes P_{(j-1,j-1)})\omega^{(i)} \\
&= \left(\sum_{k=1}^{i-j+1} P_k\otimes P_{(i-k,j-1)}\right)\omega^{(i)},
\end{aligned} \tag{6.20}$$

which yields (6.13). This completes the proof. □

We can now use some of the free parameters of the model to satisfy the conditions in Lemma 4.

Theorem 18. Consider the system (6.1) and the signal generator (3.2), and suppose that Assumptions 16 and 17 hold. Then

$$\begin{aligned}\dot{\xi} &= F_0\xi + \sum_{\chi_i\in\mathcal{T}_\xi\setminus\{0\}} F_i\xi_{\chi_i} + \sum_{\chi_i\in\mathcal{T}_\xi} G_i(\xi_{\chi_i}\otimes\xi_{\chi_i}) \\ &\quad + \sum_{\gamma_j\in\mathcal{T}_{\bar{u}}} E_j u_{\gamma_j} + \sum_{\chi_i\in\mathcal{T}_x}\sum_{\gamma_j\in\mathcal{T}_{\bar{u}}} M_{ij}\xi_{\chi_i}u_{\gamma_j}, \\ \bar{\psi}(t) &= \sum_{k=1}^{n} D_k\xi^{(k)}(t),\end{aligned} \tag{6.21}$$

where

$$F_0 = S - \sum_{\gamma_j\in\mathcal{T}_{\bar{u}}} E_j L e^{-S\gamma_j} - \sum_{\chi_i\in\mathcal{T}_\xi\setminus\{0\}} F_i e^{-S\chi_i}, \tag{6.22}$$

and

$$\begin{aligned}D_1 &= C\Pi_1, \\ D_2 &= C\Pi_2 - D_1P_{(2,1)}, \\ D_k &= C\Pi_k - D_1P_{(k,1)} - D_2P_{(k,2)} + \cdots \\ &\qquad - D_{k-1}P_{(k,k-1)},\end{aligned} \tag{6.23}$$

for $k \geq 3$, is a family of reduced-order models of system (6.1) at (S, L) that match the m-th approximate moment.

Proof. In order to match the n-th approximate moment, we only consider π and p with n terms and select $P_1 = I_v$. Then from equation (6.13), when $i = j$,

$$P_{(i,i)} = I_{v^i} \tag{6.24}$$

for all $i \geq 1$. The proposed model still has several free parameters, i.e. F_i $(i \geq 1)$, E_j, G_i, M_{ij}, $\mathcal{T}_\xi$ and $\mathcal{T}_{\bar{u}}$, which can be used to enforce additional properties of the model such as stability.

F_0 is determined by (6.22) directly from equation (6.14) and the D_k's are selected as in (6.23) (computed for the specific selection of F_i, E_j, G_i and M_{ij} from (6.13), (6.14), (6.22) and (6.24)). According to Lemma 3, system (6.21) is a reduced-order model of (6.1) by moment matching. □

Remark 9. Selecting $\mathcal{T}_\xi = \{0\}$ and $\mathcal{T}_{\bar{u}} = \{0\}$ results in a reduced-order model without time delays and this model coincides with the one presented in Section 3.2. However, by eliminating delays, the infinite-dimensional system is reduced to a finite-dimensional system, which could impact some of the specific dynamic properties of the model. For instance, delays do not always pose a negative effect to stability [128].

6.3 Numerical Example

We illustrate the results of this chaper by means of a numerical example. Consider the system (6.1) with order $n = 56$ and sets of delays $\mathcal{T}_x = \{0, 0.01\}$ and $\mathcal{T}_u = \{0.01, 0.001\}$, where $A_0 = \text{diag}(A_a, A_b, A_c, A_d)$ and $A_1 = \text{diag}(A_e, A_b, A_c, A_d)$, with

$A_a = \text{diag}(-1, -3, \cdots, -99)$,
$A_e = \text{diag}(-2, -4, \cdots, -100)$,

$$A_b = \begin{bmatrix} -1 & 5 \\ -5 & -1 \end{bmatrix}, \quad A_c = \begin{bmatrix} -1 & 10 \\ -10 & -1 \end{bmatrix}, \quad A_d = \begin{bmatrix} -1 & 15 \\ -15 & -1 \end{bmatrix}.$$

$$B_0^\top = B_1^\top = C = \begin{bmatrix} 1 & 1 & \cdots & 1 & 1 & 0 & 1 & 0 & 1 & 0 \end{bmatrix}$$

and the remaining matrices H_0, H_1, N_0, N_1, N_2 and N_3 are generated randomly using the MATLAB command `rand` such that the system are stable [96]. The signal generator (3.2) is selected as $S = \text{diag}(0, S_b, S_c, S_d)$, with $S_b = A_b + I_2$, $S_c = A_c + I_2$, $S_d = A_d + I_2$, and $L = \begin{bmatrix} 1 & 1 & 0 & 1 & 0 & 1 & 0 \end{bmatrix}$, resulting in a reduced-order model with $\nu = 7$.

The free parametrizations E_0 and E_1 are determined by assigning the eigenvalues of F_0 and F_1 as certain subsets of the spectrum of A_0. We select the same delay sets as in the original system

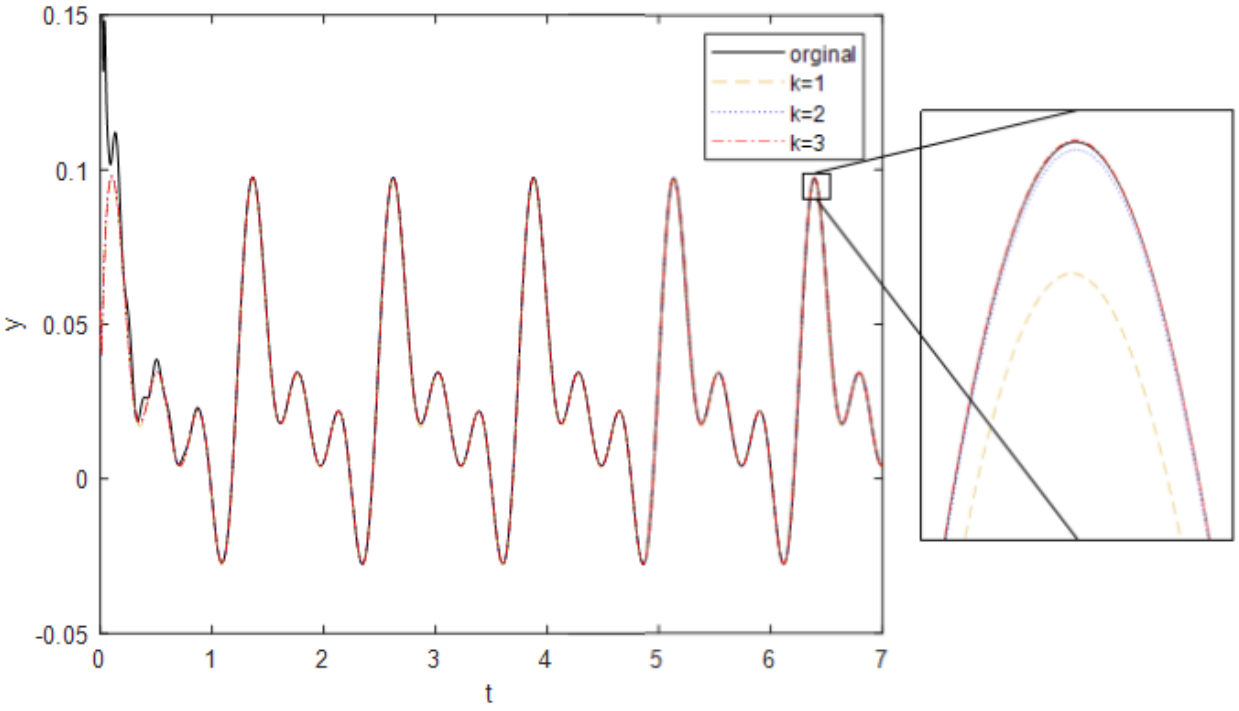

Figure 6.1: Time histories of the output of the original model (black/solid) and the output of the reduced-order model when $k = 1$ (yellow/dashed), $k = 2$ (blue/dotted), and $k = 3$ (red/dash-dotted).

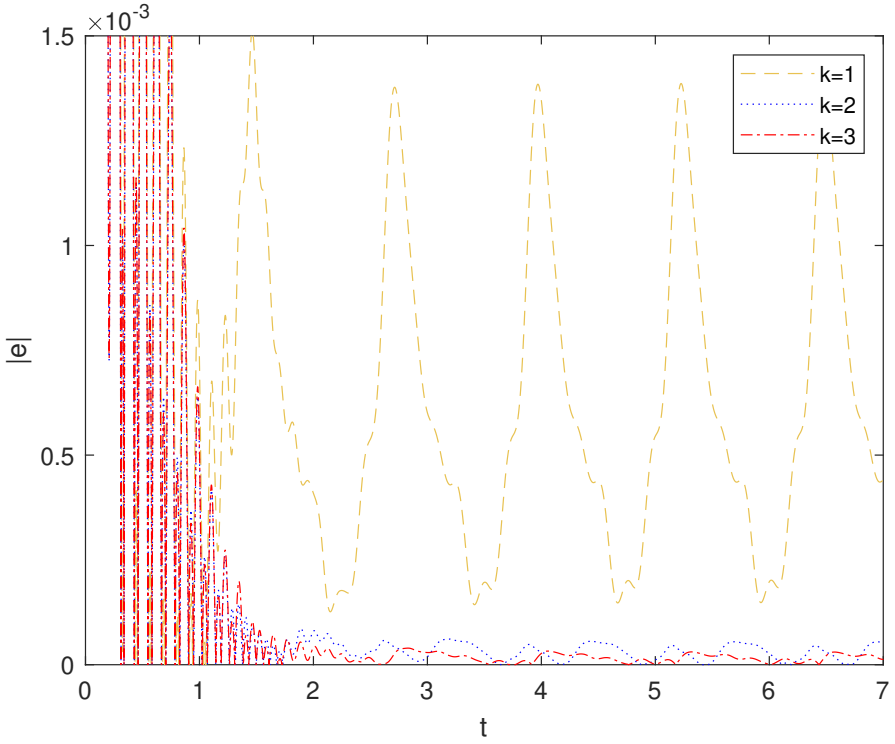

Figure 6.2: Time histories of the errors between the output of the original and the output of the reduced-order model when $k = 1$ (yellow/dashed), $k = 2$ (blue/dotted), and $k = 3$ (red/dash-dotted).

to preserve the time-delay structure. All the other free parameters in the reduced-order models are randomly generated since we do not have any other property to enforce.

We have computed the reduced-order models which match the k-th approximate moment for $k = 1$, $k = 2$, and $k = 3$, respectively. Fig. 6.1 displays the time histories of the outputs of the reduced-order models and of the original system, together with a zoom-in plot of the peak part of the steady-state responses. The time histories of the absolute error between the output of the reduced-order models and the output of the original system are reported in Fig. 6.2. The black/solid line represents the output of the original model, while the yellow/dashed, blue/dotted and red/dash-dotted lines denotes the reduced-order model with $k = 1, 2$ and 3, respectively.

As demonstrated by the figures, the reduced-order model provides good steady-state approximations of the output response. Note that a higher order k of the approximate moment for reduced-order models yields a higher approximation accuracy.

Chapter 7

Conclusions and Future Work

7.1 Original Contributions

The interconnection-based moment matching method has been developed with the primary objective to solve the model order reduction problem for imcompressible flows. By exploiting the solution of a system of Sylvester-like equations we have defined the direct nonlinear moment using a power series representation for quadratic-bilinear systems. Two families of reduced-order models have been proposed with some free parameters. We have also solved the problem of enforcing stability and a prescribed relative degree on the reduced-order models using available parameters. Applications to Naiver-Stokes type descriptor systems are given together with three examples in fluid field. The swapped moments have been defined in the same way via a power series representation. Considering together the "direct" moment and the "swapped" moment, we have proposed two families of reduced-order models that achieve two-sided approximate moment matching. The extension to quadratic-bilinear time-delay systems has been derived.

The original contributions of this Thesis can be classified as follows.

- Differently from the wide literature about the interpolation/Krylov methods (also called moment matching) of quadratic-bilinear systems, which are based on the linear notion of moment (i.e. linked to the transfer function), this work is based on the nonlinear notion

of moment (i.e. based on the steady-state response). We compute and exploit is the nonlinear moment without any reference to any type of generalized transfer functions. The reduced-order model we have constructed has a special structure and some free parameters that can be easily exploited to preserve additional properties of the model (e.g. stability). In addition, we can propose both model-based and a data-driven implementations, the latter being computationally faster.

- The proposed interconnection-based method has some advantages with respect to the general nonlinear moment matching framework presented in [60] and related papers: exploiting the structure of the class of systems under study, we have proposed an explicit way of approximating the solution of the invariance partial differential equation defining the nonlinear moment.

- With respect to [75], in which two-sided reduced-order models for general nonlinear systems were given, the two-sided approach we have developed gives easy to compute approximations of the nonlinear (swapped) moment and reduced-order models that preserve the quadratic-bilinear structure.

7.2 Future Work

There are some further research directions to be investigated by exploiting the results of this thesis. First, of great importance is the completion of the data-driven approach. While the thesis focuses solely on the direct case, future efforts could extend to examining swapped interconnections. Such exploration would enable the data-driven formulation of the two-sided approach developed in Chapter 5, potentially decreasing computational complexity.

Another research path worth pursuing involves advancing two-sided moment matching techniques for quadratic-bilinear time-delay systems, building upon the insights provided in Chapters 5 and 6. The research on this area is scarce. What we aim to do is to refine and extend the methodologies discussed in these chapters, offering a more comprehensive approach to handling the complexities associated with these types of systems.

Finally, while the focus of this thesis is primarily on systems with a single input, an intriguing area for future research involves extending these concepts to multiple inputs and multiple outputs (MIMO) systems. Such an exploration could lead to significant advancements, particularly in fields such as power systems, where the complexity and scale of the systems involved necessitate sophisticated modelling strategies.

Bibliography

[1] G. Scarciotti and A. Astolfi, "Interconnection-based model order reduction-a survey," *European Journal of Control*, p. 100929, 2023.

[2] P. Goyal, M. I. Ahmad, and P. Benner, "Model reduction of quadratic-bilinear descriptor systems via Carleman bilinearization," in *European Control Conference (ECC)*, 2015, pp. 1177–1182.

[3] E. Erturk, "Benchmark solutions of driven polar cavity flow at high Reynolds numbers," *International Journal of Mechanical Engineering and Technology*, vol. 9, no. 8, pp. 776–786, 2018.

[4] A. Quarteroni, G. Rozza *et al.*, *Reduced order methods for modeling and computational reduction*. Springer, 2014, vol. 9.

[5] P. Benner, M. Ohlberger, A. Patera, G. Rozza, K. Urban *et al.*, *Model reduction of parametrized systems*. Springer, 2017.

[6] C. W. Rowley and S. T. Dawson, "Model reduction for flow analysis and control," *Annual Review of Fluid Mechanics*, vol. 49, pp. 387–417, 2017.

[7] C. Gu, "Qlmor: A projection-based nonlinear model order reduction approach using quadratic-linear representation of nonlinear systems," *IEEE Transactions on Computer-Aided Design of Integrated Circuits and Systems*, vol. 30, no. 9, pp. 1307–1320, 2011.

[8] P. Benner and T. Breiten, "Two-sided projection methods for nonlinear model order reduction," *SIAM Journal on Scientific Computing*, vol. 37, no. 2, pp. B239–B260, 2015.

[9] N. Yadaiah and N. V. Ramana, "Linearisation of multi-machine power system: modeling and control–a survey," *International Journal of Electrical Power & Energy Systems*, vol. 29, no. 4, pp. 297–311, 2007.

[10] G. Scarciotti, "Low computational complexity model reduction of power systems with preservation of physical characteristics," *IEEE Transactions on Power Systems*, vol. 32, no. 1, pp. 743–752, 2017.

[11] Z. Gong, J. Mao, A. Junyent-Ferre, and G. Scarciotti, "Model order reduction of large-scale wind farms: A data-driven approach," *Submitted*, 2024.

[12] A. C. Antoulas, D. C. Sorensen, and S. Gugercin, "A survey of model reduction methods for large-scale systems," *Contemporary mathematics*, vol. 280, pp. 193–220, 2001.

[13] A. C. Antoulas, *Approximation of large-scale dynamical systems*. SIAM, 2005.

[14] D. F. Enns, "Model reduction with balanced realizations: An error bound and a frequency weighted generalization," in *Conference on Decision and Control*. IEEE, 1984, pp. 127–132.

[15] K. Glover, R. F. Curtain, and J. R. Partington, "Realisation and approximation of linear infinite-dimensional systems with error bounds," *SIAM Journal on Control and Optimization*, vol. 26, no. 4, pp. 863–898, 1988.

[16] J. Lam and B. Anderson, "L_1 impulse response error bound for balanced truncation," *Systems & Control Letters*, vol. 18, no. 2, pp. 129–137, 1992.

[17] B. Moore, "Principal component analysis in linear systems: Controllability, observability, and model reduction," *IEEE Transactions on Automatic Control*, vol. 26, no. 1, pp. 17–32, 1981.

[18] C. Mullis and R. Roberts, "Synthesis of minimum roundoff noise fixed point digital filters," *IEEE Transactions on Circuits and Systems*, vol. 23, no. 9, pp. 551–562, 1976.

[19] R. Ober and D. McFarlane, "Balanced canonical forms for minimal systems: A normalized coprime factor approach," *Linear Algebra and its Applications*, vol. 122, pp. 23–64, 1989.

[20] S. Gugercin and A. C. Antoulas, "A survey of model reduction by balanced truncation and some new results," *International Journal of Control*, vol. 77, no. 8, pp. 748–766, 2004.

[21] P. Benner, E. S. Quintana-Ortí, and G. Quintana-Ortí, "Efficient numerical algorithms for balanced stochastic truncation," *International Journal of Applied Mathematics and Computer Science*, vol. 11, no. 5, pp. 1123–1150, 2001.

[22] M. Green, "A relative error bound for balanced stochastic truncation," *IEEE Transactions on Automatic Control*, vol. 33, no. 10, pp. 961–965, 1988.

[23] ——, "Balanced stochastic realizations," *Linear Algebra and its Applications*, vol. 98, pp. 211–247, 1988.

[24] X. Cheng and J. M. Scherpen, "Introducing network gramians to undirected network systems for structure-preserving model reduction," in *Conference on Decision and Control*. IEEE, 2016, pp. 5756–5761.

[25] W. Gawronski and J.-N. Juang, "Model reduction in limited time and frequency intervals," *International Journal of Systems Science*, vol. 21, no. 2, pp. 349–376, 1990.

[26] R. Ober, "Balanced parametrization of classes of linear systems," *SIAM Journal on Control and Optimization*, vol. 29, no. 6, pp. 1251–1287, 1991.

[27] P. M. Wortelboer, M. Steinbuch, and O. H. Bosgra, "Iterative model and controller reduction using closed-loop balancing, with application to a compact disc mechanism," *International Journal of Robust and Nonlinear Control*, vol. 9, no. 3, pp. 123–142, 1999.

[28] K. Zhou, G. Salomon, and E. Wu, "Balanced realization and model reduction for unstable systems," *International Journal of Robust and Nonlinear Control*, vol. 9, no. 3, pp. 183–198, 1999.

[29] B. Besselink, N. van de Wouw, J. M. Scherpen, and H. Nijmeijer, "Model reduction for nonlinear systems by incremental balanced truncation," *IEEE Transactions on Automatic Control*, vol. 59, no. 10, pp. 2739–2753, 2014.

[30] K. Fujimoto and J. M. Scherpen, "Balanced realization and model order reduction for nonlinear systems based on singular value analysis," *SIAM Journal on Control and Optimization*, vol. 48, no. 7, pp. 4591–4623, 2010.

[31] J. Hahn and T. F. Edgar, "Balancing approach to minimal realization and model reduction of stable nonlinear systems," *Industrial & engineering chemistry research*, vol. 41, no. 9, pp. 2204–2212, 2002.

[32] ——, "An improved method for nonlinear model reduction using balancing of empirical gramians," *Computers & Chemical Engineering*, vol. 26, no. 10, pp. 1379–1397, 2002.

[33] A. Varga, "Balanced truncation model reduction of periodic systems," in *Conference on Decision and Control*, vol. 3. IEEE, 2000, pp. 2379–2384.

[34] S. Lall and C. Beck, "Error-bounds for balanced model-reduction of linear time-varying systems," *IEEE Transactions on Automatic Control*, vol. 48, no. 6, pp. 946–956, 2003.

[35] H. Sandberg and A. Rantzer, "Balanced truncation of linear time-varying systems," *IEEE Transactions on Automatic Control*, vol. 49, no. 2, pp. 217–229, 2004.

[36] N. Lang, J. Saak, and T. Stykel, "Balanced truncation model reduction for linear time-varying systems," *Mathematical and Computer Modelling of Dynamical Systems*, vol. 22, no. 4, pp. 267–281, 2016.

[37] P. Benner and P. Goyal, "An iterative model reduction scheme for quadratic-bilinear descriptor systems with an application to navier–stokes equations," in *Reduced-Order Modeling (ROM) for Simulation and Optimization: Powerful Algorithms as Key Enablers for Scientific Computing*. Springer, 2018, pp. 1–19.

[38] P. Benner and T. Stykel, *Model order reduction for differential-algebraic equations: a survey*. Springer, 2017.

[39] F. D. Freitas, J. Rommes, and N. Martins, "Gramian-based reduction method applied to large sparse power system descriptor models," *IEEE Transactions on Power Systems*, vol. 23, no. 3, pp. 1258–1270, 2008.

[40] S. Gugercin, T. Stykel, and S. Wyatt, "Model reduction of descriptor systems by interpolatory projection methods," *SIAM Journal on Scientific Computing*, vol. 35, no. 5, pp. B1010–B1033, 2013.

[41] M. Heinkenschloss, D. C. Sorensen, and K. Sun, "Balanced truncation model reduction for a class of descriptor systems with application to the Oseen equations," *SIAM Journal on Scientific Computing*, vol. 30, no. 2, pp. 1038–1063, 2008.

[42] K. Perev and B. Shafai, "Balanced realization and model reduction of singular systems," *International Journal of Systems Science*, vol. 25, no. 6, pp. 1039–1052, 1994.

[43] J. A. Ball, I. Gohberg, and L. Rodman, "Realization and interpolation of rational matrix functions," *Topics in interpolation theory of rational matrix-valued functions*, pp. 1–72, 1988.

[44] J. Ball and I. Gohberg, *Interpolation of rational matrix functions*. Birkhäuser, 2013, vol. 45.

[45] S. Kung and D. Lin, "Optimal Hankel-norm model reductions: Multivariable systems," *IEEE Transactions on Automatic Control*, vol. 26, no. 4, pp. 832–852, 1981.

[46] M. Safonov, R. Chiang, and D. Limebeer, "Optimal Hankel model reduction for nonminimal systems," *IEEE Transactions on Automatic Control*, vol. 35, no. 4, pp. 496–502, 1990.

[47] K. Fujimoto and J. M. Scherpen, "Model reduction for nonlinear systems based on the differential eigenstructure of Hankel operators," in *Conference on Decision and Control*, vol. 4. IEEE, 2001, pp. 3252–3257.

[48] ——, "Nonlinear balanced realization based on singular value analysis of Hankel operators," in *Conference on Decision and Control*, vol. 6. IEEE, 2003, pp. 6072–6077.

[49] ——, "Balancing and model reduction for discrete-time nonlinear systems based on Hankel singular value analysis," in *16th MTNS Conference, Leuven, Belgium*. University of Groningen, Research Institute of Technology and Management, 2004.

[50] ——, "Nonlinear input-normal realizations based on the differential eigenstructure of Hankel operators," *IEEE Transactions on Automatic Control*, vol. 50, no. 1, pp. 2–18, 2005.

[51] P. Dewilde and A.-J. Van der Veen, *Time-varying systems and computations*. Springer Science & Business Media, 1998.

[52] X. Cao, M. B. Saltik, and S. Weiland, "Hankel model reduction for descriptor systems," in *Conference on Decision and Control*. IEEE, 2015, pp. 4668–4673.

[53] A. Antoulas, J. Ball, J. Kang, and J. Willems, "On the solution of the minimal rational interpolation problem," *Linear Algebra and its Applications*, vol. 137, pp. 511–573, 1990.

[54] Z. Bai, P. M. Dewilde, and R. W. Freund, "Reduced-order modeling," *Handbook of numerical analysis*, vol. 13, pp. 825–895, 2005.

[55] K. Gallivan, A. Vandendorpe, and P. Van Dooren, "Model reduction of MIMO systems via tangential interpolation," *SIAM Journal on Matrix Analysis and Applications*, vol. 26, no. 2, pp. 328–349, 2004.

[56] ——, "Sylvester equations and projection-based model reduction," *Journal of Computational and Applied Mathematics*, vol. 162, no. 1, pp. 213–229, 2004.

[57] ——, "Model reduction and the solution of Sylvester equations," *MTNS, Kyoto*, vol. 50, 2006.

[58] T. T. Georgiou, "The interpolation problem with a degree constraint," *IEEE Transactions on Automatic Control*, vol. 44, no. 3, pp. 631–635, 1999.

[59] E. Grimme, K. Gallivan, and P. Van Dooren, "On some recent developments in projection-based model reduction," *ENUMATH-97*, no. 98–113, 1998.

[60] A. Astolfi, "Model reduction by moment matching for linear and nonlinear systems," *IEEE Transactions on Automatic Control*, vol. 55, no. 10, pp. 2321–2336, 2010.

[61] A. C. Antoulas, C. A. Beattie, and S. Güğercin, *Interpolatory methods for model reduction*. SIAM, 2020.

[62] M. F. Shakib, G. Scarciotti, A. Y. Pogromsky, A. Pavlov, and N. van de Wouw, "Model reduction by moment matching with preservation of global stability for a class of nonlinear models," *Automatica*, vol. 157, p. 111227, 2023.

[63] G. Scarciotti and A. Astolfi, "Model reduction of neutral linear and nonlinear time-invariant time-delay systems with discrete and distributed delays," *IEEE Transactions on Automatic Control*, vol. 61, no. 6, pp. 1438–1451, 2015.

[64] G. Scarciotti, Z.-P. Jiang, and A. Astolfi, "Data-driven constrained optimal model reduction," *European Journal of Control*, vol. 53, pp. 68–78, 2020.

[65] G. Scarciotti and A. Astolfi, "Data-driven model reduction by moment matching for linear and nonlinear systems," *Automatica*, vol. 79, pp. 340–351, 2017.

[66] G. Scarciotti, "Model reduction by moment matching for linear singular systems," in *Conference on Decision and Control*. IEEE, 2015, pp. 7310–7315.

[67] ——, "Moment matching for nonlinear differential-algebraic equations," in *Conference on Decision and Control*. IEEE, 2016, pp. 7447–7452.

[68] ——, "Steady-state matching and model reduction for systems of differential–algebraic equations," *IEEE Transactions on Automatic Control*, vol. 62, no. 10, pp. 5372–5379, 2017.

[69] P. Schulze, T. C. Ionescu, and J. M. Scherpen, "Families of moment matching-based reduced order models for linear descriptor systems," in *2016 European Control Conference (ECC)*. IEEE, 2016, pp. 1964–1969.

[70] G. Scarciotti and A. R. Teel, "Model order reduction of stochastic linear systems by moment matching," *IFAC-PapersOnLine*, vol. 50, no. 1, pp. 6332–6337, 2017.

[71] ——, "Model order reduction for stochastic nonlinear systems," in *Conference on Decision and Control*. IEEE, 2017, pp. 3069–3074.

[72] ——, "On moment matching for stochastic systems," *IEEE Transactions on Automatic Control*, vol. 67, no. 2, pp. 541–556, 2021.

[73] M. F. Shakib, G. Scarciotti, A. Y. Pogromsky, A. Pavlov, and N. van de Wouw, "Time-domain moment matching for multiple-input multiple-output linear time-invariant models," *Automatica*, vol. 152, p. 110935, 2023.

[74] J. Mao and G. Scarciotti, "Model reduction by matching zero-order moments for 2-D discrete systems," in *Conference on Decision and Control*. IEEE, 2023, pp. 4966–4971.

[75] T. C. Ionescu and A. Astolfi, "Nonlinear moment matching-based model order reduction," *IEEE Transactions on Automatic Control*, vol. 61, no. 10, pp. 2837–2847, 2015.

[76] A. Astolfi, "Model reduction by moment matching, steady-state response and projections," in *Conference on Decision and Control*. IEEE, 2010, pp. 5344–5349.

[77] T. C. Ionescu, A. Astolfi, and P. Colaneri, "Families of moment matching based, low order approximations for linear systems," *Systems & Control Letters*, vol. 64, pp. 47–56, 2014.

[78] T. C. Ionescu, "Two-sided time-domain moment matching for linear systems," *IEEE Transactions on Automatic Control*, vol. 61, no. 9, pp. 2632–2637, 2015.

[79] J. Mao and G. Scarciotti, "Data-driven model reduction by moment matching for linear systems through a swapped interconnection," in *European Control Conference*. IEEE, 2022, pp. 1690–1695.

[80] ——, "Data-driven model order reduction simultaneously matching linear and nonlinear moments," *IEEE Control Systems Letters*, pp. 1–1, 2024.

[81] ——, "Data-driven model reduction by two-sided moment matching," *Automatica*, vol. 166, p. 111702, 2024.

[82] Z. Zhao, J. Mao, and G. Scarciotti, "Strategies to alleviate the impact of noise in data-driven model order reduction by moment matching," in *European Control Conference (ECC)*, 2024.

[83] L. Cortelezzi and J. Speyer, "Robust reduced-order controller of laminar boundary layer transitions," *Physical review E*, vol. 58, no. 2, p. 1906, 1998.

[84] C. W. Rowley, "Model reduction for fluids, using balanced proper orthogonal decomposition," *International Journal of Bifurcation and Chaos*, vol. 15, no. 3, pp. 997–1013, 2005.

[85] K. Taira, S. L. Brunton, S. T. Dawson, C. W. Rowley, T. Colonius, B. J. McKeon, O. T. Schmidt, S. Gordeyev, V. Theofilis, and L. S. Ukeiley, "Modal analysis of fluid flows: An overview," *AIAA Journal*, vol. 55, no. 12, pp. 4013–4041, 2017.

[86] P. Astrid, S. Weiland, K. Willcox, and T. Backx, "Missing point estimation in models described by proper orthogonal decomposition," *IEEE Transactions on Automatic Control*, vol. 53, no. 10, pp. 2237–2251, 2008.

[87] J. K. White *et al.*, "A trajectory piecewise-linear approach to model order reduction of nonlinear dynamical systems," Ph.D. dissertation, Massachusetts Institute of Technology, 2003.

[88] S. Chaturantabut and D. C. Sorensen, "Nonlinear model reduction via discrete empirical interpolation," *SIAM Journal on Scientific Computing*, vol. 32, no. 5, pp. 2737–2764, 2010.

[89] W. J. Rugh, *Nonlinear system theory.* Johns Hopkins University Press, Baltimore, 1981.

[90] M. Ilyas Ahmad, P. Benner, and I. Jaimoukha, "Krylov subspace methods for model reduction of quadratic-bilinear systems," *IET Control Theory & Applications*, vol. 10, no. 16, pp. 2010–2018, 2016.

[91] M. I. Ahmad, P. Benner, P. Goyal, and J. Heiland, "Moment-matching based model reduction for Navier-Stokes type quadratic-bilinear descriptor systems," *Zeitschrift für Angewandte Mathematik und Mechanik*, vol. 97, no. 10, pp. 1252–1267, 2017.

[92] M. I. Ahmad, P. Benner, and L. Feng, "Interpolatory model reduction for quadratic-bilinear systems using error estimators," *Engineering Computations*, 2018.

[93] X. Cao, J. Maubach, S. Weiland, and W. Schilders, "A novel krylov method for model order reduction of quadratic bilinear systems," in *Conference on Decision and Control*. IEEE, 2018, pp. 3217–3222.

[94] I. V. Gosea and A. C. Antoulas, "Data-driven model order reduction of quadratic-bilinear systems," *Numerical Linear Algebra with Applications*, vol. 25, no. 6, p. e2200, 2018.

[95] M. M. A. Asif, M. I. Ahmad, P. Benner, L. Feng, and T. Stykel, "Implicit higher-order moment matching technique for model reduction of quadratic-bilinear systems," *Journal of the Franklin Institute*, vol. 358, no. 3, pp. 2015–2038, 2021.

[96] J. K. Hale, "Functional differential equations," in *Analytic Theory of Differential Equations*. Springer, 1971, pp. 9–22.

[97] L. Dugard and E. I. Verriest, *Stability and control of time-delay systems*. Springer, 1998, vol. 228.

[98] W. Michiels and S.-I. Niculescu, *Stability and stabilization of time-delay systems: an eigenvalue-based approach*. SIAM, 2007.

[99] S. Xu, J. Lam, S. Huang, and C. Yang, "H_∞ model reduction for linear time-delay systems: continuous-time case," *International Journal of Control*, vol. 74, no. 11, pp. 1062–1074, 2001.

[100] E. Jarlebring, T. Damm, and W. Michiels, "Model reduction of time-delay systems using position balancing and delay Lyapunov equations," *Mathematics of Control, Signals, and Systems*, vol. 25, no. 2, pp. 147–166, 2013.

[101] G. Scarciotti and A. Astolfi, "Model reduction of neutral linear and nonlinear time-invariant time-delay systems with discrete and distributed delays," *IEEE Transactions on Automatic Control*, vol. 61, no. 6, pp. 1438–1451, 2016.

[102] I. V. Gosea, I. P. Duff, P. Benner, and A. C. Antoulas, "Model order reduction of bilinear time-delay systems," in *European Control Conference*. IEEE, 2019, pp. 2289–2294.

[103] H. Bai, M. Thulasi, and G. Scarciotti, "Model reduction for quadratic-bilinear systems using nonlinear moments," in *European Control Conference*. IEEE, 2022, pp. 1702–1707.

[104] H. Bai, J. Mao, T. Mylvaganam, and G. Scarciotti, "Nonlinear model reduction by moment matching for Navier-Stokes type quadratic-bilinear descriptor systems," *IEEE Transactions on Control Systems Technology*, p. submitted., 2024.

[105] H. Bai and G. Scarciotti, "Two-sided interconnection-based model reduction for quadratic-bilinear systems," in *Conference on Analysis and Control of Nonlinear Dynamics and Chaos*. IFAC, 2024.

[106] H. Bai, J. Mao, and G. Scarciotti, "Model reduction for quadratic-bilinear time-delay systems using nonlinear moments," *IFAC-PapersOnLine*, vol. 56, no. 1, pp. 91–95, 2023.

[107] G. Scarciotti, A. Astolfi *et al.*, "Nonlinear model reduction by moment matching," *Foundations and Trends® in Systems and Control*, vol. 4, no. 3-4, pp. 224–409, 2017.

[108] A. Isidori, J. van Schuppen, E. Sontag, M. Thoma, and M. Krstic, "Communications and control engineering," in *Nonlinear control systems*. Springer, 1995.

[109] R. Tóth, *Modeling and identification of linear parameter-varying systems*. Springer, 2010, vol. 403.

[110] H. Rocha, "On the selection of the most adequate radial basis function," *Applied Mathematical Modelling*, vol. 33, no. 3, pp. 1573–1583, 2009.

[111] A. Padoan, G. Scarciotti, and A. Astolfi, "A geometric characterisation of persistently exciting signals generated by continuous-time autonomous systems," *IFAC-PapersOnLine*, vol. 49, no. 18, pp. 826–831, 2016.

[112] P. Kunkel and V. Mehrmann, *Differential-algebraic equations: analysis and numerical solution*. European Mathematical Society, 2006, vol. 2.

[113] A. Padoan, G. Scarciotti, and A. Astolfi, "A geometric characterization of the persistence of excitation condition for the solutions of autonomous systems," *IEEE Transactions on Automatic Control*, vol. 62, no. 11, pp. 5666–5677, 2017.

[114] Isidori and Alberto, *Nonlinear Control Systems*. Nonlinear Control Systems, 1985.

[115] C. D. Meyer, *Matrix analysis and applied linear algebra*. SIAM, 2023.

[116] J. Huang, *Nonlinear output regulation: theory and applications*. SIAM, 2004.

[117] L. N. Trefethen and D. Bau, *Numerical linear algebra*. SIAM, 2022.

[118] V. Hernández and M. Gassó, "Explicit solution of the matrix equation AXB- CXD= E," *Linear Algebra and its Applications*, vol. 121, pp. 333–344, 1989.

[119] J. A. Burns and S. Kang, "A control problem for Burgers' equation with bounded input/output," *Nonlinear Dynamics*, vol. 2, pp. 235–262, 1991.

[120] J. C. Strikwerda, *Finite difference schemes and partial differential equations*. SIAM, 2004.

[121] U. Frisch and J. Bec, "Burgulence," in *New trends in turbulence Turbulence: nouveaux aspects: 31 July–1 September 2000*. Springer, 2002, pp. 341–383.

[122] O. R. Burggraf, "Analytical and numerical studies of the structure of steady separated flows," *Journal of Fluid Mechanics*, vol. 24, no. 1, pp. 113–151, 1966.

[123] R. Schreiber and H. B. Keller, "Driven cavity flows by efficient numerical techniques," *Journal of Computational Physics*, vol. 49, no. 2, pp. 310–333, 1983.

[124] P. Huang, B. Launder, and M. Leschziner, "Discretization of nonlinear convection processes: a broad-range comparison of four schemes," *Computer Methods in Applied Mechanics and Engineering*, vol. 48, no. 1, pp. 1–24, 1985.

[125] M. Rosenfeld, D. Kwak, and M. Vinokur, "A fractional step solution method for the unsteady incompressible navier-stokes equations in generalized coordinate systems," *Journal of Computational Physics*, vol. 94, no. 1, pp. 102–137, 1991.

[126] L. Cheng and S. Armfield, "A simplified marker and cell method for unsteady flows on non-staggered grids," *International Journal for Numerical Methods in Fluids*, vol. 21, no. 1, pp. 15–34, 1995.

[127] L. Fuchs and N. Tillmark, "Numerical and experimental study of driven flow in a polar cavity," *International Journal for Numerical Methods in Fluids*, vol. 5, no. 4, pp. 311–329, 1985.

[128] Y. Halevi, "Reduced-order models with delay," *International Journal of Control*, vol. 64, no. 4, pp. 733–744, 1996.